



TECHNICAL UNIVERSITY OF CRETE
SCHOOL OF PRODUCTION ENGINEERING AND
MANAGEMENT

**INTEGRATION OF MULTIPLE
LOCAL ENERGY RESOURCES
IN A FOOD INDUSTRY
A TECHNO-ECONOMIC ANALYSIS**

By

XENOFON G. KOTAKIDIS

A THESIS SUBMITTED IN PARTIAL FULFILLMENT OF
THE REQUIRMENTS FOR THE DIPLOMA OF
PRODUCTION ENGINEERING AND MANAGEMENT

Chania, July 2022

THESIS COMMITTEE

Assistant Professor: Georgios A. Arampatzis, *Supervisor*

Professor: Spiros Papaefthimiou

Assistant Professor: Dimitris K. Ipsakis

INTENTIONALLY BLANK

Approved by the following
examining committee:

Dr. Georgios A. Arampatzis

Assistant Professor
Technical University of Crete
School of Production Engineering
and Management

Dr. Spiros Papaefthimiou

Professor
Technical University of Crete
School of Production Engineering
and Management

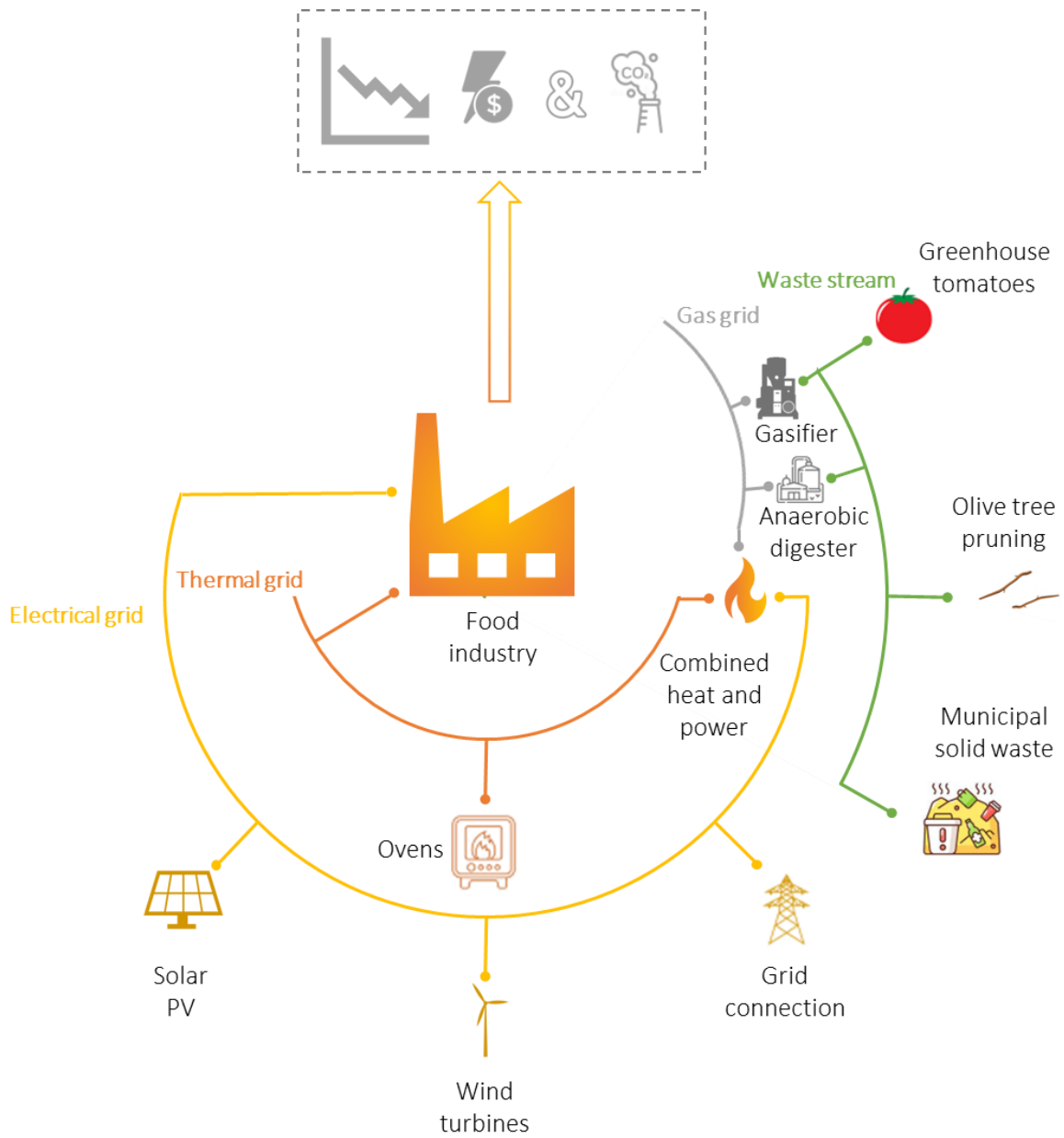
Dr. Dimitris K. Ipsakis

Assistant Professor
Technical University of Crete
School of Production Engineering
and Management

*“Nobody ever figures out what life is all about,
and it doesn't matter. Explore the world.
Nearly everything is really interesting
if you go into it deeply enough.”*

Richard P. Feynman (1918-1988)

GRAPHICAL ABSTRACT



ABSTRACT

Energy consumption in the food industry is heavily dependent on fossil fuels resulting in high greenhouse gas (GHG) emissions. Concurrently, the annual energy consumption in the food sector is expected to increase further due to the continuous global population growth. In this light, the integration of Renewable Energy Sources (RES) and the adoption of energy efficiency measures in every stage of product development can be recognized as of crucial importance. This Diploma Thesis is focused on the investigation and development of a hybrid energy system (HES) to meet the energy needs of a local bakery industry. Specifically, the proposed energy solution enables the higher penetration of RES (e.g., solar irradiation potential) as well as the exploitation of the residues from the rural activities (e.g., olive-trees pruning, tomato crops waste) taking place in the study area. The developed HES consists of technologies such as an anaerobic digestion reactor, PV system, wind turbines, gasification and CHP units. Moreover, this study aims to examine the operational aspects of the proposed system to achieve an optimal balance between RES penetration, energy cost and ecological footprint. In this context, a holistic approach was designed for a local Bakery Industry, with total annual electricity and heat consumption of 1,058 MWh and 3,036 MWh, respectively. To this end, a proper methodological framework was developed to formulate and model alternative scenarios correlating the data collected for the production processes, climatic conditions, biomass potential in the study area, as well as the data of energy consumption. Following, the developed energy-based scenarios for the HES were simulated, analysed and compared using commercially available software. The obtained results indicate that the evolved energy solution could realise the green energy transition in the food industry taking advantage of high-RES penetration to minimise the energy costs and ecological footprint.

Keywords: Renewable Energy Sources, Hybrid energy system, Waste-to-Energy, Energy Systems Modelling

Η ενεργειακή κατανάλωση στην βιομηχανία τροφίμων βασίζεται κυρίως σε ορυκτά καύσιμα και αποτελεί βασική αιτία εκπομπής των αερίων του θερμοκηπίου. Επιπλέον, η συνολική κατανάλωση ενέργειας της βιομηχανίας τροφίμων προβλέπεται να αυξηθεί λόγω του αυξανόμενου πληθυσμού. Συνεπώς η αναγκαιότητα της αξιοποίησης των Ανανεώσιμων Πηγών Ενέργειας (ΑΠΕ), καθώς επίσης και η εφαρμογή μέτρων εξοικονόμησης ενέργειας σε κάθε στάδιο της παραγωγικής διαδικασίας αναγνωρίζεται ως ιδιαίτερα σημαντική. Η παρούσα διπλωματική εργασία εστιάζεται στη μελέτη των διαφορετικών πτυχών ενσωμάτωσης ενός υβριδικού ενεργειακού συστήματος (ΥΕΣ) για την κάλυψη των ενεργειακών αναγκών μιας βιομηχανίας προϊόντων άρτου. Πιο συγκεκριμένα, η προτεινόμενη ενεργειακή λύση του ΥΕΣ προκρίνει την χρήση του τοπικού δυναμικού ΑΠΕ (π.χ. ηλιακή και αιολική ενέργεια), καθώς και την ενεργειακή αξιοποίηση γεωργικών υπολειμμάτων (π.χ. απόβλητα θερμοκηπιακών καλλιεργειών τομάτας, κλαδέματα ελιάς), η οποία συνδυάζει τις δυνατότητες της μεθόδου της αναερόβιας χώνευσης, των φωτοβολταϊκών και αιολικών συστημάτων παραγωγής ενέργειας, της αεριοποίησης και της συμπαραγωγής. Ειδικό στόχο της μελέτης συνιστά η βελτιστοποιημένη λειτουργία του προτεινόμενου συστήματος ΥΕΣ με αυξημένη διείσδυση των ΑΠΕ, μειωμένο κόστος χρήσης ενέργειας και μείωση του αποτυπώματος άνθρακα. Στο πλαίσιο της μελέτης, αναπτύχθηκε μια ολοκληρωμένη λύση για μια τοπική βιομηχανία προϊόντων άρτου, με ετήσια κατανάλωση ηλεκτρικής ενέργειας και θερμότητας ίση με 1,058 MWh και 3,036 MWh, αντίστοιχα. Για την επίτευξη των ερευνητικών στόχων της παρούσας διπλωματικής εργασίας, αναπτύχθηκε κατάλληλη μεθοδολογία, μέσω της οποίας αξιοποιήθηκαν τα δεδομένα της παραγωγικής διαδικασίας, των κλιματικών συνθηκών, της διαθεσιμότητας βιομάζας στην περιοχή μελέτης, καθώς και τα δεδομένα κατανάλωσης ηλεκτρικής ενέργειας με σκοπό τη διαμόρφωση και μοντελοποίηση σεναρίων λαμβάνοντας υπόψη το διαθέσιμο δυναμικό ΑΠΕ και των ενεργειακών αναγκών. Εν συνεχεία, η ενεργειακή ανάλυση των εναλλακτικών σεναρίων για την σύνθεση του ΥΕΣ, πραγματοποιήθηκε μέσω της προσομοίωσης σε συμβατό λογισμικό Η/Υ. Τα αποτελέσματα τα οποία εξήχθησαν, δείχνουν ότι το προτεινόμενο ΥΕΣ μπορεί να καλύψει τις ενεργειακές ανάγκες της περίπτωσης μελέτης, με ρεαλιστικό κόστος ενέργειας και αυξημένη διείσδυση των ΑΠΕ, συμβάλλοντας ουσιαστικά για τη μείωση του τελικού οικολογικού αποτυπώματος της.

Λέξεις κλειδιά: ΑΠΕ, Υβριδικό ενεργειακό σύστημα, Ενεργειακή αξιοποίηση αποβλήτων, Μοντελοποίηση ενεργειακών συστημάτων

ACKNOWLEDGEMENTS

This thesis becomes a reality with the kind of support and help of many individuals. I would like to express my sincere thanks to all of them.

Primarily, I would like to acknowledge and give my warmest thanks to my supervisor Prof. George Arampatzis who made this project possible. His continuous guidance and support throughout my thesis have been vital. I would also like to acknowledge all the research experience that Prof. Arampatzis provided me with as well as supporting and trusting me on my first steps in the field of research. You have shown me the path in addition to helping me grow personally as well as professionally. Thank you, Professor!

I would also like to express my deepest gratitude to all the members from the industrial and digital innovations research group (indigo), whom I was extremely lucky to work with, especially Dr. Nikolaos Savvakis and Dr. Nikolaos Sifakis for their continuous help and support in addition to providing fruitful ideas for the enhancement of this diploma thesis. Collaborating with you has been a pleasure and I learned so many things from you and I am extremely grateful to you for encouraging me to always work hard and chase my dreams.

Additionally, I would like to express my appreciation to Prof. Dimitris Ipsakis for his help, comments, insights, and his advices for my future M.Sc. studies at KTH Royal Institute of Technology in Stockholm, Sweden.

Also, I would love to thank all my friends especially Vassilis G., Michail Z., Ioannis F., Giorgos G., Evi K., Antonia S., Kostas S., and many others. Without you and your support this thesis would not be possible. Our endless conversations throughout all these years shaped my personality and made me the person I am today. You have been by my side since the day we all met, during the good and the bad days, and I am grateful being friends with you! I wish you all the best in your future endeavours!

To everyone mentioned above and to many more that contributed on my personal and professional development from the bottom of my heart, thank you!

Finally, I would love to thank my family for the support in each and every step throughout the years. Without you I would certainly not be here!

Xenofon G. Kotakidis

Chania, July 2022

TABLE OF CONTENTS

CHAPTER 1	1
INTRODUCTION	1
1.1 INTRODUCTION/MOTIVATION.....	1
1.2 AIM AND OBJECTIVES	5
1.3 OUTLINE OF THE THESIS.....	5
CHAPTER 2	7
REVIEW OF RELATED LITERATURE	7
2.1 UTILIZATION OF LOCAL RENEWABLE ENERGY SOURCES	7
2.1.1 SOLAR PV	9
2.1.2 WIND TURBINES.....	10
2.1.3 COMBINED HEAT AND POWER.....	11
2.2 BIOENERGY PRODUCTION THROUGH LOCAL BIOMASS RESIDUES / WASTE MANAGEMENT	12
2.2.1 ANAEROBIC DIGESTION.....	15
2.2.2 GASIFICATION	18
2.3 MEETING THE ENERGY DEMAND OF FOOD INDUSTRIES	20
2.4 ENERGY FLEXIBILITY IN FOOD INDUSTRIES.....	24
2.5 EXISTING RES UTILIZATION EXAMPLES FROM INDUSTRIES	28
2.6 STATE OF THE ART	29
CHAPTER 3	33
DESIGN AND METHODOLOGY	33
3.1 DATA COLLECTION AND PROCESSING METHODOLOGY	33
3.1.1 ENERGY CONSUMPTION DATA ANALYSIS.....	33
3.1.2 RESOURCE ANALYSIS.....	40
3.1.2.1 SOLAR RADIATION DATA	41
3.1.2.2 WIND DATA	43
3.1.2.3 TEMPERATURE DATA	44
3.1.2.4 BIOMASS DATA.....	45
3.2 SYSTEM MODELLING METHODOLOGY	52
3.2.1 PV MODULE.....	53
3.2.1.1 PV MODULE MATHEMATICAL MODEL	54
3.2.2 WIND TURBINE.....	54
3.2.2.1 WIND TURBINE MATHEMATICAL MODEL	55
3.2.3 GENERATOR.....	56
3.2.3.1 BIOGAS GENERATOR MATHEMATICAL MODEL	58
3.2.4 CONVERTER	58
3.2.5 GRID	59
3.2.6 BOILER.....	59
3.2.7 GENERAL	60
3.3 ECONOMIC MODEL.....	60
3.4 SCENARIO CONCEPTUALISATION	61
3.5 SIMULATION SOFTWARE (HOMER Pro).....	64
3.6 LIMITATIONS AND ASSUMPTIONS	67
3.7 METHODOLOGY SUMMARY	68
CHAPTER 4	69
RESULTS	69

4.1 HOMER PRO RESULTS	69
4.1.1 BASELINE CASE AND SUGGESTED SCENARIOS	69
4.1.2 OPTIMAL SYSTEM ARCHITECTURE.....	75
4.1.2.1 COST SUMMARY.....	76
4.1.2.2 ELECTRICAL DEMAND SUMMARY	79
4.1.2.3 THERMAL DEMAND SUMMARY	82
4.1.2.4 FUEL SUMMARY	84
4.1.2.5 GRID	85
4.1.3 SENSITIVITY ANALYSIS	87
4.1.3.1 SENSITIVITY ANALYSIS FOR BIOMASS PRICE	88
4.1.3.2 SENSITIVITY ANALYSIS FOR AVERAGE DAILY ENERGY AND HEAT DEMAND	90
4.1.3.3 SENSITIVITY ANALYSIS FOR GRID ENERGY PRICE	93
4.1.3.4 SENSITIVITY ANALYSIS FOR CARBON EMISSIONS PENALTY	95
4.1.3.5 SENSITIVITY ANALYSIS FOR DIESEL PRICES	98
CHAPTER 5	101
DISCUSSION	101
5.1 RESULTS DISCUSSION.....	101
5.2 RESULTS COMPARISON WITH RELEVANT LITERATURE	103
CHAPTER 6	104
CONCLUSION	104
REFERENCES	106
APPENDIX A	115
APPENDIX B.....	117
APPENDIX C	119

LIST OF FIGURES

FIGURE 1-1 MAP OF FUTURE AND CURRENT INTERCONNECTION PROJECTS IN SOUTH GREECE. (SOURCE: INDEPENDENT POWER TRANSMISSION OPERATOR IPTO, N.D.).....	3
FIGURE 1-2 WORLD ENERGY MIX, 2020. (SOURCE: LOONEY, 2021).....	4
FIGURE 1-3 WORLD ELECTRICITY PRODUCTION SOURCES PROJECTION FOR A) NEW POLICY SCENARIO B) SUSTAINABLE DEVELOPMENT SCENARIO. (SOURCE: CURTO ET AL., 2019).....	4
FIGURE 1-4 SUSTAINABLE DEVELOPMENT GOALS REGARDING ENERGY AND CLIMATE CHANGE.....	5
FIGURE 1-5 OUTLINE OF THE THESIS PROCEDURE.....	6
FIGURE 2-1 VALUE CREATION CHAIN OF OLIVE PRUNING. (ADAPTED FROM: KOUGIOUMTZIS ET AL., 2019).....	9
FIGURE 2-2 OPERATIONAL PRINCIPLES OF SOLAR PV. (SOURCE: FRANCESCO & UMBERTO, 2019).....	10
FIGURE 2-3 MAIN COMPONENTS OF A TYPICAL MODERN WIND TURBINE. (SOURCE: LYNN, 2012).....	11
FIGURE 2-4 A TYPICAL CONFIGURATION OF A CHP UNIT. (SOURCE: TIAL KIO ET AL., 2021).....	12
FIGURE 2-5 A) REFERENCE GREENHOUSE PLANT SYSTEM AND B) GREENHOUSE PLANT SYSTEM WITH AD. (SOURCE: DANEVAD & CARLOS-PINEDO, 2021).....	14
FIGURE 2-6 ENERGY VALORISATION OF OLIVE DERIVED WASTE (SOLIDS LINES REPRESENT INDUSTRY PROCESSES WHEREAS DASHED LINES SYMBOLIZE APPLICATIONS AT RESEARCH STAGE). (SOURCE: GARCÍA MARTÍN ET AL., 2020).....	15
FIGURE 2-7 AD'S INPUT AND OUTPUT FLOWS. (SOURCE: MEEGODA ET AL., 2018).....	16
FIGURE 2-8 SUMMARY OF THE USES AND PRODUCTS OF THERMOCHEMICAL BIOMASS CONVERSION TECHNOLOGIES. (SOURCE: MOLINO ET AL., 2016).....	19
FIGURE 2-9 A TYPICAL PRODUCTION SYSTEM AND ITS INTERACTION WITH THE ENVIRONMENT. (SOURCE: BEIER, 2017).....	20
FIGURE 2-10 PERCENTAGE OF TOTAL COST RELATED TO ENERGY AND WATER CONSUMPTION ACROSS DIFFERENT INDUSTRIAL SECTORS IN THE UK. NOTE: GVA (GROSS VALUE ADDED). (SOURCE: GRIFFIN ET AL., 2016).....	21
FIGURE 2-11 MAIN ENERGY DEMAND FOR FOOD AND DRINK INDUSTRIAL SECTORS IN THE UK. (SOURCE: GRIFFIN ET AL., 2016).....	22
FIGURE 2-12 ESTIMATED CARBON INTENSITY FOR SEVERAL FOOD PRODUCTS FOR THE US. (SOURCE: BOEHM ET AL., 2018).....	23
FIGURE 2-13 ENERGY FLEXIBILITY STRATEGIES. (SOURCE: BEIER, 2017; PIERRI ET AL., 2021).....	26
FIGURE 2-14 LOAD SHAPING STRATEGIES IN DSM. (SOURCE: BEIER, 2017).....	26
FIGURE 2-15 MAIN INDUSTRIAL FACILITIES OF PLASTIKA KRITIS (UPPER) AND PART OF THE WIND FARM LOCATED IN CRETE. (SOURCE: COMPANY PROFILE - PLASTIKAKRITIS.COM, N.D.).....	28
FIGURE 3-1 THE GEOGRAPHICAL LOCATION OF THE AREA OF STUDY.	34
FIGURE 3-2 DROPS IN ELECTRIC POWER DEMAND DURING THE SUMMER BREAK AND THE CHRISTMAS PERIOD.	35
FIGURE 3-3 TOTAL ELECTRICITY CONSUMPTION AND ELECTRIC POWER DEMAND PROFILES.	35
FIGURE 3-4 ACTIVE ELECTRIC POWER DEMAND THROUGHOUT A WEEK DURING MAY 2020 (LEFT) AND COMPARISON BETWEEN ELECTRIC POWER DEMAND DURING A WEEKDAY AND SUNDAY DURING A TYPICAL MONTH (RIGHT).	36
FIGURE 3-5 ACTIVE ELECTRIC POWER DEMAND THROUGHOUT A WEEK DURING JULY 2020 (LEFT) AND COMPARISON BETWEEN ELECTRIC POWER DEMAND DURING A WEEKDAY AND SUNDAY DURING A PEAK MONTH (RIGHT).	37
FIGURE 3-6 ANNUAL ACTIVE ELECTRIC POWER DEMAND INFORMATION.	37
FIGURE 3-7 TOTAL THERMAL CONSUMPTION AND THERMAL POWER DEMAND PROFILES.	38
FIGURE 3-8 ACTIVE THERMAL POWER DEMAND THROUGHOUT A WEEK DURING MAY 2020 (LEFT) AND COMPARISON BETWEEN THERMAL POWER DEMAND DURING A WEEKDAY AND SUNDAY DURING A TYPICAL MONTH (RIGHT).	38

FIGURE 3-9 ACTIVE THERMAL POWER DEMAND THROUGHOUT A WEEK DURING JULY 2020 (LEFT) AND COMPARISON BETWEEN THERMAL POWER DEMAND DURING A WEEKDAY AND SUNDAY DURING A PEAK MONTH (RIGHT).	39
FIGURE 3-10 ANNUAL THERMAL POWER DEMAND INFORMATION.	39
FIGURE 3-11 ENERGY DEMAND SPLIT AT THE LOCAL BAKERY.....	40
FIGURE 3-12 AVERAGE MONTHLY RADIATION AND CLEARNESS INDEX AT THE STUDY AREA. (SOURCE: NASA POWER PREDICTION OF WORLDWIDE ENERGY RESOURCES, N.D.; PFENNINGER & STAFFELL, 2016; STAFFELL & PFENNINGER, 2016)	43
FIGURE 3-13 MONTHLY AVERAGE WIND SPEED AT THE STUDY AREA. (SOURCE: NASA POWER PREDICTION OF WORLDWIDE ENERGY RESOURCES, N.D.; PFENNINGER & STAFFELL, 2016; STAFFELL & PFENNINGER, 2016).....	44
FIGURE 3-14 MONTHLY AVERAGE TEMPERATURE AT THE STUDY AREA. (SOURCE: NASA POWER PREDICTION OF WORLDWIDE ENERGY RESOURCES, N.D.; PFENNINGER & STAFFELL, 2016; STAFFELL & PFENNINGER, 2016).....	45
FIGURE 3-15 LAND USAGE IN THE MUNICIPALITY OF KISSAMOS FOR AGRICULTURAL ACTIVITIES. NOTE: THE CIRCLE REPRESENTS A 12.5 KM RADIUS OF ECONOMICALLY EXPLOITABLE LAND. (SOURCE: 7H YΠΠΕ - ΓΕΩΓΡΑΦΙΑ ΔΗΜΩΝ ΝΟΜΟΥ ΧΑΝΙΩΝ, N.D.).....	46
FIGURE 3-16 A) SCHEMATIC DIAGRAM OF THE REFERENCE WASTE TO ENERGY SYSTEM B) SCHEMATIC DIAGRAM OF THE HOMER EQUIVALENT WASTE TO ENERGY SYSTEM.	51
FIGURE 3-17 POWER CURVE OF THE GENERIC 10KW WIND TURBINE. (SOURCE: TERLOUW & BAUER, 2021) ..	55
FIGURE 3-18 SCHEMATIC DIAGRAM OF THE PROPOSED HRES.....	62
FIGURE 3-19 CORE CAPABILITIES OF THE HOMER PRO SOFTWARE. (SOURCE: RAM ET AL., 2021)	65
FIGURE 3-20 INPUT AND OUTPUT VARIABLES IN HOMER PRO SOFTWARE. (SOURCE: P. KUMAR & VALLABHBHAI, 2016; RAM ET AL., 2021)	65
FIGURE 3-21 MAIN SCREEN OF THE HOMER PRO SOFTWARE.....	66
FIGURE 3-22 SUMMARY OF THE PROPOSED METHODOLOGICAL FRAMEWORK DEVELOPED.....	68
FIGURE 4-1 SCHEMATIC DIAGRAM OF THE BASELINE SYSTEM.	69
FIGURE 4-2 A) NPC, INITIAL CAPITAL, AND CDE OF CURRENT SUPPLY AND SCENARIOS B) LCOE, LCOTE AND CARBON SAVINGS OF CURRENT SUPPLY AND SCENARIOS.	71
FIGURE 4-3 A) ELECTRICAL ENERGY PRODUCTION FOR EVERY SCENARIO AND LEVELIZED COST PER TECHNOLOGY, B) THERMAL ENERGY PRODUCTION PER TECHNOLOGY AND RENEWABLE FRACTION FOR EVERY SCENARIO, AND C) DIESEL AND BIOMASS CONSUMPTION PER SCENARIO.....	74
FIGURE 4-4 SCHEMATIC OF THE SYSTEM (LEFT), COMPARISON OF CUMULATIVE DISCOUNTED CASH FLOWS (RIGHT).....	76
FIGURE 4-5 COST FLOWS OF THE OPTIMAL SYSTEM.	78
FIGURE 4-6 MONTHLY ELECTRICAL ENERGY PRODUCTION PER TECHNOLOGY.	79
FIGURE 4-7 HOURLY ELECTRICAL POWER GENERATION ACCORDING TO HOMER FOR A TYPICAL WEEK (19 TH WEEK).....	81
FIGURE 4-8 DATA MAPS FOR ELECTRICITY PRODUCTION OF EVERY COMPONENT OF THE PROPOSED HRES.	82
FIGURE 4-9 MONTHLY THERMAL ENERGY PRODUCTION PER TECHNOLOGY.	82
FIGURE 4-10 HOURLY THERMAL POWER GENERATION ACCORDING TO HOMER FOR A TYPICAL WEEK (19 TH WEEK).....	83
FIGURE 4-11 DATA MAPS FOR THERMAL ENERGY PRODUCTION OF EVERY COMPONENT OF THE PROPOSED HRES.....	84
FIGURE 4-12 DATA MAPS FOR BIOGAS AND DIESEL CONSUMPTION.....	85
FIGURE 4-13 DATA MAPS FOR ENERGY PURCHASES AND SALES FROM OR TO THE GRID.....	87
FIGURE 4-14 THE EFFECT OF THE BP ON LCOE AND IRR.	89
FIGURE 4-15 THE EFFECT OF THE BP ON CO ₂ EMISSIONS AND THE RENEWABLE FRACTION.	90
FIGURE 4-16 THE EFFECT OF THE BP ON BIOGAS ELECTRICITY/HEAT CONTRIBUTION (%TOTAL GENERATION).90	90
FIGURE 4-17 THE EFFECT OF THE ELECTRIC AND THERMAL DEMAND ON LCOE AND IRR	92
FIGURE 4-18 THE EFFECT OF ELECTRIC AND THERMAL DEMAND ON CDE AND THE RENEWABLE FRACTION. ...	92

FIGURE 4-19 THE EFFECT OF ELECTRIC AND THERMAL DEMAND ON BIOGAS ELECTRICITY/HEAT CONTRIBUTION (%TOTAL GENERATION).	93
FIGURE 4-20 THE EFFECT OF GRID ENERGY PRICE ON LCOE AND IRR.....	94
FIGURE 4-21 THE EFFECT OF GRID ENERGY PRICE ON CDE AND THE RENEWABLE FRACTION.	95
FIGURE 4-22 THE EFFECT OF GRID ENERGY PRICE ON BIOGAS ELECTRICITY/HEAT CONTRIBUTION (%TOTAL GENERATION).	95
FIGURE 4-23 THE EFFECT OF CDE PENALTIES ON LCOE AND IRR.	97
FIGURE 4-24 THE EFFECT OF CDE PENALTIES ON CDE AND THE RENEWABLE FRACTION.	97
FIGURE 4-25 THE EFFECT OF CDE PENALTIES ON BIOGAS ELECTRICITY/HEAT CONTRIBUTION (%TOTAL GENERATION).	98
FIGURE 4-26 THE EFFECT OF DIESEL PRICE ON LCOE AND IRR.	99
FIGURE 4-27 THE EFFECT OF DIESEL PRICE ON CDE AND THE RENEWABLE FRACTION.	100
FIGURE 4-28 THE EFFECT OF DIESEL PRICE ON BIOGAS ELECTRICITY/HEAT CONTRIBUTION (%TOTAL GENERATION).	100

LIST OF TABLES

TABLE 2-1 ESTIMATED PRODUCTION OF TOMATO WASTES FROM GREENHOUSE SYSTEMS.	8
TABLE 2-2 ESTIMATED PRODUCTION OF OLIVE PRUNING DERIVED BIOMASS. NOTE: (AR: AS RECEIVED, DB: DRY BASIS).....	8
TABLE 2-3 AVERAGE MSW PRODUCTION PER CAPITA IN EUROPE IN 2020.....	9
TABLE 2-4 METHANE POTENTIAL FROM AD AND CHEMICAL CHARACTERISTICS OF ROTTEN TOMATO (RT), GREEN TOMATO (GT), TOMATO BRANCHES (TB), AND FRESH TOMATO LEAVES AND STEMS (TLSF).....	17
TABLE 2-5 METHANE POTENTIAL FROM AD AND CHEMICAL CHARACTERISTICS OF THE ORGANIC FRACTION OF MSW.....	17
TABLE 2-6 CHEMICAL CHARACTERISTICS OF OTP. NOTE: (N/G: NOT GIVEN)	19
TABLE 2-7 THERMAL AND ELECTRICAL ENERGY DEMAND TO PRODUCE OF ONE METRIC TON OF SEVERAL FOOD PRODUCTS ACROSS SIX EUROPEAN COUNTRIES (AUSTRIA, FRANCE, GERMANY, SPAIN, POLAND, AND THE UK).	21
TABLE 2-8 TECHNICAL POTENTIAL FOR INSTALLED RES FOR THE FOOD AND TOBACCO INDUSTRY SECTOR BY 2030 (AN AMBITIOUS SCENARIO). NOTE: UNITS IN EJ/YR.....	23
TABLE 2-9 ESTIMATION OF ENERGY SAVINGS, CDE MITIGATION, AND PAYBACK PERIODS FOR THE FOOD AND BEVERAGE INDUSTRY ACROSS SIX EUROPEAN COUNTRIES (AUSTRIA, FRANCE, GERMANY, SPAIN, POLAND, AND THE UK).	24
TABLE 2-10 COMPARISON BETWEEN RES AND FOSSIL FUEL ENERGY GENERATION. (SOURCE: BEIER, 2017)...	25
TABLE 2-11 DIFFERENCES BETWEEN PROCESS AND DISCRETE MANUFACTURING SYSTEMS. (SOURCE: PIERRI ET AL., 2020).....	27
TABLE 2-12 ASSESSMENT OF POTENTIAL ENERGY FLEXIBILITY METHODS IN PROCESS INDUSTRY. (SOURCE: PIERRI ET AL., 2020).....	27
TABLE 2-13 SIMILAR STUDIES SUMMARY.	32
TABLE 3-1 SUMMARY OF THERMAL AND ELECTRIC LOAD.	40
TABLE 3-2 METEOROLOGICAL CONDITIONS IN STUDY AREA.	41
TABLE 3-3 BA DATA FOR THE AREA OF INTEREST.	45
TABLE 3-4 BIOMASS FOR GASIFICATION PROPERTIES.	47
TABLE 3-5 GASIFICATION OF OLIVE PRUNING - ENERGY POTENTIAL FOR THE AREA OF STUDY.	48
TABLE 3-6 MSW GENERATION DATA FOR THE AREA OF INTEREST.	48
TABLE 3-7 AD OF MSW - ENERGY POTENTIAL FOR THE AREA OF STUDY.	49
TABLE 3-8 AD OF TOMATO RELATED WASTE - ENERGY POTENTIAL FOR THE AREA OF STUDY.	49
TABLE 3-9 TOTAL ANNUAL FUEL PRODUCTION PER TECHNOLOGY.	49
TABLE 3-10 MEAN COST AND INPUT PARAMETERS OF BIOMASS.	50
TABLE 3-11 CHEMICAL CHARACTERISTICS OF THE PRODUCED GASES.	52
TABLE 3-12 FUEL CHARACTERISTICS USED IN THE CHP UNIT.	52
TABLE 3-13 TECHNICAL AND ECONOMIC PARAMETERS OF SOLAR PV.	53
TABLE 3-14 SOLAR PV ECONOMY OF SCALE.	53
TABLE 3-15 TECHNICAL AND ECONOMIC PARAMETERS OF WT.	54
TABLE 3-16 TECHNICAL AND ECONOMIC PARAMETERS OF THE GENERATOR WITH GASIFICATION AND AD.....	57
TABLE 3-17 TECHNICAL AND ECONOMIC PARAMETERS OF THE CONVERTER.	59
TABLE 3-18 DIFFERENT HRES CONFIGURATIONS ANALYZED IN HOMER PRO SOFTWARE.....	62
TABLE 3-19 SCENARIOS.....	63
TABLE 3-20 ADVANTAGES AND DISADVANTAGES OF THE HOMER PRO SOFTWARE. (SOURCE: P. KUMAR & VALLABHBHAI, 2016; RAM ET AL., 2021)	66
TABLE 4-1 COST OF THE BASELINE CASE.	70
TABLE 4-2 OPTIMIZATION RESULTS.....	73
TABLE 4-3 SYSTEM ARCHITECTURE.....	75

TABLE 4-4 OPTIMAL SYSTEM ECONOMICS.	76
TABLE 4-5 NPCS.	77
TABLE 4-6 ELECTRICITY PRODUCTION SUMMARY.	79
TABLE 4-7 THERMAL ENERGY PRODUCTION SUMMARY.	83
TABLE 4-8 FUEL CONSUMPTION SUMMARY.	85
TABLE 4-9 GRID MONTHLY SUMMARY.	86
TABLE 4-10 LIST OF SENSITIVITY ANALYSIS VARIABLES.	88
TABLE 4-11 SUMMARY OF THE RESULTS IN BP SENSITIVITY ANALYSIS.	89
TABLE 4-12 SUMMARY OF THE RESULTS IN AVERAGE DAILY ELECTRICITY AND THERMAL ENERGY CONSUMPTION SENSITIVITY ANALYSIS.	91
TABLE 4-13 SUMMARY OF THE RESULTS IN ENERGY PRICE SENSITIVITY ANALYSIS.	94
TABLE 4-14 SUMMARY OF THE RESULTS IN CARBON EMISSION PENALTIES SENSITIVITY ANALYSIS.	96
TABLE 4-15 SUMMARY OF THE RESULTS IN DIESEL PRICES SENSITIVITY ANALYSIS.	99
TABLE 5-1 RESULTS COMPARISON WITH RELEVANT LITERATURE. NOTE: (N/E: NOT EXAMINED, N/G: NOT GIVEN)	103

NOMENCLATURE

SYMBOLS

SYMBOLS	UNITS (SI)	DESCRIPTION
K_T	–	Clearness index
H_{ave}	$kWh/m^2/day$	Monthly average radiation on a horizontal surface of the earth
$H_{o,ave}$	$kWh/m^2/day$	Extra-terrestrial horizontal radiation
n	–	The day of the year
N	–	Number of days in a month
G_{on}	kW/m^2	Intensity of solar radiation at the top of Earth's atmosphere
θ_z	degrees [°]	Zenith angle
φ	degrees [°]	Latitude
δ	degrees [°]	Solar declination
ω	degrees [°]	Hour angle
H_o	$kWh/m^2/day$	Average extra-terrestrial horizontal radiation for the day
ω_s	degrees [°]	Sunset hour angle
f_{Load}	%	Load factor
P_{PV}	kW	Output of a PV array
Y_{PV}	kW	Rated capacity of the PV array
f_{PV}	%	PV derating factor
\bar{G}_T	kW/m^2	Current solar radiation incident on the PV array

$\bar{G}_{T,STC}$	1 kW/m^2	Incident solar radiation on the PV array under STC
a_p	$\%/^{\circ}\text{C}$	Temperature coefficient of power
T_c	$^{\circ}\text{C}$	Current PV cell temperature
$T_{c,STC}$	$25 \text{ }^{\circ}\text{C}$	PV cell temperature under STC
U_{hub}	m/s	Wind speed at the hub height of the wind turbine used in the simulation
U_{anem}	m/s	Wind speed at the anemometer height
z_{hub}	m	Hub height of the wind turbine
z_{anem}	m	The anemometer height
z_0	m	Surface roughness length.
P_{WTG}	kW	Wind turbine power output
$P_{WTG,STP}$	kW	Power output at standard test conditions
ρ	kg/m^3	Actual air density
ρ_0	1.225 kg/m^3	Air density under standard test conditions
C_{acap}	€	Annualized capital cost of each component
C_{cap}	€	Initial capital cost for each component
K	years	System lifetime
i	$\%$	Annual interest rate
m	$-$	Total number of all system components
$C_{OM,j}$	€	Annual O&M cost for the j^{th} component
C_f	€	Total annual fuel cost
$C_{R,j}$	€	Annual replacement cost of the j^{th} component

E_{total}	$kWh/year$	Total annual energy consumption
$E_{prim,AC}$	$kWh/year$	Total AC load served
$E_{prim,DC}$	$kWh/year$	Total DC load served
E_{def}	$kWh/year$	Total deferrable load served
$E_{grid,sales}$	$kWh/year$	Total yearly grid sales
LCOE	$€/kWh_{el}$	Levelized cost of electricity
u	–	Number of waste streams
$MOWS_i$	$ton/year$	Annual waste mass generation of i^{th} waste stream
EP_i	$MJ/year$	Annual energy potential of the i^{th} waste stream
TAP	$MJ/year$	Annual energy potential of all waste streams
$C_{1,i}$	$€/ton$	Cost of collection and storage for 1 ton of the i^{th} waste
$C_{2,i}$	$€/km/ton$	Cost of transporting 1 ton of the i^{th} waste for 1 km
$D_{1,i}$	km	Average distance travelled for the i^{th} waste stream
CDE	$kg CO_{2eq}/kWh$	Carbon dioxide emissions from grid per unit of produced power
F_{PE}	2.9	Primary energy factor and is used to convert the final to primary energy (factory to consumer)
F_D	$0.989 kg CO_{2eq}/kWh$	Diesel factor
F_{FF}	%	Fossil fuels' factor (grid penetration)
LCOTE	$€/kWh_{th}$	Levelized cost of thermal energy
TE_{boiler}	$kWh/year$	Annual thermal output of the boiler
AC_{boiler}	$€/year$	Annualized cost of the boiler.
F	$kg/hour$	Generator's fuel consumption

F_0	$kg/hour/kW$	Fuel curve intercept coefficient
Y_{gen}	kW	The rated capacity of the generator
F_1	$kg/hour/kW$	Fuel curve slope
P_{gen}	kW	The electrical output of the generator
η_{gen}	%	Electrical efficiency of the generator
\dot{m}_{fuel}	kg/hr	Mass flow rate of the fuel
p_{gen}	P_{gen}/Y_{gen}	The relative output of the generator

ACRONYMS

ACRONYM: DESCRIPTION

AD: Anaerobic Digestion

BAT: Batteries

BOD: Biochemical Oxygen Demand

BA: Biomass Availability

BP: Biomass Price

BG: Biogas Generator

CAC: Capital Cost

COD: Chemical Oxygen Demand

CHP: Combined Heat and Power

C/N: Carbon/Nitrogen Ratio

CDE: Carbon Dioxide Emissions

DG: Diesel Generator

DSM: Demand Side Management

DW: Dry Weight

FC: Fuel Cell

FM: Fresh Matter

GT: Green Tomato

GVA: Gross Value Added

**HVAC: Heating, Ventilation, Air
Conditioning/Cooling**

IRR: Internal Rate of Return

LCOE: Levelized Cost Of Electricity

**LCOTE: Levelized Cost of Thermal
Energy**

LHV: Lower Heating Value

LF: Load Factor

MSW: Municipal Solid Waste

NPC: Net Present Cost

NEC: Not Elsewhere Classified

**O&M C: Operational and Maintenance
Cost**

OTP: Olive Tree Pruning

PM: Particulate Matter

PHS: Pumped Hydro Storage

PV: Photovoltaics

RES: Renewable Energy Sources

RC: Replacement Cost

ROI: Return On Investment

RT: Rotten Tomato

SDG: Sustainable Development Goal

SEC: Specific Energy Consumption

STC: Standard Test Conditions

TOC: Total Organic Carbon

TLC: Thermal Load Controller

TB: Tomato Branches

TS: Total Solids

VRE: Variable Renewable Energy

VAT: Value Added Tax

VFAs: Volatile Fatty Acids

VS: Volatile Solids

WG: Waste Generation

WT: Wind Turbines

CHAPTER 1

INTRODUCTION

Subchapter 1.1 examines the status of renewable energy sources (RES) in the global economy, including trends, growth attempts, and roadblocks to their continued development. Additionally, it provides the primary motivation behind this diploma thesis. Subchapter 1.2 presents the main objectives of the diploma thesis, and the thesis's main outline is presented in Subchapter 1.3.

1.1 INTRODUCTION/MOTIVATION

Energy is one of the essential elements for the sustainable development of a society and is directly correlated to the quality of people's lives and economic development, making energy supplies a crucial issue in human existence. The energy supply sector has seen tremendous transformations over the last century. Due to the exponential population growth in combination with continually increasing industrialization, the energy demand is following a similar trend. This transition improved the quality of life and living conditions for billions of people.

Energy resources can be classified into three main categories: fossil fuels, renewable sources, and nuclear resources. Fossil fuels are limited, and their price varies greatly thanks to several factors (i.e., transportation costs, availability, mining costs). Fossil fuels also generate massive amounts of greenhouse gas (GHG) emissions, which in turn cause global warming and climate change. Nuclear energy produces zero-carbon emissions while having high energy density characteristics; however, it produces highly toxic radioactive waste that threatens human health concurrently being an extremely water-intensive process. These are the key factors contributing to the rising popularity of RES. According to (Hersh, 2006), RES can be defined as “*energy flows which are continuously replenished by natural processes*”. Fossil and nuclear resources are described in terms of finite quantities, whereas RES are described in terms of flows. Due to the finite nature of fossil and nuclear fuels, they will eventually be exhausted.

Some RES are variable renewable energy (VRE) sources and are often characterized by a non-dispatchable nature. VRE sources' power output cannot be increased as desired and can only be reduced (curtailment). This characteristic leads to losses of unexploited potential. On the contrary, fossil fuel power plants can control the power output to a certain extent, which is one of the main differentiating factors between RES and fossil fuels. Additionally, RES energy generation is also stochastic (volatile); therefore, short-term fluctuations can lead to a relatively significant reduction in power generation capabilities. Volatility is the main characteristic of solar and wind energy. Biomass and hydropower, however, are not characterized by high volatility.

The amount of fuel that can be extracted, and consequently the total available energy potential, depends on the availability of technologies that can extract the fuel at an acceptable cost. The environmental impact of the extraction process is significant and should be carefully assessed, but it

is outside of the scope of this thesis. One of the main advantages of RES is that they are flows; hence it is impossible to overconsume because the extracted energy for a particular period does not impact the amount of energy flow in the subsequent periods. Technical and economic constraints introduce an upper limit on the available energy for extraction. Another advantage is that due to the nature of RES, it is possible to eliminate current inequalities in access to energy for developing countries and rural areas that are inaccessible from the current electrical grid. Reduced life cycle GHG emissions from power and heat generation is another advantage of RES.

Indeed, RES are distinguished by their wide range of energy supply alternatives that can help with the decentralization of the energy mix. According to the Texas Renewable Energy Industries Association, RES can be divided into three main categories: directly (solar thermal energy and solar photovoltaics (PV)) or indirectly (hydropower, wind power and biofuels) derived from the sun as well as natural movements and mechanisms of the environment (geothermal energy).

The necessity of the implementation of RES is evident from the Paris Agreement, signed in 2016, where 195 United Nations Framework Convention on Climate Change (UNFCCC) participating members agreed to reduce the emissions of GHGs to keep the increase of the mean global temperature to well below 2°C above pre-industrial levels, setting a goal of net-zero emissions by 2050. Before the Paris Agreement, there had been a wide range of growth in renewables; however, this agreement has rapidly altered the rate of change to a low carbon energy system transition. This led to a remarkable transformation of the electricity system's shape. Currently, power production from RES is decentralized, small- to medium-scale, and located depending on climatic and topographical parameters as well as the geographical position of the consumer, minimizing transmission and distribution losses. The distance between source and consumer is mainly a function of the RES type. For example, wind power generation tends to increase the distance because of the very own nature of this technology. When introducing new renewable incentives, energy system design is crucial yet sometimes underestimated. Poor system design can lead to certain technical challenges, such as an increased rate of change of frequency (ROCOF), reduction of renewables, and power quality issues (McIlwaine et al., 2021).

Other essential factors that need to be considered for the integration of RES are the cost of energy, public acceptance, integration of RES electricity production to the existing electrical grid, government support, and increased use of public transportation and energy efficiency because of behavioural changes (McIlwaine et al., 2021).

Decentralized smart energy systems are vital in transitioning towards a net-zero carbon society. In the current years, a transition of the centralized energy system to a more decentralized (onsite generation) is apparent. This transition is beneficial for industrial and, more specifically, production and manufacturing industrial sites, where massive amounts of energy (heat, electricity) are consumed.

The area of study is located on the island of Crete in Greece. The island is characterized by high wind and solar potential for energy production. As of 2022, the total number of inhabitants is estimated to be around 600,000; however, the number doubles during the summer due to the relatively high tourism activity. The vast variations in the island's inhabitants result in considerable variations in the island's electrical load demand throughout the year. The island is grid-connected with the mainland. The first connection with Peloponnesus was finished in May 2021, when an interconnection of 150 kV AC with a total capacity of 2×200 MVA was installed (*Independent*

Power Transmission Operator / IPTO, n.d.; Tial Kio et al., 2021). This interconnection offers economic and environmental benefits. For example, the cost of energy production in off-grid islands is significantly higher compared to the mainland and interconnection between them the island and the mainland can dramatically reduce the energy-related costs. Moreover, the large-scale deployment of local RES can bring economic growth and benefits regarding the decarbonization of the energy system. Additionally, it can reduce GHG emissions because off-grid islands tend to rely on fossil fuels. Moreover, this interconnection can increase the RES penetration and offer the possibility to exploit the high-RES potential of the area. Moreover, another interconnection is planned for 2023 offering an expansion of 1,000 MW capacity (*Independent Power Transmission Operator / IPTO*, n.d.; Tial Kio et al., 2021). It is estimated that with the two interconnections, Crete's total annual CO₂ emissions (CDE) will be reduced by 60 % compared to the current energy system. *Figure 1-1* presents the interconnections of Crete with Attica and Peloponnese.



Figure 1-1 Map of future and current interconnection projects in south Greece. (Source: Independent Power Transmission Operator | IPTO, n.d.)

As it can be seen from *Figure 1-2* the world's current energy relies mainly on fossil fuels. More than 80 % of the total energy production is based on fossil fuels. The lowest contribution is nuclear energy, and renewables produce 6 % of the total energy. These values vary depending on the continent, with more technologically advanced continents such as Europe and North America relying less on coal than Pacific Asia and Africa (Looney, 2021). Oil dependence is present on every continent.

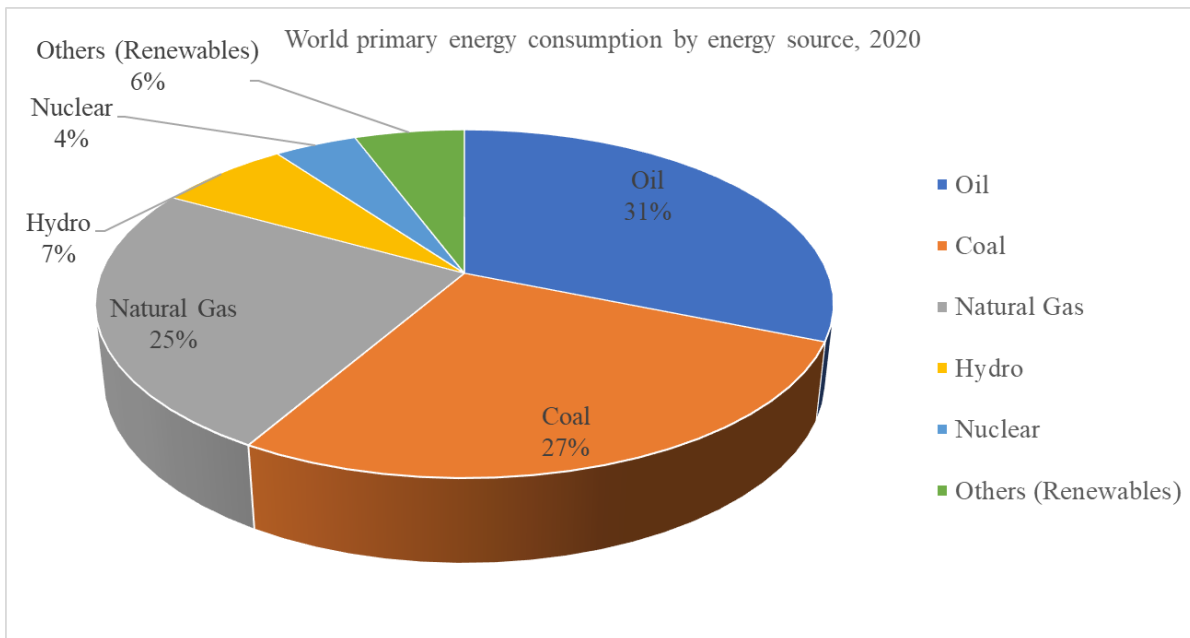


Figure 1-2 World energy mix, 2020. (Source: Looney, 2021)

Figure 1-3 A) depicts a new policy scenario in which existing energy policy is incorporated and proclaimed policy intentions are implemented. Figure 1-3 B) presents a sustainable development scenario based on an integrated strategy to meet international targets for climate change, air quality, and energy access. In the sustainable development scenario, oil usage will be dramatically reduced, and the share of nuclear and RES such as wind, solar PV and hydro is projected to increase in the upcoming years. These projections were made in 2017 by the International Energy Agency.

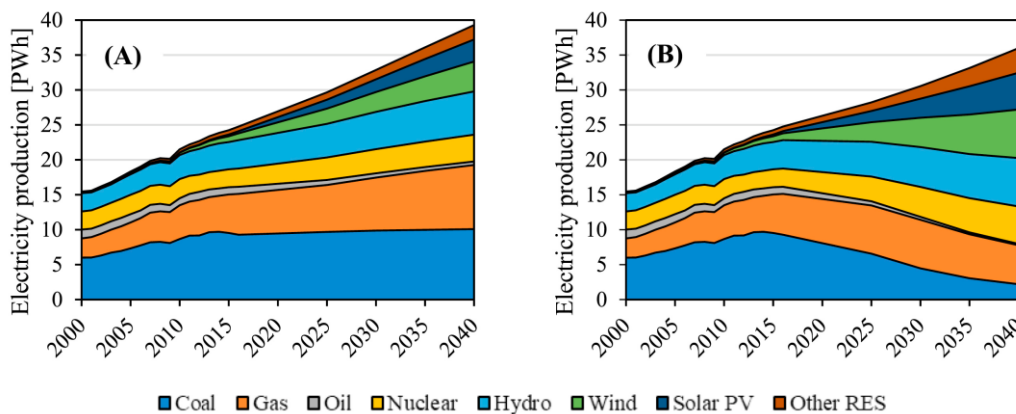


Figure 1-3 World electricity production sources projection for A) new policy scenario B) Sustainable development scenario. (Source: Curto et al., 2019)

1.2 AIM AND OBJECTIVES

This thesis aims to model and optimize an energy system that utilizes locally available resources to meet the needs of one local bakery industry and develop a proper methodological framework to model hybrid energy systems that can utilize biomass resources. Furthermore, this study aims to investigate the operational aspects of the proposed system to determine the best balance between RES penetration, energy cost, and ecological impact. The objectives of the study are to:

- Describe the energy consumption/demand and the current supply system of the industry;
- Assess the available energy resources (RES potential) and the annual waste streams. The main waste streams that were investigated in this study are olive tree pruning (OTP), organic fraction of municipal solid waste (MSW) and tomatoes unfit for the market;
- Design an energy system with multiple scenarios to develop a robust and future-proof energy system;
- Select the most suitable waste-to-energy technologies and model the hybrid renewable energy system (HRES) in HOMER Pro software, and
- Simulate all the developed scenarios and, through a sensitivity analysis, describe the optimal energy system.

Lastly, a vital aim of this study is to promote the economic and environmental sustainability recognized by the Sustainable Development Goals (SDGs). More specifically, SDGs regarding energy generation goals (SDG-7) and the environment (SDG-13) are supported by this study to achieve a sustainable society in the following decades.



Figure 1-4 Sustainable development goals regarding energy and climate change.

1.3 OUTLINE OF THE THESIS

The methodological steps followed for this diploma thesis are presented in *Figure 1-5*. The methodology used is broken down into several stages to achieve the aim of the study. Firstly, an initial literature review helped define the study's aim.

During the initial literature review, it was observed that there is a significant lack of research papers addressing both the thermal and electrical needs of an industrial site. Additionally, it was found that HOMER Pro software has not been used with the intent to use a combination of gasification and anaerobic digestion (AD); thus, this diploma thesis aims to fill the gap in this research area.

The development of the objective followed the initial literature review.

The next step was an extensive literature review on gasification of OTP, AD of tomato and MSW, as well as the energy flexibility of hybrid energy systems. This step required a literature review regarding the biomass and energy conversion technologies used to model the proposed hybrid energy system.

Numerous scientific papers were studied to formulate a proper methodological framework to develop, model and simulate a complex hybrid energy system using HOMER Pro. Data for the energy consumption of the case study and data regarding the RES potential of the area of study were collected and later assessed.

Finally, the results were assessed and interpreted to find the optimal hybrid energy system to meet the industrial sites' electrical and thermal demands.



Figure 1-5 Outline of the thesis procedure.

CHAPTER 2

REVIEW OF RELATED LITERATURE

This chapter's literature review was conducted to investigate all related technologies and is divided into four main subchapters. Subchapter 2.1 presents a comprehensive assessment of the literature on biomass collection and other technologies such as PV, wind turbines (WT), and combined heat and power (CHP) systems. In subchapter 2.2, a detailed presentation of technologies such as AD and gasification for the valorisation of local agricultural waste and biomass residues for bioenergy production is provided. Based on the most recent studies, a comprehensive introduction of the current situation for the coverage of the energy demand of the food industry sector may be found in subchapter 2.3. The food industry's energy flexibility and strategies to increase it are discussed in subchapter 2.4. In Subchapter 2.5, an example of RES utilization for an industrial facility on the island of Crete is presented. Lastly, in Subchapter 2.6, a synopsis of comparable research in the literature is offered.

2.1 UTILIZATION OF LOCAL RENEWABLE ENERGY SOURCES

Biomass is available in one form or another almost everywhere on Earth. According to the scientific community, it is recognized that using biomass for energy production can increase the flexibility of renewable energy systems. Increased energy flexibility can be achieved because bioenergy can be utilized on demand.

Valorisation of biomass can be utilized in numerous ways, for example, biomass to heat and power, biomass to chemicals, and biomass as a transport fuel. This thesis examines the utilization of biomass for heat and power generation.

As an industrialized island with substantial agricultural activity, Crete's high biomass and waste generation capabilities enable the use of alternative RESs with less volatility compared to more conventional approaches (e.g., solar PV, WT). Biomass in Crete is mainly based on extensive olive and olive oil production. Given the abundance of agricultural waste, these materials appear to be viable options for use as AD and gasification fuels.

Several by-products and residues arise from the harvesting and milling process, and in more particular:

- Olive husk
- Trimmed leaves and twigs
- OTP

Furthermore, a variety of additional biomass of similar nature is produced in Crete, including:

- Vineyard pruning
- Grape pomace

- Greenhouse residues

This thesis focuses on utilizing OTP along with greenhouse residues and tomatoes unfit for market exploitation (e.g., misshapen, rotten) for the production of biofuels. A considerable amount of tomato residues produced in greenhouse systems is reportedly discarded because it is unfit for selling. Additionally, the biodegradable fraction of MSW is utilized to produce biofuels. According to research conducted by (Almeida, Rodrigues, Gaspar, et al., 2021; Tial Kio et al., 2021), the estimated yearly residue production for tomatoes is presented in *Table 2-1*.

Table 2-1 Estimated production of tomato wastes from greenhouse systems.

Estimated average tomato residue production ($\text{tons} \cdot \text{ha}^{-1} \cdot \text{year}^{-1}$)	Reference
15	Almeida, Rodrigues, Gaspar, et al., 2021; Pane et al., 2015
10 – 50	Tial Kio et al., 2021

Table 2-2 presents the estimated production of olive pruning-derived waste, according to the literature. OTP is a waste produced from maintenance and reshaping work conducted on olive trees.

Table 2-2 Estimated production of olive pruning derived biomass. Note: (ar: as received, db: dry basis)

Estimated average olive pruning production ($\text{tons} \cdot \text{ha}^{-1} \cdot \text{year}^{-1}$)	Dry or wet	Comments	Reference
1.5	N/A		Contreras et al., 2020
1.31	Dry		Velázquez-Martí et al., 2011
3	Wet	OTP was collected after fruit-harvesting, air-dried at room temperature to 10% moisture content.	Cara et al., 2006; Martínez-Patino et al., 2017
3	Wet	Moisture content was determined after drying.	Mamaní et al., 2021
2.5 – 3.0	Wet	15-20% of the total ar mass is moisture. After solar drying 10% moisture is detected.	Vera et al., 2014
1.5	N/A		Najafi et al., 2021
3.23	Dry		Kougioumtzis et al., 2019

As reported by (Contreras et al., 2020), existing usage possibilities for olive-derived biomass are minimal while also introducing new environmental challenges for their sustainable disposal. Currently, OTP are mainly used for producing pellets (Vera et al., 2014) or for direct combustion (García Martín et al., 2020). Nevertheless, because of their potential to increase energy flexibility, extensive research is being conducted into alternate uses of biomass to take advantage of their

chemical composition and the prospects of producing renewable energy, biofuels, and compounds through these low-cost residues.

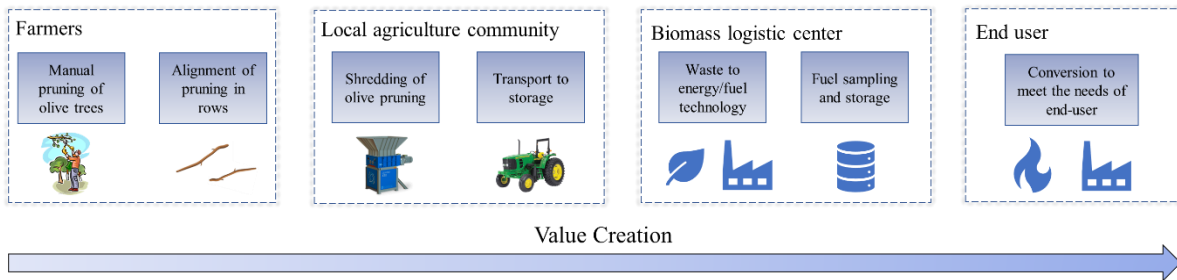


Figure 2-1 Value creation chain of olive pruning. (Adapted from: Kougioumtzis et al., 2019)

Storage is one of the most critical processes in the waste valorisation process, especially when changes in the waste's physicochemical parameters can significantly impact the conversion process' performance. Excess aggregation of moisture and non-combustible (e.g., pebbles, glass) material is critical in ligneous woody biomass. The quality of the resulting biofuel is substantially influenced by pre-treatment (e.g., drying) of the biomass.

MSW, which primarily consists of household, business, commercial, institutional, and industrial waste streams, is another local waste with a substantial organic percentage. MSW has a high biomass content of (~50%) and can thus be used for energy production using waste valorisation methods alone or in combination with other wastes (R. A. Meyers & Kaltschmitt, 2019). Particularly in the literature, some studies have been conducted to investigate the co-digestion of MSW with other substrates (Mata-Alvarez et al., 2014).

In Europe, MSW generation varies greatly. These variations reflect differences in consumption patterns and economic prosperity. Another factor that significantly affects MSW generation is the way MSW is collected and treated. Table 2-3 presents the average European MSW production per capita.

Table 2-3 Average MSW production per capita in Europe in 2020.

Average MSW production per capita ($kg \cdot year^{-1}$)	Reference
505	Waste Statistics - Statistics Explained, 2021

2.1.1 SOLAR PV

Solar energy is the product of the nuclear fusion of hydrogen nuclei to helium and is the most abundant and inexhaustible form of all RES. Currently, the incident solar energy exceeds the total energy demand worldwide (Strezov & Anawar, 2019).

PV technology enables the conversion of solar energy to electricity via a PV cell, utilizing the photovoltaic phenomenon. PV technology is a relatively mature technology and is currently supplying a considerable amount of electricity worldwide. The main reason behind the vast adoption of this technology is zero-carbon emissions (CE) during energy generation. Additionally, they produce no noise when in use while also being able to be deployed in densely populated areas.

They also require little to no maintenance because they do not have moving parts, resulting in a superb lifetime (~20-30 years). Furthermore, solar energy provides energy during peak energy demand. Solar PV can also be used as a standalone system and in grid-connected systems. This technology is also highly modular, thus enabling the deployment of small-scale PV systems (mW) and large-scale systems (MW). Lastly, PV has high compatibility and can be operated with other RES technologies such as WT, thus creating HRESs (Strezov & Anawar, 2019; Τσούτσος & Κανάκης, 2013). For all the above reasons, solar PV is one of the most appealing renewable technologies that will enable the transition towards a green and sustainable future. In *Figure 2-2*, the operating principles of a solar PV cell are illustrated.

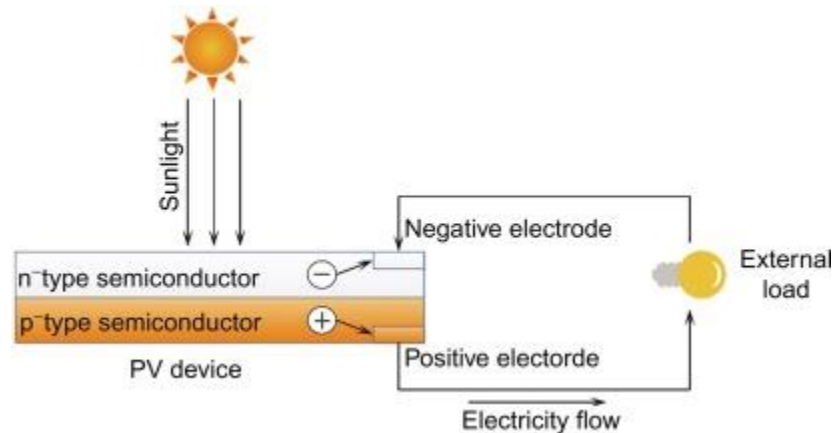


Figure 2-2 Operational principles of solar PV. (Source: Francesco & Umberto, 2019)

2.1.2 WIND TURBINES

The energy derived from wind is exploited to generate power by harnessing the kinetic energy of air by a wide range of machines and technologies with a vast range of economic performances (wind energy conversion devices). Wind, and therefore wind energy, is a product of the uneven heating of the Earth's atmosphere from the sun. The passage of air between the blades of WT exerts a force that causes the blades to spin. This rotational move leads to electricity generation via the rotation of a generator.

Today, nearly all WT manufactured and used are of the horizontal axis type, and most of them have a three-bladed rotor. Due to the continuous advancements in manufacturing and material science, two-bladed WTs are now being used, which reduces the total cost of instalment and development while also prolonging the life expectancy of these machines (Lynn, 2012). The wind turbine tower contains a housing, or nacelle, which contains a gearbox, generator, and anemometer. The rotor governs the generator with a gearbox. The blades' rotation converts the wind's kinetic energy to electrical energy through the components shown in *Figure 2-3*.

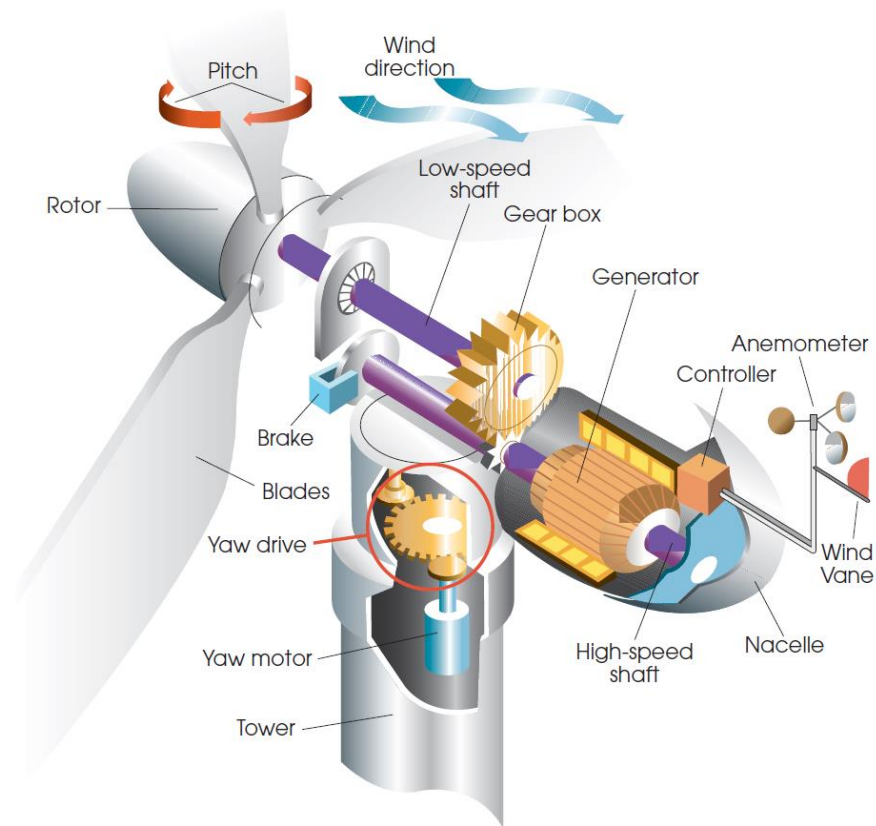


Figure 2-3 Main components of a typical modern wind turbine. (Source: Lynn, 2012)

2.1.3 COMBINED HEAT AND POWER

Combine heat and power (CHP) plants can deliver both electricity and heat simultaneously while also using a common fuel or energy source as an energy source. This characteristic leads to an overall increase in efficiency, reducing CDE. Its main use for industries is meeting the industry's thermal needs because the cost of transportation of surplus electricity is substantially lower than transporting surplus heat. Therefore, CHP plants can be viewed as a heat source, with electricity being a by-product.

Most modern CHP units can reach efficiencies more than 90% according to (Intergovernmental Panel on Climate Change (IPCC), 2007) while also minimizing the losses related to network thanks to the on-site generation characteristics of CHP's.

The 4 main components of every CHP plant are:

- Prime mover (engine);
- Electricity generator;
- Heat recovery system;
- Control system

Every CHP plant can be described based on the characteristics of the four main components and the type of fuel used for energy production. According to (Kerr, 2008), natural gas is the primary fuel used for CHP plants; however, the recent EU Horizon 2020 project ROBINSON aims the develop a renewable fuel-based CHP plant using syngas as the primary fuel, mixed with biomethane and hydrogen (Tial Kio et al., 2021).

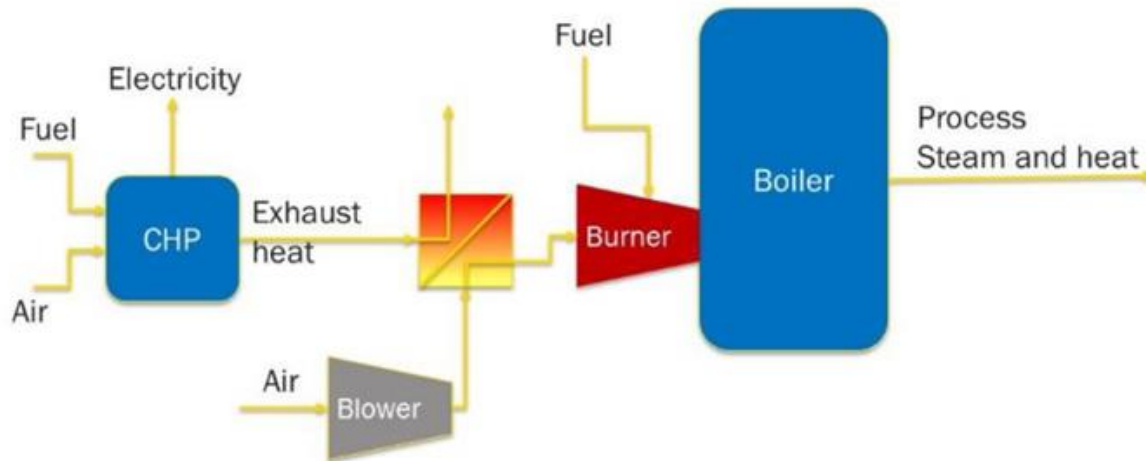


Figure 2-4 A typical configuration of a CHP unit. (Source: Tial Kio et al., 2021)

HRESs consisting of PVs, WT and CHP units are a reliable and tested method of energy generation. Many studies have been conducted on the economic feasibility of these technologies.

2.2 BIOENERGY PRODUCTION THROUGH LOCAL BIOMASS RESIDUES / WASTE MANAGEMENT

Another challenge that modern societies face is the generation of waste (WG), and the organic fractions of waste have the highest production rates on a global scale. If organic waste is not adequately managed, it might lead to potential environmental issues. As previously stated, Mediterranean areas such as Crete have a large agricultural sector that contributes significantly to the economy and waste reduction.

Bioenergy is classified in the category of RES because the energy stored in biomass is solar-derived. Energy is stored in chemical bonds after the natural process of photosynthesis (Mizanur et al., 2021). Bioenergy is generated by biomass combustion, either alone or as a mixture with other fuels (e.g., coal, hydrogen, natural gas).

The constant rise in energy demand and the necessity of increasing the RES penetration into the existing grid make AD and gasification increasingly popular technologies for waste valorisation-based renewable energy generation. Food and industrial wastes and sewage sludges represent an underutilized renewable source for producing heat and power, chemicals, and transport fuels. The proper use of biomass will result in a reduction in the use of fossil fuels. AD and gasification are the two key bioenergy production technologies discussed in greater depth in this diploma thesis.

Although AD has long been acknowledged as a viable waste management solution, the value of using AD technology for energy production has only recently been apparent. This is mainly an aftereffect of the relatively high energy potential of its main product, biogas. The use of AD serves a dual purpose. It provides a sustainable waste management and energy generation approach, which is critical given the need to reduce fossil fuel usage and GHG emissions.

Similarly, gasification is a waste-to-energy process that produces green biofuels, aiding in the green energy transition. This method is especially appealing in places where substantial amounts of ligneous biomass may be harvested. Crete, the research location, has a lot of agricultural activity, notably in the field of olive production, and therefore it is a viable solution for utilizing olive-derived biomass.

Figure 2-5 a) demonstrates the reference/current tomato collection process, where most of the waste is discarded, and a small portion of it is composted. *Figure 2-5 b)* presents the proposed tomato collection process. In the proposed system, the continuous greenhouse waste from tomatoes is utilized from an AD plant. This plant can also take advantage of other organic waste such as MSW and manure. Anaerobic digestion's main product is biogas which can be utilized from a CHP unit to provide heat and electricity to the end-user. Additionally, lesser amounts of CO₂ and solid/liquid digestate are produced from AD that can be utilized from the greenhouse plant, thus creating a circular economy model.

The existing energy valorisation technologies for olive-derived wastes are shown in *Figure 2-6*. The drying step can be considered the first step in the OTP process. Because of the small size of OTP waste, no pelletization or grinding is required. It is also clear that the gasification of OTP is still in its preliminary stages of development, but current research indicates it is a potential future technology.

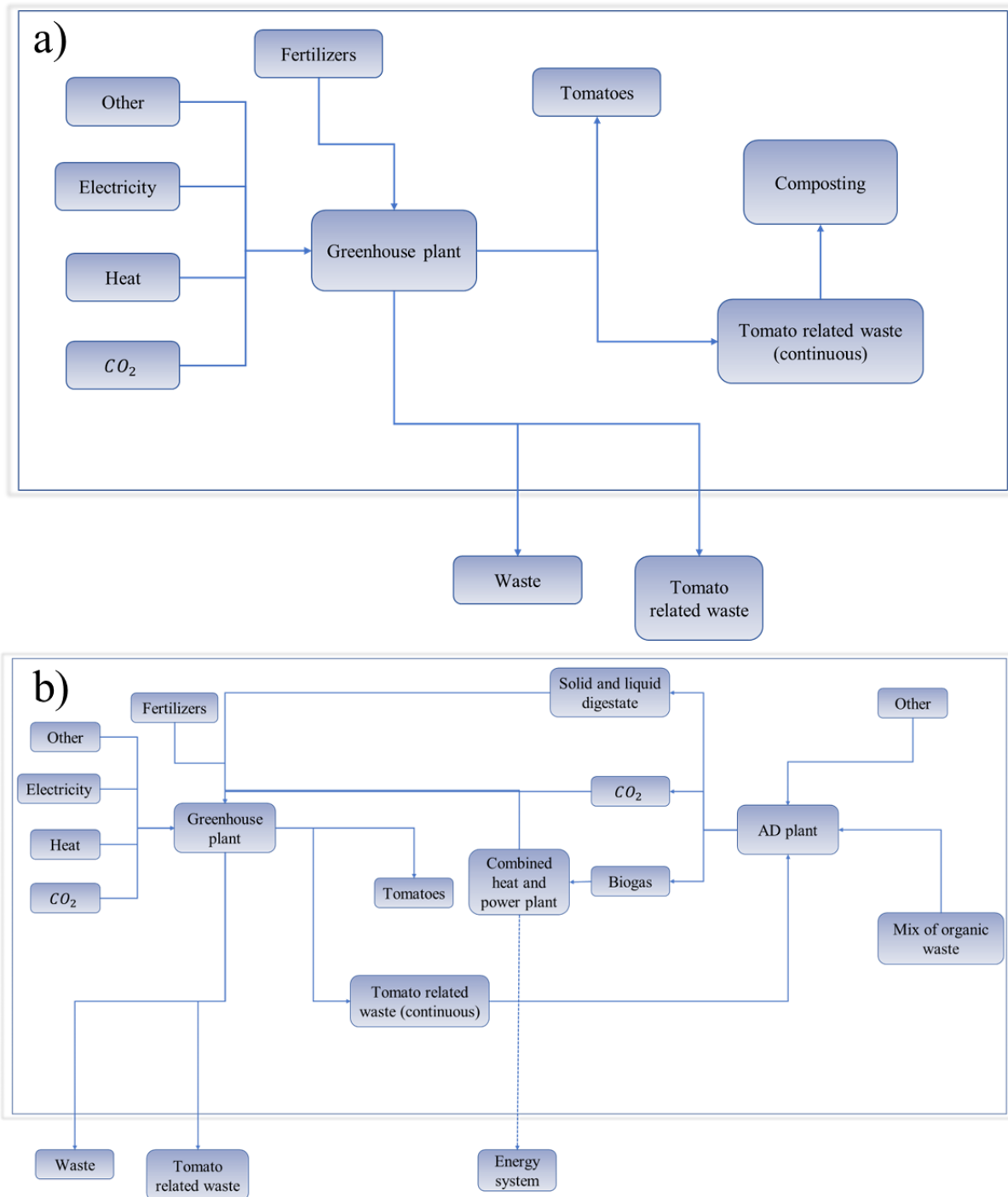


Figure 2-5 a) Reference greenhouse plant system and b) greenhouse plant system with AD. (Source: Danevad & Carlos-Pinedo, 2021)

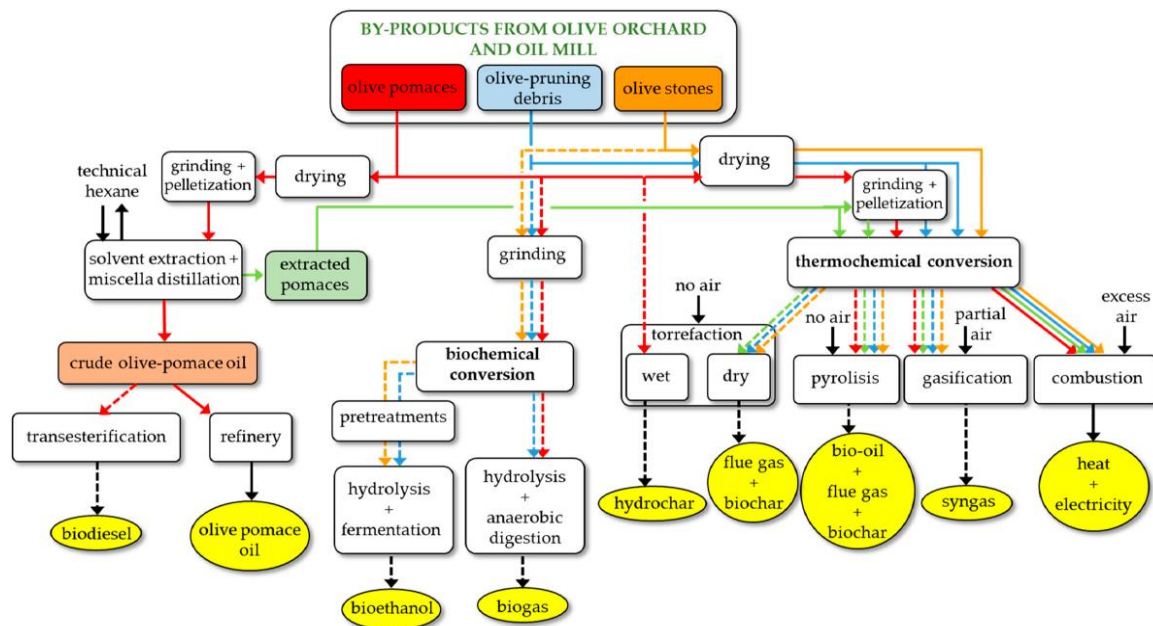


Figure 2-6 Energy valorisation of olive derived waste (Solids lines represent industry processes whereas dashed lines symbolize applications at research stage). (Source: García Martín et al., 2020)

2.2.1 ANAEROBIC DIGESTION

The breakdown of organic materials by a wide range of microorganisms in the absence of oxygen is known as AD. In nature, similar processes can be found. Initially created for waste management, AD has been effectively applied to treating organic waste substrates such as food waste, animal manure, wastewater, sludge, and MSW. As previously stated, recent research has focused on optimizing energy production through AD, which generates enormous quantities of biogas. Another by-product of this procedure is organic nitrogen-rich residue, which can be used for agricultural purposes. The fuel generated from AD is primarily composed of 40-70 (% vol) of methane (CH_4) as well as carbon dioxide (CO_2), traces of ammonia (NH_3), hydrogen (H_2), and hydrogen sulfide (H_2S). Because of the high concentration of methane gas in the end products of AD, it is a viable technology for energy generation, as it may be burned directly or converted to heat and power via CHP reactors. AD is considered an environmentally friendly process for energy production because extensive amounts of methane gases are prevented from being released into the atmosphere, further contributing to the greenhouse effect, considering CH_4 is one of the primary GHGs. Additionally, by burning biomethane, only carbon-neutral CO_2 is released into the atmosphere. Integration of this technology can enhance concepts such as industrial symbiosis, where industrial waste can be used as feedstock in the anaerobic digesters.

Anaerobic digesters are categorized based on their design and operational principles. The mode of operation (continuous or batch), solids content (solid-state or liquid), and temperature (thermophilic, mesophilic, and psychrophilic) are all parameters that define the category of the reactor. A variety of microorganisms also drive the AD process. They are classified according to their metabolic routes, which include hydrolytic, fermentative, acetogenic, and methanogenic

(Pellera, 2017). A graphical illustration of AD's influent and output flows are presented in *Figure 2-7*.

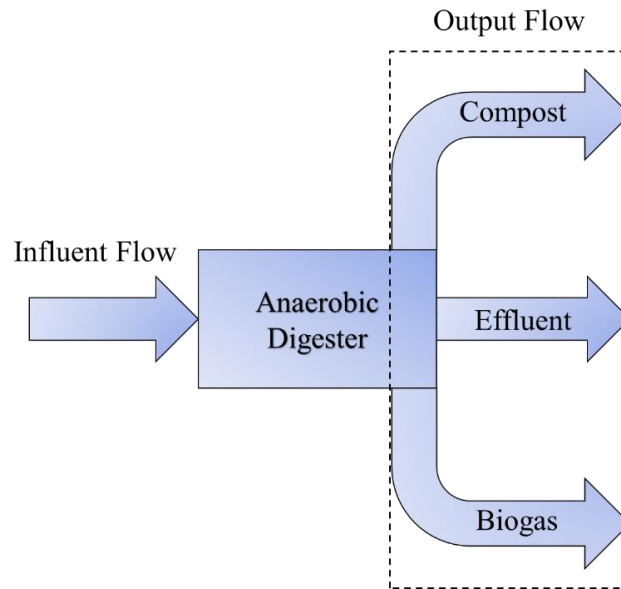
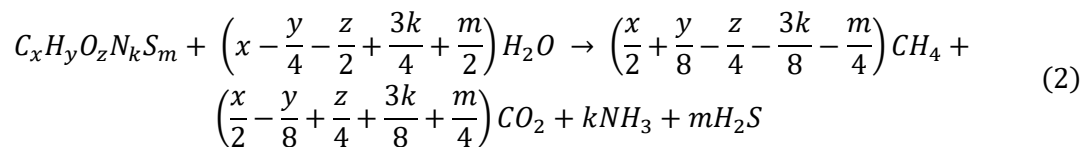
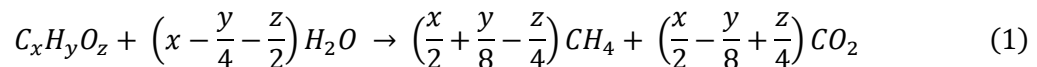


Figure 2-7 AD's input and output flows. (Source: Meegoda et al., 2018)

The organic fractions of the substrate, fresh matter (FM), and especially total solids (TS), volatile solids (VS), chemical oxygen demand (COD), biochemical oxygen demand (BOD), and carbon-nitrogen (C/N) ratio are significant, and the most used in the literature, characteristics of organic substrates for the production of methane from AD reactors. TS are defined as the mass of the dried FM after water and other volatile substances (i.e., alcohols) subtraction from the drying process. VS parameter is based on the mass of TS. Specifically, VS is determined by subtracting the inert solid fraction from TS. BOD is a metric of the biodegradable organic matter in sludge. It is, therefore, a measure of the amount of oxygen needed to sustain anaerobic microorganisms for a predefined amount of time (5 days). Correspondingly, COD is a metric of the amount of oxygen stored in sludge that oxidizing agents can utilize.

The maximum theoretical biogas potential (methane yield) under the assumption that all available substrate is converted to CO_2 or CH_4 is shown in *Equation 1*. This equation is valid based on the condition that the organic materials present in the AD process are entirely degradable. The theoretical methane yield, including sulfur and nitrogen present in the organic matter, is presented in *Equation 2* (Meegoda et al., 2018; R. A. Meyers & Kaltschmitt, 2019a).



However, experimental methane yields, particularly in continuous batch reactors, are difficult to calculate, and experiments and further research is needed to collect data on the process. In this

diploma thesis, agricultural and MSW are utilized for methane production. More notably, tomato waste from greenhouse crops is considered the main agricultural waste. Following research conducted by (Almeida, Rodrigues, Gaspar, et al., 2021; Almeida, Rodrigues, Teixeira, et al., 2021; Jagadabhi et al., 2011), the chemical characteristics of tomatoes and methane yield ($NmL_{CH_4}g^{-1} VS_{added}$) of AD are provided in *Table 2-4*.

Table 2-4 Methane potential from AD and chemical characteristics of rotten tomato (RT), green tomato (GT), tomato branches (TB), and fresh tomato leaves and stems (TLSF).

Residue type	PH	Moisture (%)	TS (%)	VS (%TS)	COD ($mg O_2 g^{-1} VS$)	Cellulose (%TS)	Lignin (%TS)	Hemicellulose (%TS)	Methane yield	Reference
RT	4.75	94.00	5.99	86.0	1517	15.45	7.87	16.33	294	Almeida, Rodrigues, Gaspar, et al., 2021; Almeida, Rodrigues, Teixeira, et al., 2021
GT	4.00	92.24	7.76	88.0	1223	23.15	4.11	31.02	304	Almeida, Rodrigues, Gaspar, et al., 2021; Almeida, Rodrigues, Teixeira, et al., 2021
TB	6.82	28.65	71.4	80.0	1592	23.99	20.27	17.57	140	Almeida, Rodrigues, Gaspar, et al., 2021; Almeida, Rodrigues, Teixeira, et al., 2021
TLSF	5.10	N/A	10.0	7.6 ¹	N/A	12.5	1.4	7.9	320	Jagadabhi et al., 2011

The theoretical methane yield for AD of the organic fraction of MSW is equal to $570 NmL_{CH_4}g^{-1} VS_{added}$ (Mlaik et al., 2022). However, actual experimental data show that methane yield greatly depends on the organic loading rate. Also, according to (Mu et al., 2018), AD of MSW is an economical way of treating the organic fraction of MSW. It is also clear that co-digestion with food waste is an efficient method for increasing the total energy potential of AD.

Table 2-5 presents the chemical characteristics of MSW and methane yields from the AD of the organic fraction of MSW according to the literature.

Table 2-5 Methane potential from AD and chemical characteristics of the organic fraction of MSW.

Study ID	PH	Moisture (%)	TS (% WW)	VS (% TS)	Ash (% TS)	Range of methane yield ($NmL_{CH_4}g^{-1} VS_{added}$)	Reference
1	4.7	73.02	26.97	93.90	N/A	260 – 290	Mlaik et al., 2022
2	6.93	N/A	34.82	46.9	53.10	334 – 430	Mu et al., 2018
3	N/A	N/A	23.4 – 33.1	83.4 – 93.3	6.7 – 16.6	N/A	Hansen et al., 2007

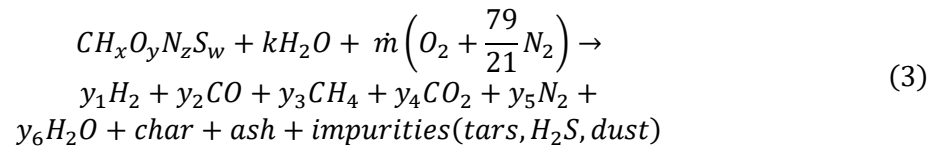
¹ 7.6% of the total tomatoes mass.

Based on *Table 2-5* it can be observed that the chemical composition of MSW varies greatly, and it depends on the area of the study.

2.2.2 GASIFICATION

Agricultural waste generates substantial amounts of waste that can be considered biomass. For example, the olive oil industry generates enormous amounts of pruning waste. Olive pruning accounts for more than 60% of the total WG of the olive oil industry, according to (Martín-Lara et al., 2017; Sánchez & San Miguel, 2016). OTP is a lignocellulosic material mainly composed of lignin, cellulose, and hemicellulose. Gasification is one of the leading technologies that allow the clean and renewable energy utilization of OTP through waste valorisation. A more widely used method is the direct combustion of OTP. However, drawbacks such as low energy density, low energy efficiency and substantial amounts of GHG emissions limit the potential of this technology. The higher thermal conversion efficiency, while also being a mature technology, thanks to its extensive use in the gas industry, makes gasification a promising technology. However, more research is needed to develop cost-effective solutions compared to traditional technologies such as direct burning (Arregi et al., 2018).

Gasification is a partial oxidation process of biomass performed at high temperatures (>700 °C). The main parameters of this process are the amount of oxygen or steam used. Gasification is not a combustion process; therefore, the main product of this process is syngas (H₂ and CO). It also produces condensable organic compounds as a by-product (García Martín et al., 2020; Iáñez-Rodríguez et al., 2019). The process of gasification for a hydrocarbon with the chemical formula CH_xO_yN_zS_w using air as an oxidizing agent is shown in *Equation 3* (Fryda, 2006; Skoulou, 2009; Vera et al., 2014).



The chemical formula of the hydrocarbon is based on elemental analysis. The second and third elements of *Equation 3* represent the biomass moisture content and air introduced in the gasification process, respectively. Based on the values y₁-y₆, the composition of the produced gas is determined; therefore, the fuel properties can be derived.

The formation of tars is the main gasification problem that affects the process's thermal efficiency (Trabold & Badditt, 2018). It also generates an environmental concern thanks to tar's toxic and carcinogenic nature. Operational concerns like stream blockages and syngas degradation are also problems caused by tar formation, and several studies have been performed to minimize tar production (Iáñez-Rodríguez et al., 2019). However, most of the proposed methods in these research studies resulted in increased operation-related costs and decreased overall process efficiency.

The products and uses of thermochemical conversion processes are summarized in *Figure 2-8*.

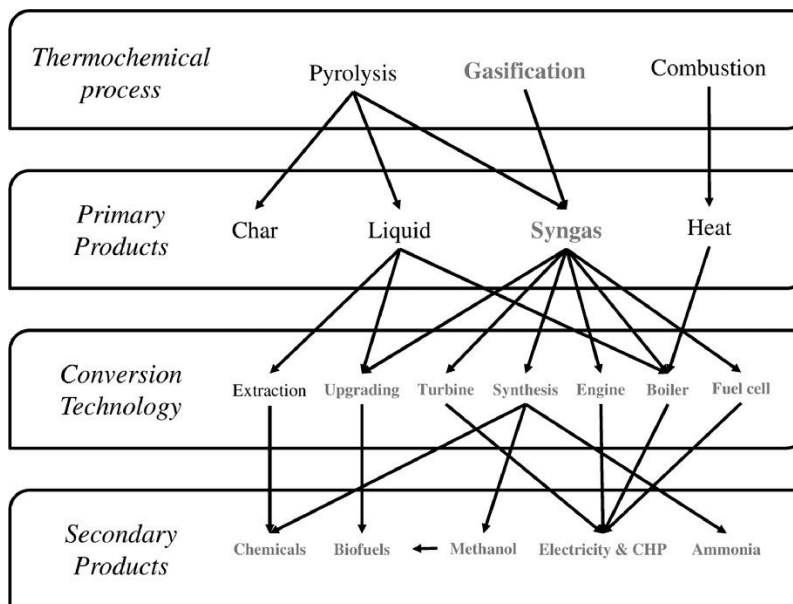


Figure 2-8 Summary of the uses and products of thermochemical biomass conversion technologies. (Source: Molino et al., 2016)

Information about the elemental analysis of OTP is scarce in the literature. According to Table 2-6, there are little to no Sulphur traces on OTP wastes.

Table 2-6 Chemical characteristics of OTP. Note: (N/G: Not Given)

Cellulose (%DW)	Lignin (%DW)	Hemi-cellulose (%DW)	Ash (%)	Volatile Matter (%)	Fixed Carbon (%)	Moisture (%)	Elemental Analysis					Reference
							N (%)	C (%)	H (%)	S (%)	O (%)	
21.6	17.7	14.5	3.9	N/G	N/G	N/G	N/G	N/G	N/G	N/G	N/G	Contreras et al., 2020
31.88	9.26	17.26	3.29	77.5	11.57	7.64	0.24	48.52	6.92	2.09	42.39	Mamaní et al., 2021
N/G	N/G	N/G	4.75	N/G	N/G	7.1	0.7	49.9	6.0	N/G	43.4	Skoulou, 2009
36.6	20.8	19.7	N/G	N/G	N/G	N/G	0.8	44.6	6.7	0.0	47.9	García Martín et al., 2020
N/G	N/G	N/G	3.50	78.46	17.13	10.00	0.55	47.10	6.18	0.10	42.57	Vera et al., 2014

Waste-to-energy technologies that produce biofuels have been under the microscope for the last decades. A considerable number of studies have been published that investigate the operational aspects of these technologies. However, there is a gap in scientific papers regarding the integration of these technologies in an industrial setting. This study aims to fill this gap by studying the economic feasibility of HRESs that take advantage of waste-to-energy technologies such as gasification and/or AD.

2.3 MEETING THE ENERGY DEMAND OF FOOD INDUSTRIES

Every manufacturing system requires energy to transform an input into output. Energy demand is determined by the current stage and task of the input transformation's manufacturing process. The main energy carriers needed from manufacturing systems are electricity, heat, compressed air heating, and cooling (Beier, 2017). However, a typical production system contains many separate sub-processes for the final translation of input to output, as shown in *Figure 2-9*; a quantitative energy intensity analysis of all processes is required.

A constant base load demand is observable in every energy audit at a factory level. This is caused because every factory has a constant energy demand regardless of the production rate (e.g., security, lighting, HVAC). Additionally, a constant base-load demand is evident for every production process and originates from turned-on controls (e.g., heating, or cooling pumps, lubrication systems). Likewise, energy demand is a function of the performance levels (i.e., production rate). Hence, total electricity demand can be divided into two main categories: base-load demand and production power. Production power can be affected to a limited extent by varying the production rate of a product.

On a manufacturing system level, the sum of the energy demand of individual components/machines represents the total amount of energy demand. Random disturbances result in a highly dynamic and stochastic energy demand profile, especially on the system level of technical building services and HVAC, where energy demand is dependent on climatic influences with a stochastic nature.

According to (Beier, 2017), on a factory level, the energy demand is primarily based on production activities. The factory's typical energy demand profile can be influenced by changes in the production activities during weekdays and weekends, changes in shift schedule, temperature, and break times.

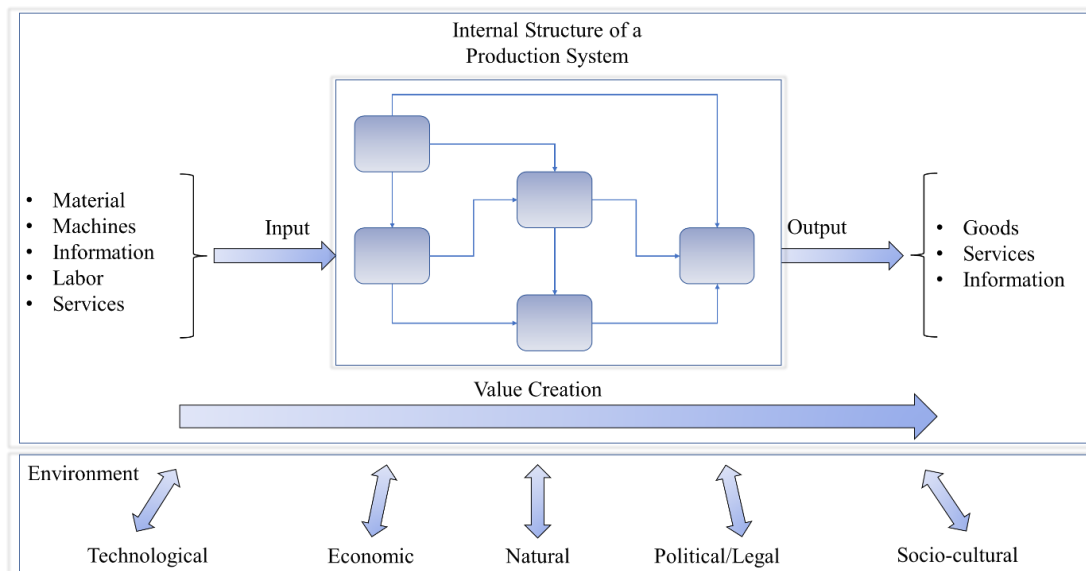


Figure 2-9 A typical production system and its interaction with the environment. (Source: Beier, 2017)

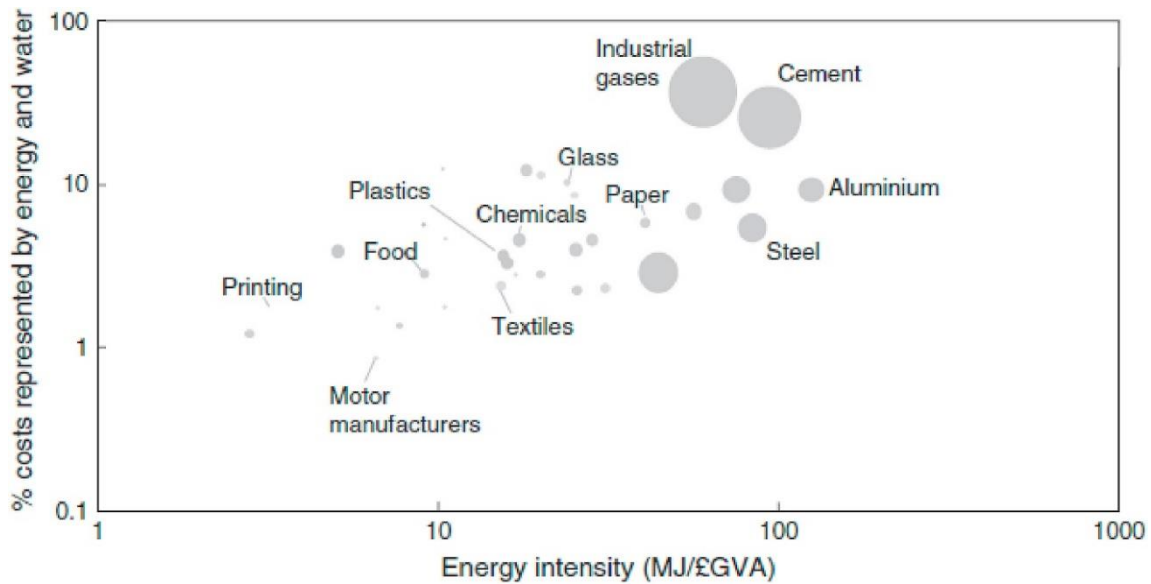


Figure 2-10 Percentage of total cost related to energy and water consumption across different industrial sectors in the UK. Note: GVA (Gross Value Added). (Source: Griffin et al., 2016)

As Figure 2-10 indicates, in the case of the UK, the industrial sector of the food industry stands as a process with moderate energy intensity while also having relatively high energy costs. Additionally, the food industry, according to (Griffin et al., 2016), has higher energy costs, as a percentage of the total costs, compared to motor manufacturers, printing, and textiles. The higher energy costs result from the relatively excessive cost of preparing, packaging, and transporting food products.

In the case of bakery products, the main energy-intensive processes the industry depends upon are heat processing processes, namely baking (i.e., the use of ovens to make the food edible) as well as processes in the category of concentration by heat, for example, drying (i.e., applying heat to remove water). Furthermore, post-processing operations require copious amounts of energy, such as packaging, where bakery products are placed into plastic, paper or cardboard packages in an artificially produced atmosphere or vacuum (Sovacool et al., 2021). An approach that focuses on the thermal and electrical energy required for producing one metric ton of product in several food industry sectors is presented in Table 2-7.

Table 2-7 Thermal and electrical energy demand to produce of one metric ton of several food products across six European countries (Austria, France, Germany, Spain, Poland, and the UK).

Type of industry	Thermal Energy (kWh/t)			Electrical Energy (kWh/t)			Reference
	Lowest Thermal Energy	Mean Thermal Energy	Highest Thermal Energy	Lowest Electrical Energy	Mean Electrical Energy	Highest Electrical Energy	
Bakery	243	1335	3039	150	590	1834	S. Meyers et al., 2016
Meat Processing	20	612	1668	85	366	957	
Meat	20	510	1668	77	354	957	
Dairy	129	1055	3957	21	625	3636	
Sugar	1398	1759	3076	185	282	560	
Fruits and Vegetables	124	459	1235	85	253	1235	

Another approach used in literature to calculate and examine energy consumption profiles across different food-related industrial sectors is presented in *Figure 2-11*, where the most energy-intensive subsectors are meat and poultry as well as bakery industries. Additionally, in *Figure 2-12*, the estimated carbon equivalent emissions associated with food production in the US are presented.

Studies focused on the baking and bread manufacturing sector showed an average value of specific energy consumption (SEC) of 5.21 MJ/kg in the UK (Ladha-Sabur et al., 2019). Bakery products, particularly rusk products, are consumed regularly in the Mediterranean diet. Baking is considered the most energy-demanding process regarding bakery products (Ladha-Sabur et al., 2019), a direct effect of the low values of heat transfer through the air via convection. In most cases of bakery goods, more than 65% of the total energy consumption is allocated to baking.

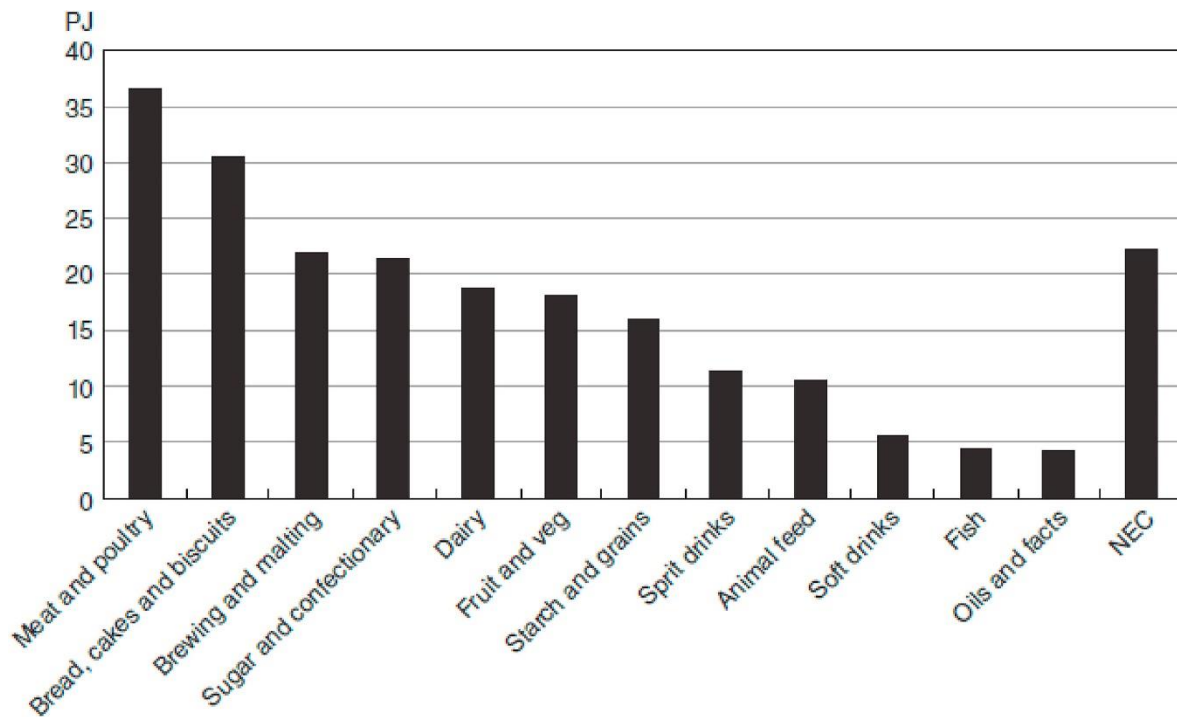


Figure 2-11 Main energy demand for food and drink industrial sectors in the UK. (Source: Griffin et al., 2016)

According to the International Renewable Energy Agency, the food and tobacco industry have great potential for integrating RES for electricity and heat demand coverage. The only industrial sectors that exceed the potential of the food and tobacco industry are the pulp and paper industry sector. According to projections published by (Renewable Energy Agency, 2015), RES can cover 60 % of existing heat demand for processes that require low to medium temperatures. Following *Table 2-8*, the RES with the highest potential for integrating RES is biomass, followed by solar thermal, heat pump, geothermal, and solar cooling. The food industry sector, and more importantly, bakery industries, can further benefit from the integration of heat pumps because they can increase the efficiency of conventional air dryers. Heat pumps can also reduce air humidity (Wang, 2014).

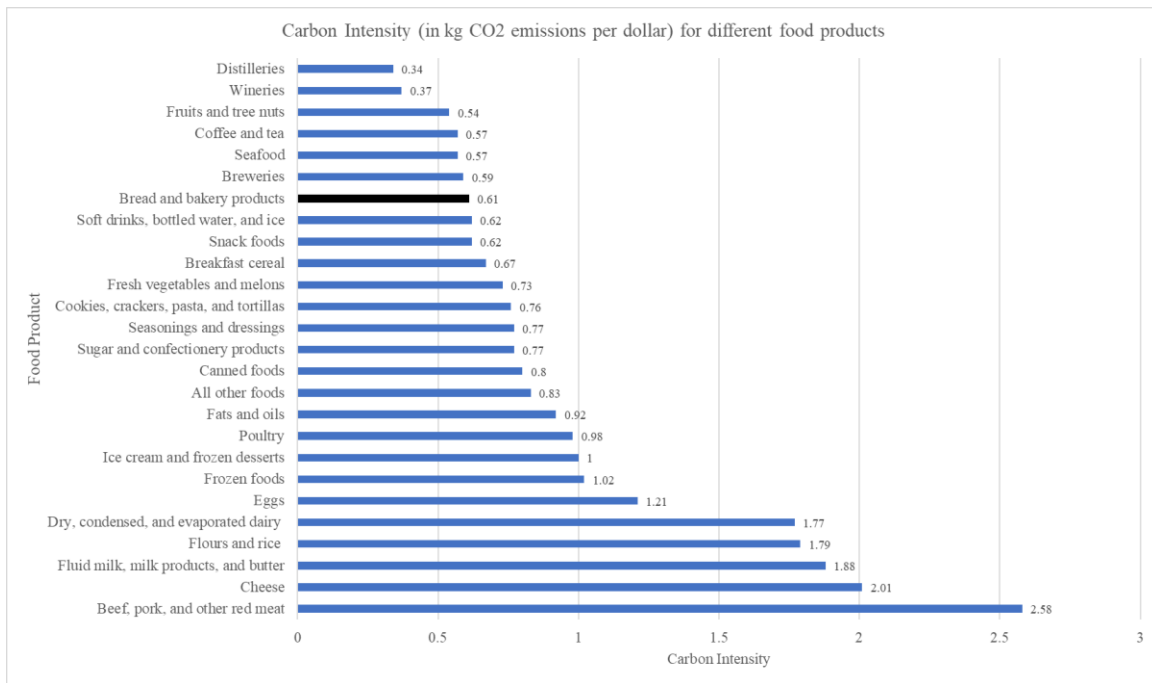


Figure 2-12 Estimated carbon intensity for several food products for the US. (Source: Boehm et al., 2018)

Further utilization of biomass resources for the substitution of conventional fuels (e.g., coal, natural gas) will help reduce GHG emissions as well as help promote electrification of the industrial processes needed for food manufacturing by switching from fuel-burning boilers to electric heating equipment with higher conversion efficiencies (Department of Energy and Climate Change and the Department for Business, 2015).

Table 2-8 Technical potential for installed RES for the food and tobacco industry sector by 2030 (an ambitious scenario). Note: units in EJ/yr.

Type of RES	Low temperature	Medium temperature	High temperature	Total	Reference
Biomass	2.8	1.9	NA	4.8	Renewable Energy Agency, 2015
Solar Thermal	0.9	0.6	NA	1.4	
Solar Cooling	0.1	NA	NA	0.1	
Geothermal	0.2	NA	NA	0.2	
Heat pump	0.4	NA	NA	0.4	

One study (S. Meyers et al., 2016) at a national level examined the effects of implementing cost-effective energy generation methods in the food and beverage industry across six European countries (Austria, France, Germany, Spain, Poland, and the UK). Having installed these energy-saving technologies, it was discovered that there were significant energy and carbon savings, as well as short payback times.

Table 2-9 Estimation of energy savings, CDE mitigation, and payback periods for the food and beverage industry across six European countries (Austria, France, Germany, Spain, Poland, and the UK).

<i>Energy generation method</i>	Estimated energy savings (in MWh) identified	(tCO₂e) mitigation	Short payback time (years)	Long payback time (years)	Reference
<i>Biomass</i>	1415	370	6.6	26.8	S. Meyers et al., 2016
<i>Solar heat</i>	3720	970	14.9	45.9	
<i>Solar PV</i>	50	15	13.7	NA	
<i>CHP</i>	64,900	15,415	1.1	3.6	
<i>Heat pump</i>	70	20	7.8	NA	

Furthermore, based on a recent study by (K. R. Kumar et al., 2021), the industrial sector of the tea industry in India can benefit from RES integration. Expressly, 83% of the total thermal energy demand can be provided from bioenergy via waste valorisation technologies. This study found that evacuated tube solar collectors can supply the energy requirements for the drying processes. Additionally, a hybrid system combining solar, and biomass could be used for the drying and withering process. Solar PV, WT, and micro-hydro power systems could also be used to meet electricity needs. The technologies were selected based on the availability of the renewable resources' potential.

Lastly, according to the literature, a small number of published scientific articles regarding the integration of HRESs in the food and beverages industrial sector can be found. Moreover, there is a significant gap, especially in techno-economic analyses of waste-to-energy technology integration in the food and beverage industries. This study aims to fill this gap by investigating the economic aspects of HRES integration in the bakery industry. An in-depth analysis of the sociotechnical systems and policy options for the decarbonization of the food and beverage industry is presented by (Sovacool et al., 2021).

2.4 ENERGY FLEXIBILITY IN FOOD INDUSTRIES

The decentralization of the electrical grid and the integration of RES offers new opportunities for a flexible energy production system. Increased energy efficiency in energy-intensive activities alone will not suffice to minimize anthropogenic GHG emissions and address climate change mitigation. As a result, RES must deliver power to the industry to further minimize GHG emissions. An electrical grid consisting of only fossil fuel-based production units can be considered a dispatchable resource (Beier, 2017). Due to the unpredictable nature of VRE generation, which results from non-controllable elements (i.e., weather conditions), large-scale integration of RES into the current electrical grid renders the grid a non-dispatchable resource. Therefore, energy flexibility measures must be employed to cope with the extensive VRE sources' energy supply problem. For example, wind and solar energy generation are very volatile. They may fluctuate substantially within seconds to minutes due to various factors (e.g., ambient temperature, wind speed, cloud coverage, and solar irradiation).

Furthermore, the electrical system's demand side (e.g., industry, households) is volatile. However, recurring patterns are observed. Because there is no direct connection between VRE generation and

demand, the remaining energy supply mix must be flexible to compensate for VRE's lack of energy flexibility. According to (Eamonn Lannoye et al., 2012), flexibility is defined as “*the ability to schedule and leverage resources to satisfy the net system load, while assuming that the other part of the load is served by VRE*”.

A comparison between RES and fossil-fuel-based energy production is shown in *Table 2-10*. Volatility, storability, and dispatchability metrics are among the metrics presented. Wind and solar are considered unfavorable due to their involatile nature and lack of dispatchability. It is also clear that large-scale biomass energy generation may compensate for the disadvantages of wind and solar energy.

Table 2-10 Comparison between RES and fossil fuel energy generation. (Source: Beier, 2017)

<i>Energy Source</i>	Volatility	Storability	Dispatchability
<i>Solar</i>	–	–	– –
<i>Biomass</i>	+	+ +	+
<i>Wind</i>	– –	– –	– –
<i>Fossil Fuel</i>	+ +	+ +	+ +

Demand side management (DSM) and energy storage are critical assets for increasing RES penetration (Beier, 2017; Bird et al., 2013). Several energy storage technologies have been developed (Després et al., 2017): compressed air, pumped hydro, hydrogen production, batteries (BAT), supercapacitors, and flywheels. However, according to (Tang et al., 2021), energy storage is the least cost-efficient alternative for increasing energy flexibility. Lastly, the most inefficient mean of increasing energy flexibility is RES curtailment.

Embodied energy storage is another excellent technique to increase energy flexibility through energy storage. Due to the nature of food industries where the products require a certain amount of energy (e.g., heating, cooling), energy during low-cost hours can be allocated as embodied energy, benefiting from the fluctuating energy prices, and lowering the production costs associated with energy consumption. Daryanian et al. first suggested the concept of embodied energy storage in 1989. Furthermore, Lorenz et al. proposed in 2012 that industries may be utilized to store energy from variable sources like wind and solar. This concept epitomizes “*energy efficiency 2.0.*” As a result, instead of being passive consumers, industries will become active participants in the energy sector. It is critical to examine the restrictions and constraints of the production system, such as available material flow, adjusting the production sequence, and satisfying the required demand. This shows a strong link between the industrial facility's ability to alter its energy demand and the amount of energy demand covered by VREs.

DSM is a consumer-side energy flexibility measure. The consumer in DSM aims to change and adjust their energy consumption behaviours in response to available energy sources and pricing (price-based demand response). (Beier, 2017) proposes several load shape measures for increased energy flexibility, which are depicted in *Figure 2-14*. These measures include (Pierri et al., 2020):

- Peak clipping, decrease of peak demand;
- Valley shifting, increase of off-peak energy demand;
- Load shifting, reprogramming of the electrical demand schedule;
- Energy efficiency, decrease of total energy demand.

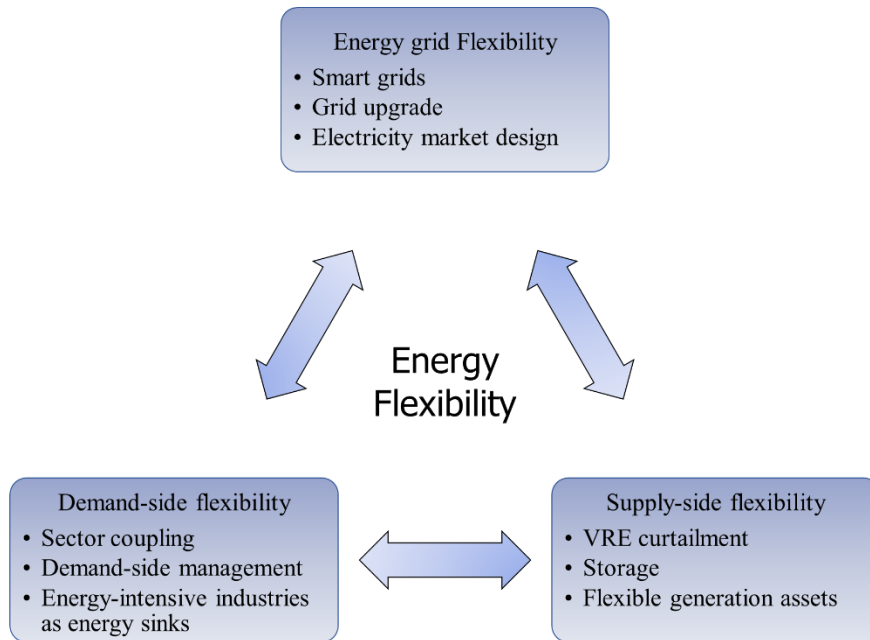


Figure 2-13 Energy flexibility strategies. (Source: Beier, 2017; Pierri et al., 2021)

DSM for increased energy flexibility has increased thanks to considerable developments in areas such as control and communication technology in smart grids. These advances enable better grid economics and increased reliability to the consumer. These benefits can be achieved by choosing the optimal energy modes with the lowest marginal costs.

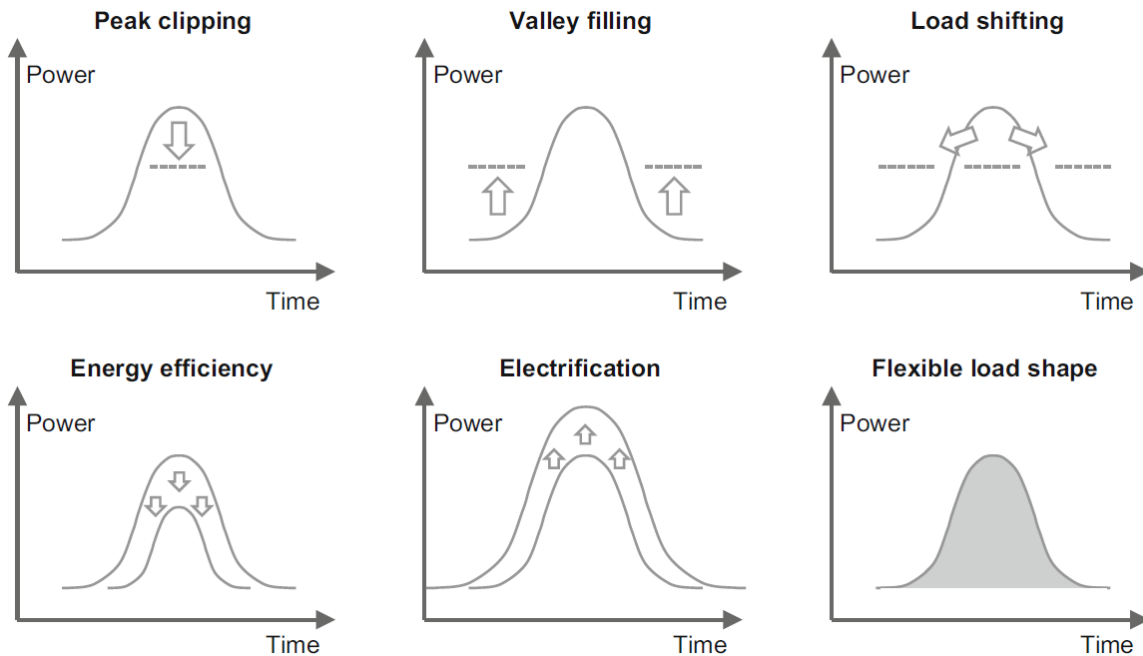


Figure 2-14 Load shaping strategies in DSM. (Source: Beier, 2017)

Food manufacturing industries are considered process industries, with production systems that can be continuous or batch. A continuous flow production system is defined as a continuous flow of input or output. The beginning and end of the production are difficult to identify; thus, it is left unspecified in continuous processes. In batch production systems, however, the start and finish are pre-defined, and the production consists of several batches. The discrete manufacturing mode consists of multiple single-phase manufacturing processes. As stated by (Pierri et al., 2020), extensive research has been undertaken to enhance energy flexibility in discrete manufacturing; however, in continuous manufacturing, integrating energy flexibility measures can be challenging, and further research is required. The lack of research in continuous processes stems from the inability to immediately reallocate or interrupt manufacturing stages to deploy demand-side management methods. Differences between process and discrete manufacturing systems are presented in *Table 2-11*.

Table 2-11 Differences between process and discrete manufacturing systems. (Source: Pierri et al., 2020)

<i>Characteristics</i>	Process Industry	Discrete Manufacturing
<i>Energy Intensity</i>	High	Low
<i>Process Mode</i>	Continuous/Batch	Discrete
<i>Processes Interdependencies</i>	Strong	Relatively low
<i>Processes Decoupling</i>	Not always feasible	Feasible

The results of an assessment of potential energy flexibility measures to enhance DSM on a process industry production plant (Beier, 2017; Pierri et al., 2020) are presented in *Table 2-12*. In total four system levels have been investigated.

Table 2-12 Assessment of potential energy flexibility methods in process industry. (Source: Pierri et al., 2020)

<i>System Level</i>	Strategy	Load Shaping Category	Feasibility Level
<i>Factory</i>	Affecting customer demand	Flexible load shape	Medium
	Energy monitoring and management	Energy efficiency and Flexible load shape	High
	Rescheduling of production	Load shifting	Medium
<i>Technical Building Services</i>	Sensor installation for energy consumption	Energy efficiency	High
	Waste heat recovery	Energy efficiency and Valley filling	High
	Energy storage system	Peak clipping and Valley filling	High
	On-site RES generation	Load shifting and Peak clipping	High
<i>Production Unit</i>	Adjustment of machine configuration	Load shifting	Low
	Process interruption	Peak clipping	Low
	Modifying the process sequence	Peak clipping	Low
	Waste heat recovery	Energy efficiency	High
<i>Machine</i>	Shutting down machines	Peak clipping	Medium
	Integration of new energy sources	Peak clipping and Energy efficiency	High

Many studies have been conducted on industrial systems' energy flexibility. This study aims to investigate the effects of integrating different strategies for increasing energy flexibility, videlicet integration of new energy sources and waste heat recovery strategies in this diploma thesis.

2.5 EXISTING RES UTILIZATION EXAMPLES FROM INDUSTRIES

Industries located on the island of Crete that utilize RES to meet their energy needs exist. One notable example is PLASTIKA KRITIS. It is an industry-leading producer of masterbatches and agricultural films. PLASTIKA KRITIS serves the industrial sector of plastics, horticultural, agricultural, as well as leading projects related to water management & environment protection. Since 2003 it has been utilizing energy produced from RES. More specifically wind farm with an 11.9 MW capacity is in Crete that produces more than 40.000 MWh annually. Moreover, five additional PV stations with a total capacity of 2.34 MW were built to meet the industry's energy needs. Currently, almost 99% of the total consumed energy of the company facilities is produced from RES according to (*COMPANY PROFILE - Plastikakritis.Com, n.d.*).

In *Figure 2-15*, the main industrial facilities of the company and part of the wind farm located in Crete are presented, respectively.



Figure 2-15 Main industrial facilities of PLASTIKA KRITIS (upper) and part of the wind farm located in Crete. (Source: COMPANY PROFILE - Plastikakritis.Com, n.d.)

2.6 STATE OF THE ART

During the last years, a continuous increase in research into biomass-based HRESs has been observed. Additionally, in the literature, it is observed the increased usage of HOMER Pro software to model and evaluate these HRES. In the literature review, a few research papers were found that use HOMER Pro software and biomass technologies to meet an industrial site's electrical and thermal needs. Furthermore, only a few research papers have been published addressing the electric load of industrial/commercial/residential facilities using HOMER Pro software. Lastly, most of the research papers with biomass-based HRESs are used to model an energy system to meet the needs of small and remote communities or university campuses, usually in islands or rural areas, by utilizing technologies such as gasification or AD. This study aims to provide a methodological framework for combining the above-mentioned technologies. A summary of the reviewed studies is presented in *Table 2-13*.

According to a research article published in 2020 by the authors (Jahangir & Cheraghi, 2020), using local biomass resources to supply the electricity in rural areas is an acceptable alternative compared to the current supply in terms of LCOE. The proposed optimal system of this study has a LCOE equal to 0.128 \$/kWh, a competitive electricity price for the village. The proposed system consisted of solar PV, WT, biogas generator (BG), and BAT. This study shows that more than 99 % of the total electrical energy is supplied from the BG. Moreover, it was found that the CDE were reduced by 99 % compared to the current energy solution (coal-based plants). Lastly, it was also found that the price of biomass and the inflation rate dramatically affected the cost of power generation.

In (Malik et al., 2020), it was found that in the case of the institute building of the Centre for Energy and Environmental Engineering located in the western Himalayan hilly region, the optimal HRES consisted of PV/BG/grid. In this HRES, the biomass gasifier contributed by generating more than 60 % of the total required energy. The LCOE of the system was found equal to 0.102 \$/kWh with a renewable penetration factor of 83 %. Lastly, the proposed HRES saves 27.8 Mt CO₂ from being released into the atmosphere compared to a diesel-only solution.

A stand-alone HRES consisting of PV/BG/BAT utilizing local waste streams to meet the needs of a small community in Nigeria was investigated (Eziyi & Krothapalli, 2014). This study found that by utilizing the local waste streams and gasification technology, a cost reduction of 30 % can be achieved regarding the LCOE. Additionally, this study proposes the idea that waste heat generated by the BG can be utilized to purify water, thus increasing the system's efficiency while also providing a technology that can enable sustainable rural development.

A study by (Ahmad et al., 2018) found that a BG that utilizes animal manure can provide 60 % of the total electrical load. Adding solar PV and WT lowers the grid dependency to almost 12 %. This results in 19.97 Mt CO₂ savings per year while also providing good LCOE equal to 0.057 \$/kWh. The authors also notice the high risk of implementing a project of this scale for possible investors. Lastly, it is concluded that a system of this scale is techno-economically feasible, with grid-connected solutions offering better economic performance than the off-grid system.

In (Yimen et al., 2018), the authors investigated the integration of a HRES that utilizes local livestock manure to meet the needs of a village located in Cameroon. A grid extension was

investigated; however, the proposed HRES provided better economic performance than the grid extension required to connect the village to the grid. The system provided a 100 % renewable penetration factor with storage. The LCOE equaled 0.256 €/kWh, a competitive price for 100 % renewable HRESs.

The study conducted in 2021 by (Yimen et al., 2021) investigated the effect of utilizing livestock manure by AD or forest residues by gasification. It showed that AD integration resulted in a 29 % decrease in LCOE, whereas gasification led to a decrease of 40 %. It also showed that a small fraction of the total available biomass resource was utilized. It also found that the transportation costs of livestock manure dramatically affected the system's economics and architecture. On the contrary, the transportation cost of forest waste did not affect the share of power in the proposed HRES.

In a 2017 study regarding off-grid solar-biomass systems, (Shahzad et al., 2017) proposed the use of solar PV, a battery array, and a BG to meet the electrical needs of an agricultural farm with six households. This study found that the proposed HRES resulted in LCOE equal to 5.51 PKR/kWh, a 46.76 % decrease compared to the current grid supply. It also emphasizes that HRESs are reliable and effective solutions for energy crises in rural and decentralized areas with low grid stability.

In a study published in 2020 by (Chambon et al., 2020), it was found that the implementation of HRES mini-grids offered higher grid reliability for off-grid power. Additionally, it was found that a standalone gasification unit for off-grid systems provided better economic indexes than solar PV, even though it is not as commercially attractive. In the case of the grid-connected system, the cost of energy reduction ranged from 30 to 50 % while also providing convincing evidence that a hybrid system can cover the needs of a small village with weak, moderate, and robust grid reliability.

A study that uses biomass gasification was tested by (Rajbongshi et al., 2017), and it provided strong evidence that a biomass gasification system can be a competitive option compared to a PV system. This study found that the grid-connected hybrid system had a LCOE of 0.064 \$/kWh, a 55.86 % decrease compared to the reference off-grid system. This study shows that grid-connected systems offer more competitive LCOE than off-grid systems, with low grid availability and stability.

The investigation conducted by (Bhattacharjee & Dey, 2014) has shown that for the electrical needs of a rice husk facility, a BG and a PV cannot realize the electrical demand without a grid connection. The study showed that in the extreme case that electricity rates increase to 1 \$/kWh, the proposed hybrid system will have a LCOE equal to 0.143 \$/kWh. By utilizing locally available resources (solar and biomass), the proposed HRES can conserve almost 92 % of the grid electricity consumption, therefore reducing the CDE of the system substantially.

In (R. Kumar & Channi, 2022), the authors proposed a hybrid energy system that utilizes local agricultural residues from the rural area to provide energy to the village. This study showed that this village could be 100 % energy self-sufficient by installing PV, a BG, and BAT. This study also shows a reduction of 99.9 % in carbon dioxide emissions (CDE) compared to the grid-only system. This study also indicates that installing BGs in rural areas is highly beneficial, particularly in developing countries.

A feasibility study using a HRES consisting of PV/WT/BAT/BG was evaluated by (Sigarchian et al., 2015). This study used locally produced biogas to provide the necessary energy while also

replacing a diesel generator (DG). Additionally, it was found that the proposed HRES had a LCOE of 0.25 \$/kWh, a 19.35 % decrease from the LCOE found by utilizing a DG in parallel with solar PV and wind. In rural areas, it is also common to only use a DG. In this case, the proposed HRES with a BG offers a 55 % price decrease while saving 48 tCO₂ annually.

In (Salehin et al., 2014), the authors conducted a feasibility study for a PV/DG/BG/BAT hybrid system for off-grid electrification of an island in Bangladesh. In this study, livestock manure on the island was utilized to produce biogas. This study showed that it is possible to provide the island's electrical needs with locally available energy resources, with a renewable penetration of 99 %, while having a competitive LCOE of 0.217 \$/kWh.

The work conducted by (Al-Najjar et al., 2022) presents the overall performance of a grid-connected HRES. The proposed optimal system consists of PV/BG, thus utilizing the solar and biomass potential of the area. The hybrid energy system decreased grid dependency by almost 70 % while reducing CDE.

In (Castellanos et al., 2015), it was found that 61 % of the total electrical load can be met with a CHP unit by utilizing locally available biomass with a CHP. Additionally, the excess heat produced by the CHP unit can be used to provide the necessary heat required for the optimum operation of the AD plant. In this work, they also emphasized that by using AD, the liquid and solid by-products can be used as fertilizer to improve crop yields.

A 2021 study by (Vendoti et al., 2021) showed that a HRES consisting of PV/WT/BG/FC/BAT could meet the needs of the case study village, with a LCOE equal to 0.214 \$/kWh and 0 % shortage capacity. Compared to the base case system, the proposed HRES offers a simple payback time of 4.43 years.

The authors (Thirunavukkarasu & Sawle, 2022) in their study evaluated an HRES to meet the needs of an Indian tea plant. This industrial plant required electrical, thermal, and hydrogen loads to properly function. This study evaluated off-grid and grid-connected systems, with the latter being a more cost-effective solution. It also provides robust evidence that a CHP unit with a thermal load controller (TLC) could provide the necessary thermal load in industrial applications.

In (Jahangiri et al., 2021), the authors investigated the effectiveness of installing a HRES to meet the electrical and thermal needs of a building in Iran. It was found in this study that the utilization of biomass with a CHP plant is economically unjustifiable. However, via hydrogen production and TLC, this HRES can meet the electrical and thermal loads of the building with a renewable fraction equal to 47 %. However, due to the increased LCOE, thanks to the expensive hydrogen production, a grid-connected system is economically justified if the grid extension is lower than 1.47 km.

Lastly, (Ribó-Pérez et al., 2021) provide an extensive methodology for modelling gasifiers in HOMER Pro software. Additionally, they provide results of the electrification of two case studies utilizing locally available biomass to produce syngas. In this study, it was found that in both case studies, the gasifier acts as a backup system; however, with increased amounts of available biomass, the generators can manage higher loads. In the first case study located in Columbia, the decrease of the LCOE ranges from 50 to 94 %. Comparable results were found in the case study of Zambia, where the estimated LCOE is lower than connecting the community to the electric grid.

There is a research gap when it comes to techno-economic analyses for industrial systems that require electricity and heat. Additionally, no research papers propose a method of using a combination of waste-to-energy technologies in HOMER Pro software. This study provides the necessary methodological framework to develop proper models in HOMER Pro software that take advantage of two (or more) waste-to-energy technologies. Lastly, it also fills the gap concerning the use of HOMER Pro software in the food industry, where heat and electricity are the main energy carriers.

Table 2-13 Similar studies summary.

<i>Location of study</i>	Study area	Load type	System components	Grid connection	Software	Biomass resource	Biomass to energy technology	Reference
<i>Iran</i>	Village	Electrical	PV/WT/BG/BA	Off-grid	HOMER Pro	Mix of municipal animal and agricultural wastes	Gasification	Jahangir & Cheraghi, 2020
<i>India</i>	Institute building	Electrical	PV/BG	On-grid	HOMER Pro	Forest residues	N/A	Malik et al., 2020
<i>Nigeria</i>	Small community	Electrical	PV/BG/BAT	Off-grid	HOMER Pro	N/A	Gasification	Eziyi & Krothapalli, 2014
<i>Pakistan</i>	Town	Electrical	PV/WT/BG	On-grid	HOMER Pro	Livestock manure	Gasification	Ahmad et al., 2018
<i>Cameroon</i>	Village	Electrical	PV/BG/WT/PHS	Off-grid	HOMER Pro	Livestock manure	Gasification	Yimen et al., 2018
<i>Cameroon</i>	Rural community	Electrical	PV/WT/BG/BAT	Off-grid	HOMER Pro	Livestock manure or forest waste	Gasification or AD	Yimen et al., 2021
<i>Pakistan</i>	Agricultural farm and residences	Electrical	PV/BG/BAT	Off-grid	HOMER Pro	Livestock manure	AD	Shahzad et al., 2017
<i>India</i>	Village	Electrical	Different combinations of PV/BG/DG	Off-grid and on-grid	HOMER Pro	Woody biomass	Gasification	Chambon et al., 2020
<i>India</i>	Village	Electrical	PV/BG/DG/BAT	Off-grid and on-grid	HOMER Pro	Local village residues	Gasification	Rajbongshi et al., 2017
<i>India</i>	Small industry	Electrical	PV/BG	On-grid	HOMER Pro	Agricultural residues	Gasification	Bhattacharjee & Dey, 2014
<i>India</i>	Village	Electrical	PV/BG/BAT	Off-grid	HOMER Pro	Agricultural residues	Gasification	R. Kumar & Channi, 2022
<i>Kenya</i>	Village	Electrical	PV/WT/BAT/DG/BG	Off-grid	HOMER Pro	Livestock manure	AD	Sigarchian et al., 2015
<i>Bangladesh</i>	Island	Electrical	PV/DG/BG/BAT	Off-grid	HOMER Pro	Livestock manure	AD	Salehin et al., 2014
<i>N/A</i>	Residential buildings	Electrical	PV/BG	On-grid	HOMER Pro	Waste (MSW, agricultural)	AD	Al-Najjar et al., 2022
<i>India</i>	Village	Electrical	PV/BG/BT	Off-grid	HOMER Pro	Biomass	AD	Castellanos et al., 2015
<i>India</i>	Village	Electrical	PV/WT/BG/FC/BAT	Off-grid	HOMER Pro	Livestock manure	AD	Vendoti et al., 2021
<i>India</i>	Industry	Electrical and thermal	PV/BG/HYDRO/DG/TLC	Off-grid and on-grid	HOMER Pro	Industrial waste	Gasification	Thirunavukkarasu & Sawle, 2022
<i>Iran</i>	Building	Electrical and thermal	PV/WT/FC/BAT/BG	Off-grid	HOMER Pro	Livestock manure	Gasification	Jahangiri et al., 2021
<i>Zambia and Columbia</i>	Two rural communities	Electrical	PV/BG/BAT	On-grid	HOMER Pro	Forest and agricultural biomass	Gasification	Ribó-Pérez et al., 2021

CHAPTER 3

DESIGN AND METHODOLOGY

This Chapter presents the various phases of the developed methodological framework to formulate and evaluate scenarios utilizing data from production processes, climatic conditions, biomass potential, and energy consumption data. Real-time series for electricity consumption data were used in this study, kindly provided by the bakery industry. Furthermore, the computational approaches employed in this diploma thesis to answer the research questions and the software used for the modelling, simulation, and comparison of the proposed energy-based scenarios for the HES are discussed. Lastly, the main limitations and assumptions used in this study are presented in this Chapter. The main research objectives of this diploma thesis are:

- Is it economically feasible to utilize local RES in combination with bioenergy production through local biomass residues from agricultural activities to meet the needs of a local bakery industry?
- What is the most economically viable grid-connected HRES solution to meet the needs of this industry?
- What will be the economic and environmental impact of the energy utilization of local energy sources on islands?
- What is the effect of variations in the system control variables on the system's economic performance?

3.1 DATA COLLECTION AND PROCESSING METHODOLOGY

In this section, the microgrids' electrical and energy demand time series were collected and later assessed to provide helpful information. Additionally, an assessment of the RES potential followed.

3.1.1 ENERGY CONSUMPTION DATA ANALYSIS

In this section, the energy consumption data collected for a local bakery industry are analyzed and visualized to adapt the HRES solution to the specific energy needs of the industry. During most of the production processes, electricity and heat are consumed. In *Figure 3-3*, the monthly electric usage profile of the bakery industry for the year 2020 is shown. A strong connection between energy consumption and time of the year is apparent. This seasonality is caused by the increase in production during the summer months.

The location of the area of study is presented in *Figure 3-1*.

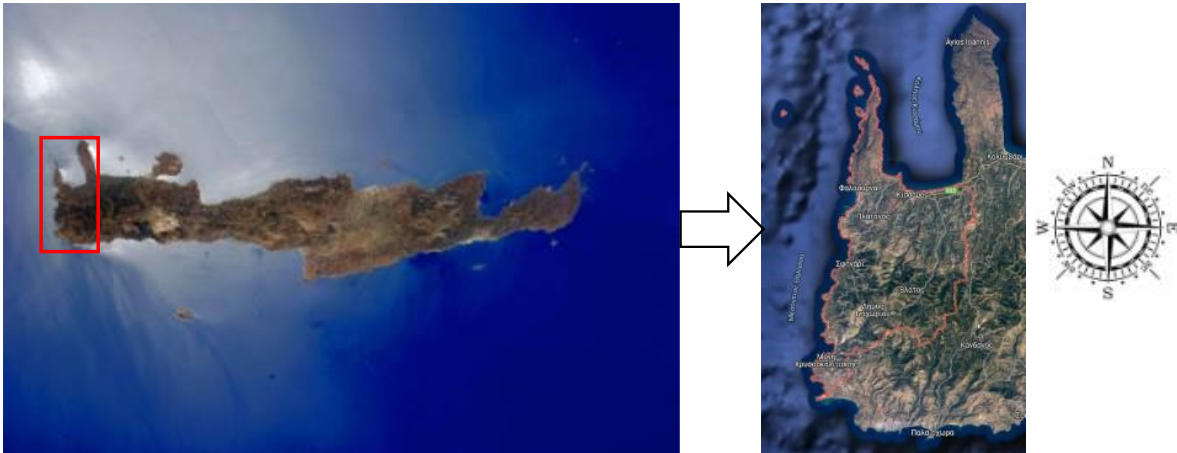


Figure 3-1 The geographical location of the area of study.

More specifically, the monthly total electricity consumption fluctuated from 66,175.1 kWh (December 2020) to 121,163.1 kWh (July 2020), while the mean value was calculated equal to 88,149.5 kWh. In 2020 the total electricity consumption was 1,057,794.1 kWh, and 41.47% of the yearly total energy consumption was consumed from July to October. On average, 2890.5 kWh were consumed daily to meet the electric needs of the industry.

The peak power demand varied from 155.9 kW_{el} (March 2020) to 270.1 kW_{el} (August 2020). The average power demand throughout the year was calculated equal to 120.4 kW_{el}.

Based on the collected data, May can represent the typical operational month, as the total monthly energy consumption and average power demand equaled 88,432.3 kWh and 119.1 kW_{el}, respectively. Both values have small deviations from their respective means. Additionally, during May, the power demand varied from 37.2 to 205.4 kW_{el}.

According to *Figure 3-3* and *Appendix A*, the total monthly electricity consumption and average power demand for August 2020 decreased slightly. The drop in energy consumption can be attributed to the summer pause of rusk production. Similar findings can be found during the end of the year 2020 when the production pause during the Christmas period can be identified. The drop in electric power demand can be observed in *Figure 3-2*.

A significant index for electricity demand and consumption is the load factor (LF). *Equation 4* is used for the calculation of the LF.

$$f_{Load} = \frac{\text{Energy used during a time period (kWh)}}{\text{Maximum demand (kW)} \times \text{Time (hrs)}} \cdot 100 \quad (4)$$

For the data collected from the bakery industry, the electrical f_{load} (%) was found equal to 44,7 %.

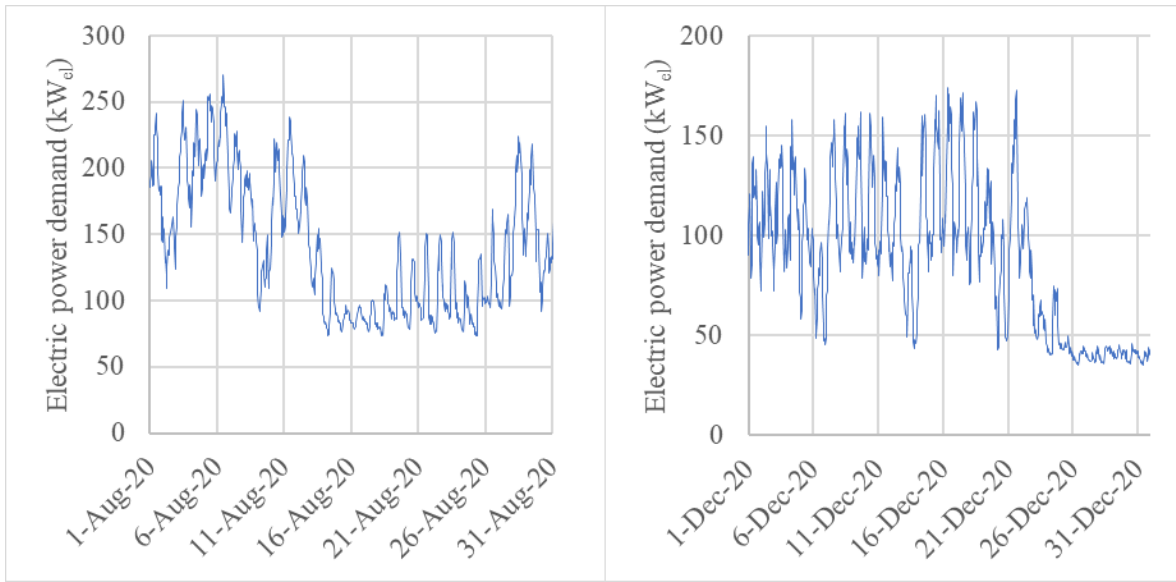


Figure 3-2 Drops in electric power demand during the summer break and the Christmas period.

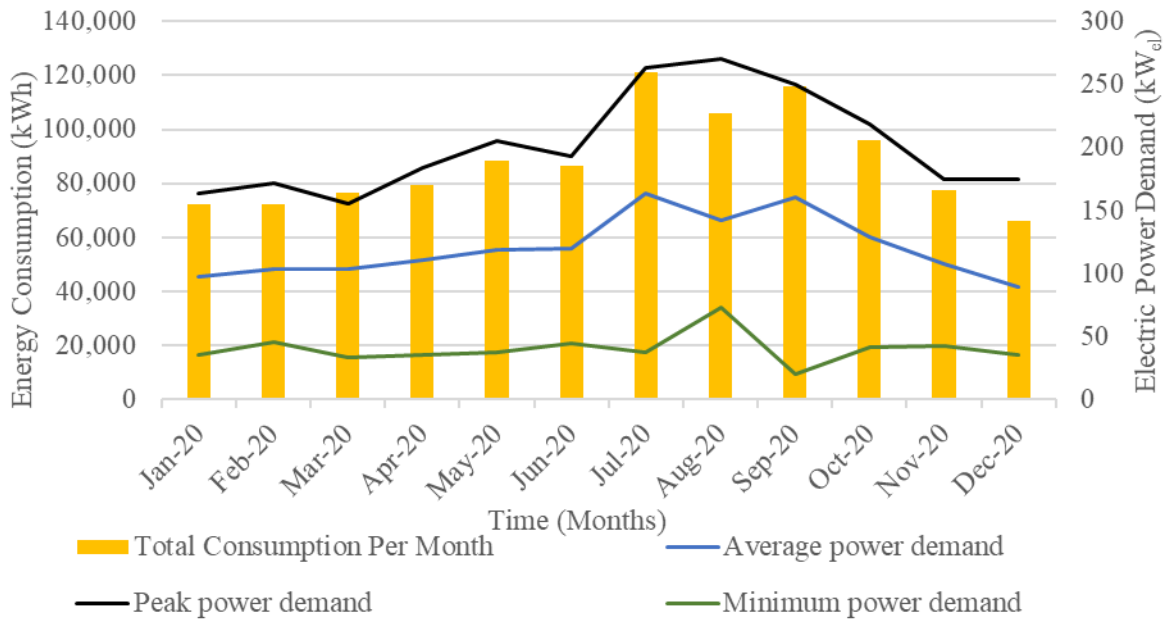


Figure 3-3 Total electricity consumption and electric power demand profiles.

In Figure 3-4 (left), the electric power demand in the industrial facility during the 19th week of the reference year is presented. This week corresponds to the beginning of May 2020. During the reference week, the total energy consumption was equal to 19,653 kWh. During the weekdays (Monday-Friday), the electric power demand profile follows a similar pattern, whereas the demand is sufficiently lower during the weekend (Saturday-Sunday). During the 19th week, the electric power demand fluctuates from 78.2 to 168.4 kW_{el}. It is observed that higher demand is located during the morning and early evening hours (07:00 – 18:00). During late evening and early morning hours (19:00 – 06:00), the electric power demand stays below 100 kW_{el}. However, according to Figure 3-4 (right), during the weekend days, there is reduced industrial activity leading to a 40 %

decrease in electricity consumption. This may be caused because the factory runs lighter shifts on Sundays due to labour costs, decreased customer demand or performing maintenance.

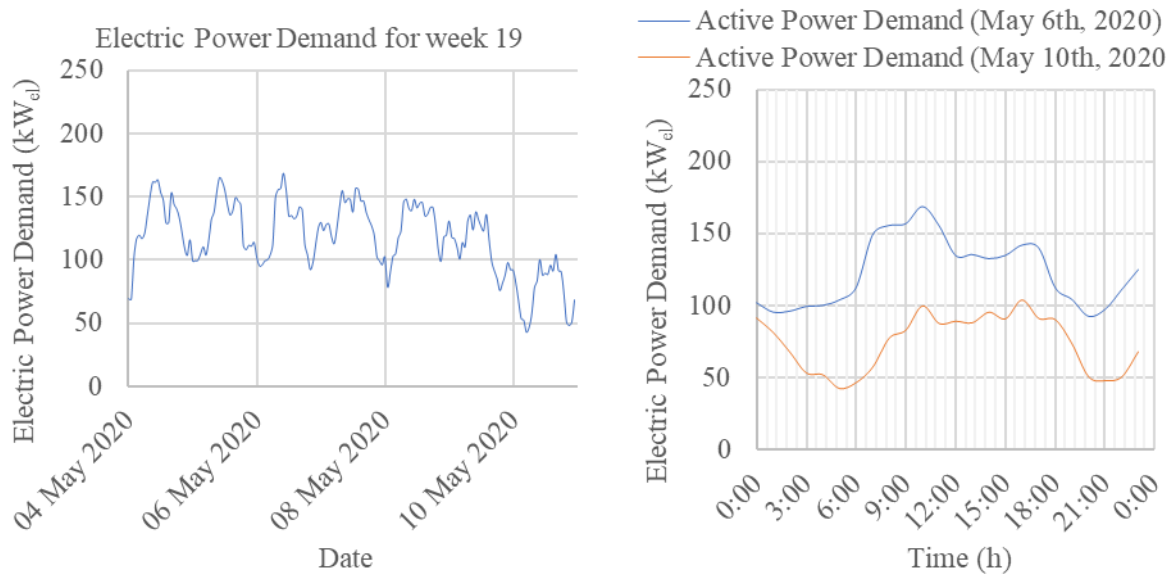


Figure 3-4 Active electric power demand throughout a week during May 2020 (left) and comparison between electric power demand during a weekday and Sunday during a typical month (right).

Similarly, the electric power demand to serve the needs of the industrial facility during the 30th week are presented in *Figure 3-5*. These graphs represent the peak load scenario located in July. According to *Figure 3-5 (left)*, weekdays (Monday-Friday) present the same variations as the reference week (19th). The electric power demand during weekdays varies from 126.1 to 236.3 kW_{el}. The weekly electricity consumption for the peak week was found equal to 30,065.7 kWh, an increase of 52 % compared to the reference week during May. Comparing the two different operational modes presented in *Figure 3-5 (right)*, on Sundays, the energy power demand is sufficiently lower. Furthermore, on July 21st, the total electricity consumption was found equal to 4,428.2 kWh, whereas, on July 26th, the consumption equaled 3,470.32 kWh, a decrease of 22 % between a peak weekday and a Sunday. Comparing the two different operational modes presented in *Figure 3-5 (right)*, the energy power demand is sufficiently lower on Sundays.

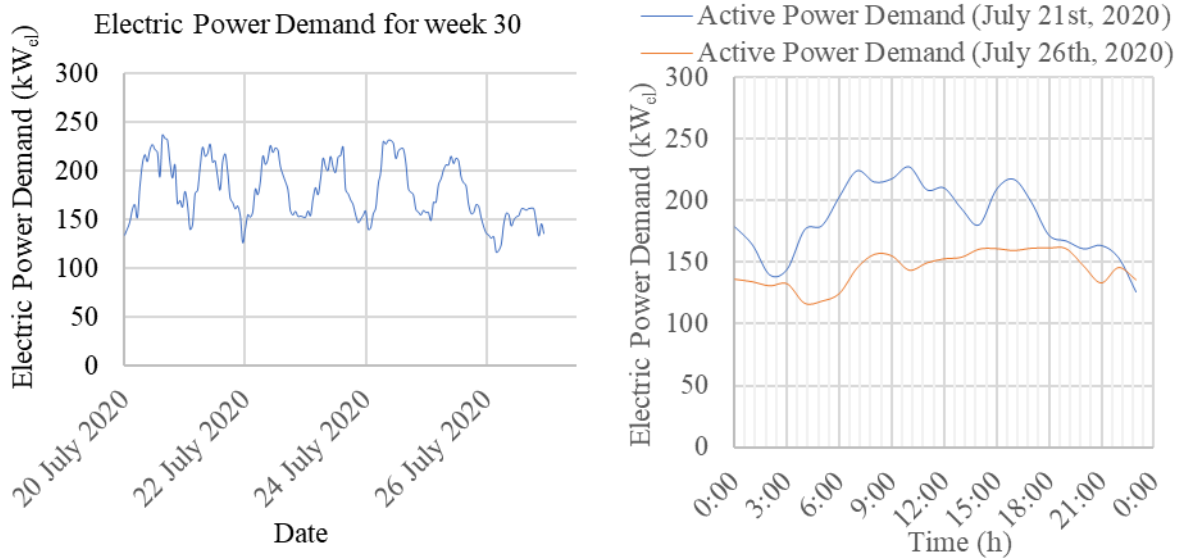


Figure 3-5 Active electric power demand throughout a week during July 2020 (left) and comparison between electric power demand during a weekday and Sunday during a peak month (right).

Figure 3-6 shows that the electrical energy power demand mainly varies from 80 to 130 kW_{el}. Values higher than 130 kW_{el} appear with lower frequency, and a similar pattern appears for electric power demand values lower than 80 kW_{el}.

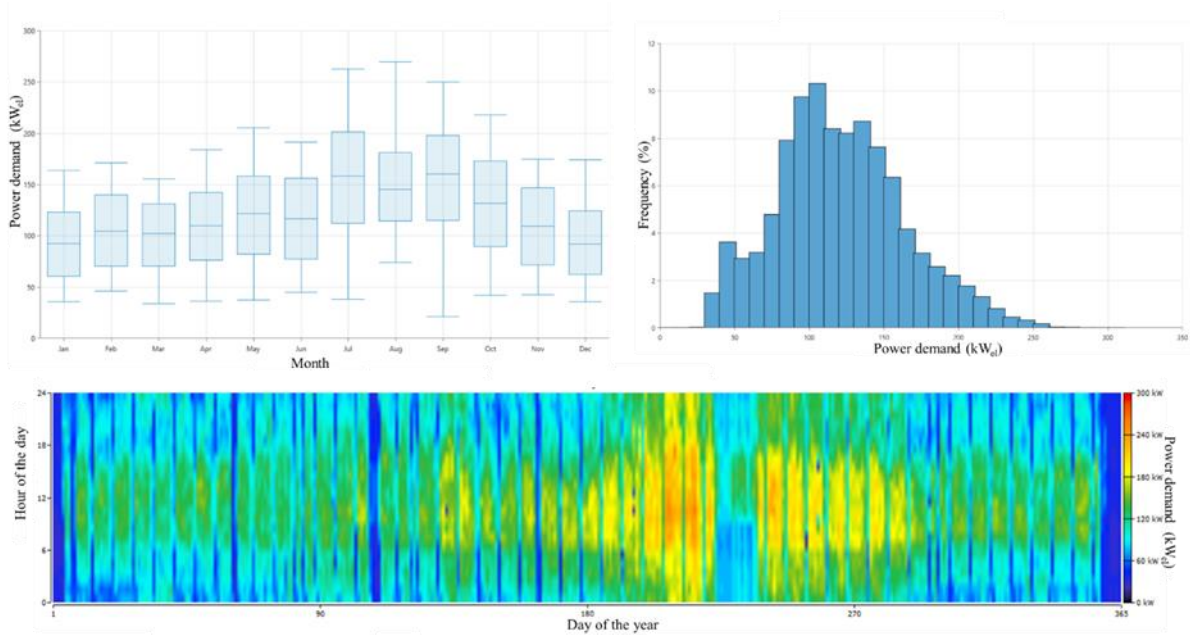


Figure 3-6 Annual active electric power demand information.

Similar findings can be found concerning the thermal energy usage related to the production processes. Typical profiles for heat consumption and thermal power demand are presented in the following figures.

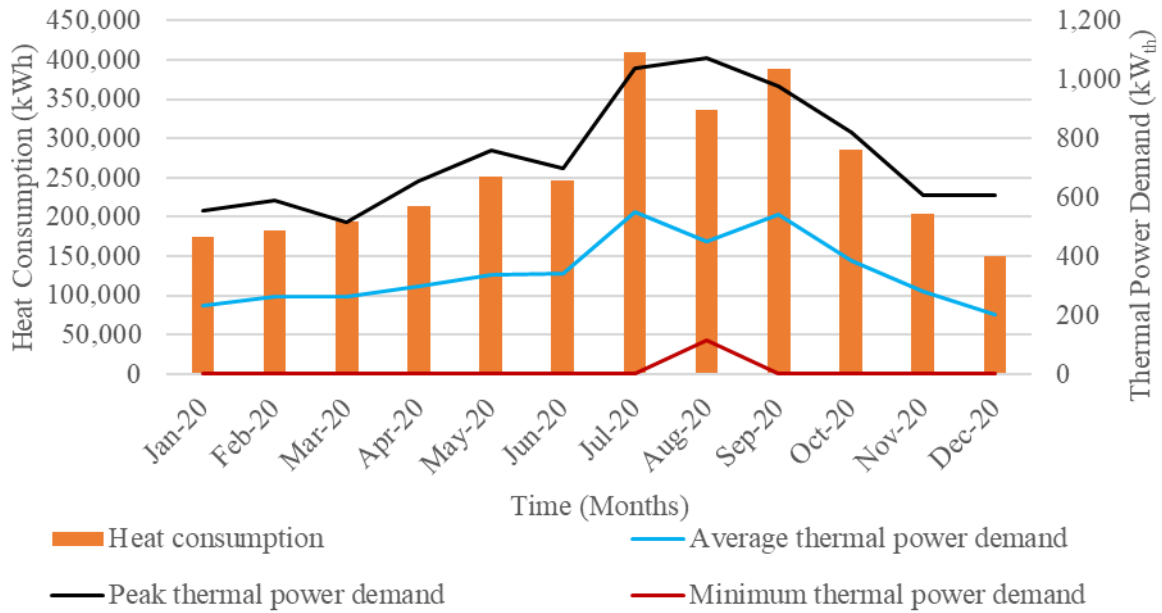


Figure 3-7 Total thermal consumption and thermal power demand profiles.

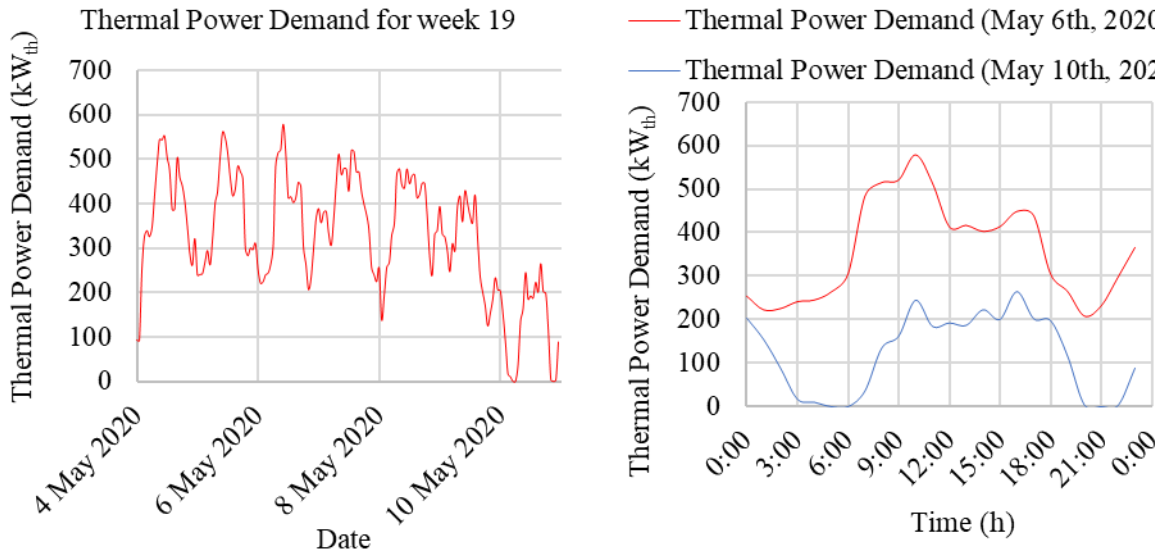


Figure 3-8 Active thermal power demand throughout a week during May 2020 (left) and comparison between thermal power demand during a weekday and Sunday during a typical month (right).

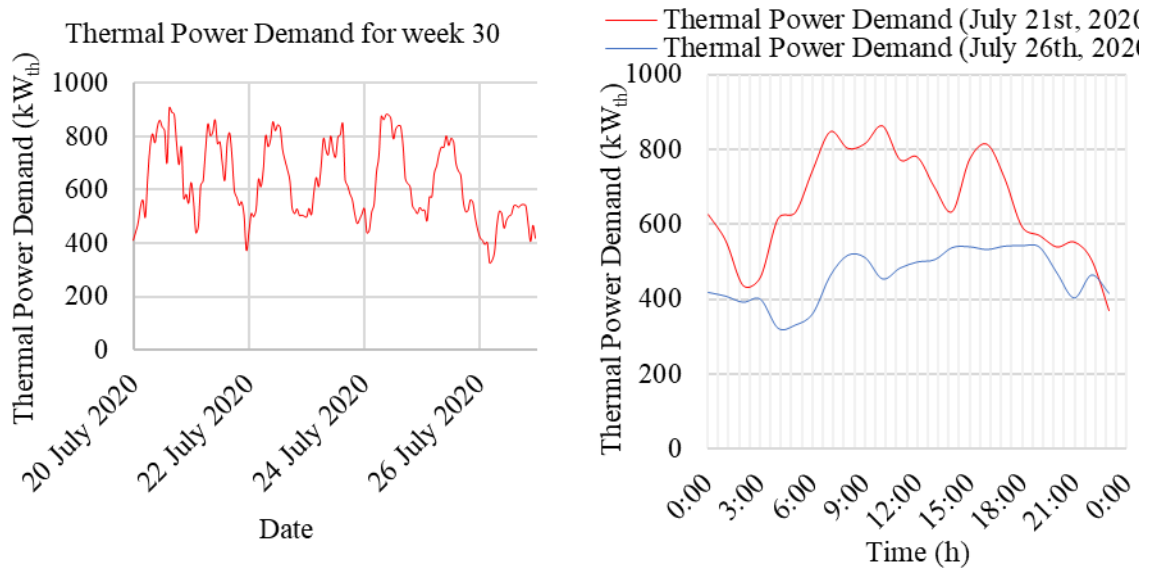


Figure 3-9 Active thermal power demand throughout a week during July 2020 (left) and comparison between thermal power demand during a weekday and Sunday during a peak month (right).

In *Figure 3-10*, the frequency of the thermal power demand is presented. It follows a bell curve distribution. However, the value of 0 kW_{th} appears with the highest frequency.

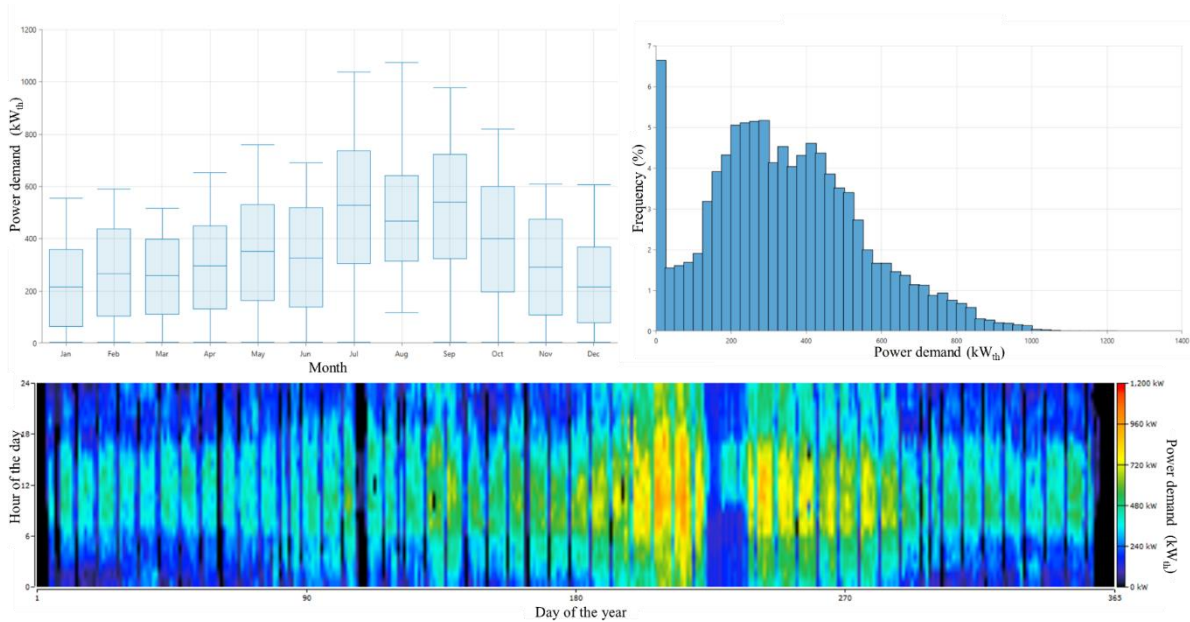


Figure 3-10 Annual thermal power demand information.

Additionally, in the Data-Map shown in *Figure 3-10*, during Easter and Christmas periods, the thermal power demand decreased dramatically.

In summary, 74.16 % of the total energy consumption in the study area is dedicated to meeting the thermal energy needs of the industry, whereas the remaining is related to electricity consumption.

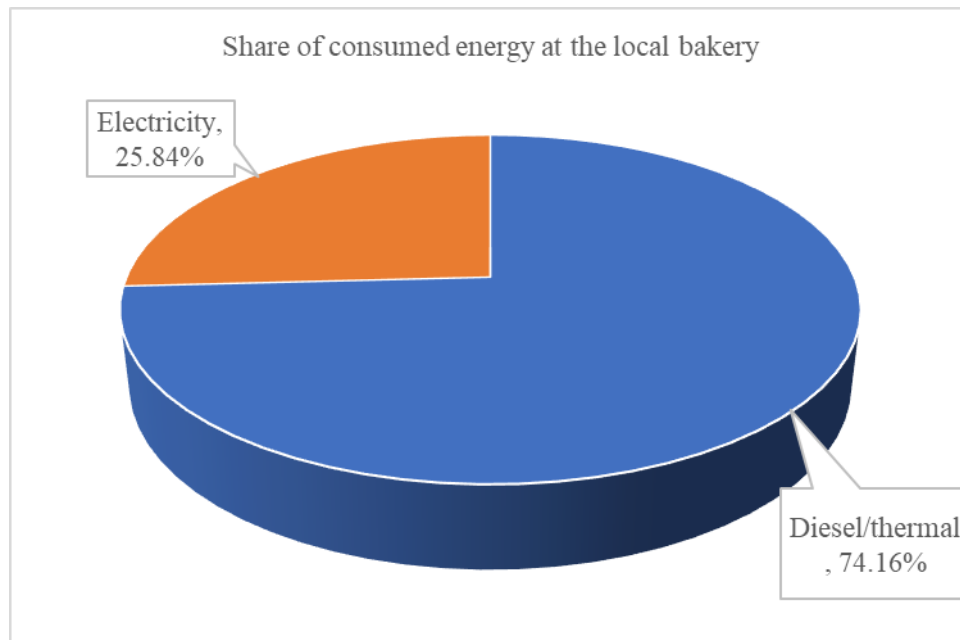


Figure 3-11 Energy demand split at the local bakery.

A detailed summary of both the electric and thermal power demand is presented in *Table 3-1*.

Table 3-1 Summary of thermal and electric load.

<i>Parameter</i>	Electric	Thermal	Unit
<i>Average daily energy demand</i>	2,894.1	8,305.3	<i>kWh/day</i>
<i>Average load</i>	120.59	346.06	<i>kW</i>
<i>Peak load</i>	270.05	1,074.2	<i>kW</i>
<i>LF</i>	45	32	%
<i>Hourly variability</i>	12.272	41.790	%
<i>Day-to-day variability</i>	23.538	40.945	%

3.1.2 RESOURCE ANALYSIS

Additionally, a resource analysis was conducted to assess the available RES potential. These metrics include solar radiation, wind speed, temperature, and biomass availability (BA). The meteorological conditions are an essential factor that significantly affects technology selection. Data for meteorological conditions were obtained from the NASA Prediction Of Worldwide Energy Resource (POWER) database and were compared with data collected from the website RENEWABLES NINJA (Pfenninger & Staffell, 2016; Staffell & Pfenninger, 2016). This was done to compare and assess multiple datasets to increase the simulations' accuracy in this diploma thesis.

The coordinates of the study area, as well as the average solar radiation, average wind speed, and average temperature, are presented in *Table 3-2*.

Table 3-2 Meteorological conditions in study area.

<i>Study area</i>	Latitude	Longitude	Average solar radiation (<i>kWh/m²</i> <i>/day</i>)	Average wind speed (<i>m/s</i>)	Average Temperature (°C)	Reference
<i>Local Bakery</i>	35°25'37.6"N	23°38'35.3"E	5.36	6.32	18.66	NASA POWER Prediction Of Worldwide Energy Resources, n.d.
			5.29	7.63	19.11	Pfenninger & Staffell, 2016; Staffell & Pfenninger, 2016

Biomass potential was assessed based on the available agricultural waste generated in the study area and later converted to fuel based on the conversion rates found in the literature review. Furthermore, MSW from the municipality of Kissamos was assessed for co-digestion with the tomato residues.

3.1.2.1 SOLAR RADIATION DATA

Data obtained from POWER is a monthly average over 22 years (July 1983 – June 2005), whereas data from RENEWABLES NINJA is from the dataset MERRA-2 in 2019.

Figure 3-12 reveals the variation of the average daily radiation in the area of interest. Solar radiation peaks during the summer months, while in the winter months, it decreases dramatically. It is also clear that solar radiation is similar between these two datasets; thus, they can be used interchangeably. *Figure 3-12* indicates that the study area's solar energy harvesting potential is significant. The average solar radiation from the POWER database was equal to 5.355 *kWh/m²/day*, 1.5 % higher than the MERRA-2 dataset.

Additionally, in *Figure 3-12*, the clearness index from the POWER and MERRA-2 datasets are presented, and the HOMER Pro software calculates the clearness index. The clearness index from the POWER dataset and the HOMER Pro software calculations are similar; however, the data from MERRA-2 appears to be different.

After importing the solar radiation data on the Earth's surface from MERRA-2 dataset, HOMER Pro software then calculates the clearness index as a function of the average radiation, the month of the year, and the latitude. The clearness index is a dimensionless number describing the fraction of the solar radiation on a horizontal surface at the top of the Earth's atmosphere that makes it through the atmosphere to strike the Earth's surface. In *Equation 5*, the clearness index is defined:

$$K_T = \frac{H_{ave}}{H_{o,ave}} \quad (5)$$

where H_{ave} is the monthly average radiation on a horizontal surface on Earth's surface and $H_{o,ave}$ is the equivalent at the top of the Earth's atmosphere.

For a specified latitude $H_{o,ave}$ can be calculated for every month of the year. Firstly, HOMER Pro calculates the intensity of solar radiation at the top of Earth's atmosphere using *Equation 6*.

$$G_{on} = G_{sc} \times \left(1 + 0.033 \times \cos\left(\frac{360 \times n}{365}\right) \right) \quad (6)$$

Where G_{sc} is the solar constant and is equal to 1.367 kW/m^2 and n is the number of the year.

To calculate the radiation on a horizontal plane HOMER Pro uses *Equation 7*.

$$G_o = G_{on} \times \cos(\theta_z) \quad (7)$$

where θ_z is the zenith angle given in degrees.

This angle is calculated from *Equation 8*.

$$\cos(\theta_z) = \cos(\varphi) \times \cos(\delta) \times \cos(\omega) + \sin(\varphi) \times \sin(\delta) \quad (8)$$

Where φ is the latitude, δ is the solar declination, and ω is the hour angle. All these angles are in degrees.

For the calculation of the solar declination HOMER Pro uses *Equation 9*.

$$\delta = 23.45^\circ \times \sin\left(360^\circ \times \frac{284 + n}{365}\right) \quad (9)$$

where n is the day of the year.

The total daily extraterrestrial radiation per square meter is derived from the integration for G_o and is given by *Equation 10*.

$$H_o = \frac{24}{\pi} \times G_{on} \left[\cos(\varphi) \times \cos(\delta) \times \sin(\omega_s) + \frac{\pi \times \omega_s}{180^\circ} \times \sin(\varphi) \times \sin(\delta) \right] \quad (10)$$

where ω_s is the sunset hour angle and H_o is the average extraterrestrial horizontal radiation for the day.

The sunset hour angle is calculated from *Equation 11*.

$$\cos(\omega_s) = -\tan(\varphi) \times \tan(\delta) \quad (11)$$

After calculating H_o for every day of the month, HOMER Pro then calculates the average for every month based on *Equation 12*.

$$H_{o,ave} = \frac{\sum_{n=1}^N H_o}{N} \quad (12)$$

where N is the number of days in the month.

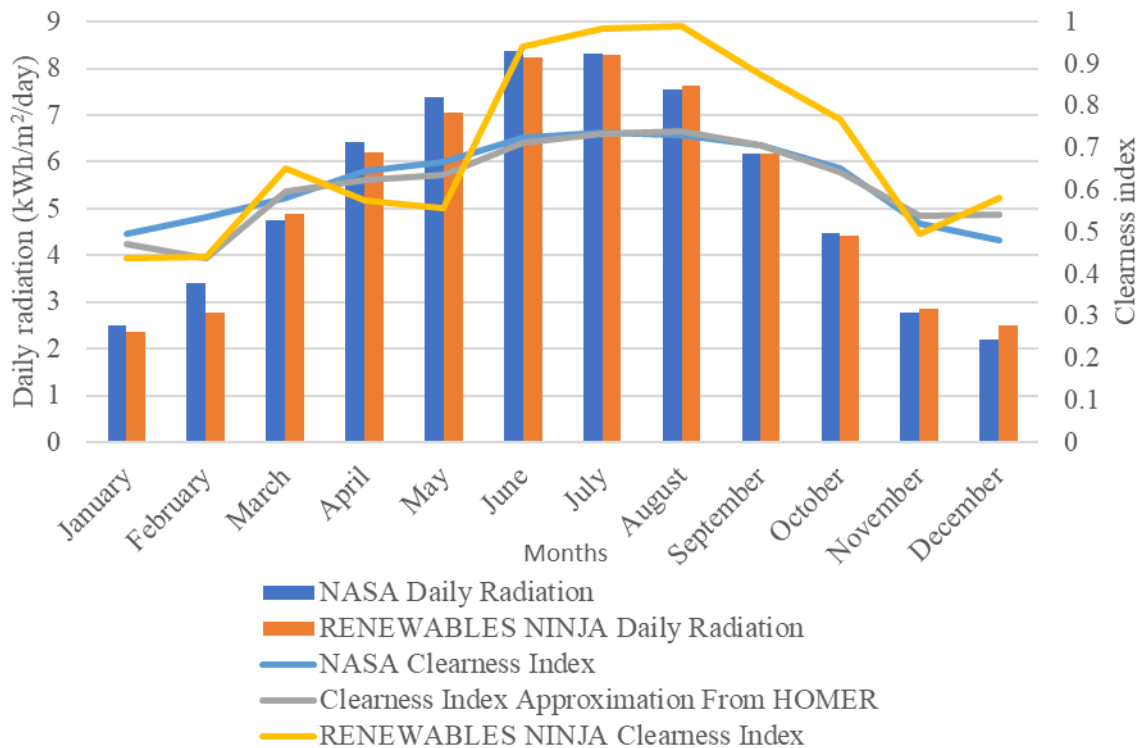


Figure 3-12 Average monthly radiation and clearness index at the study area. (Source: NASA POWER | Prediction Of Worldwide Energy Resources, n.d.; Pfenninger & Staffell, 2016; Staffell & Pfenninger, 2016)

Because of the minuscule differences between the two datasets, data (regarding solar radiation and clearness index) from POWER is used in this work.

3.1.2.2 WIND DATA

Data obtained from POWER is the monthly average wind speed 50m above the earth's surface over 30 years (January 1984 – December 2013). Data from RENEWABLES NINJA was a part of the MERRA-2 dataset of the year 2019.

Figure 3-13 shows the variation of the monthly average wind speed over a year. What can be seen in this figure is the variability of the wind speed; however, in both datasets, it can be easily recognized that during the winter months, the average wind speed is higher compared to the summer months. The lowest average monthly wind speeds were recorded during the summer months. The average wind speed throughout the year concerning the data from RENEWABLES NINJA is equal to 7.64 m/s , whereas, for the POWER dataset, it equaled 6.32 m/s , a decrease of 17.2 % compared to the MERRA-2 dataset.

For the POWER dataset, wind speeds peak at 7.46 m/s (monthly average), whereas in MERRA-2, a higher monthly peak is observed, with the highest average monthly value reported in January equalling 10.027 m/s .

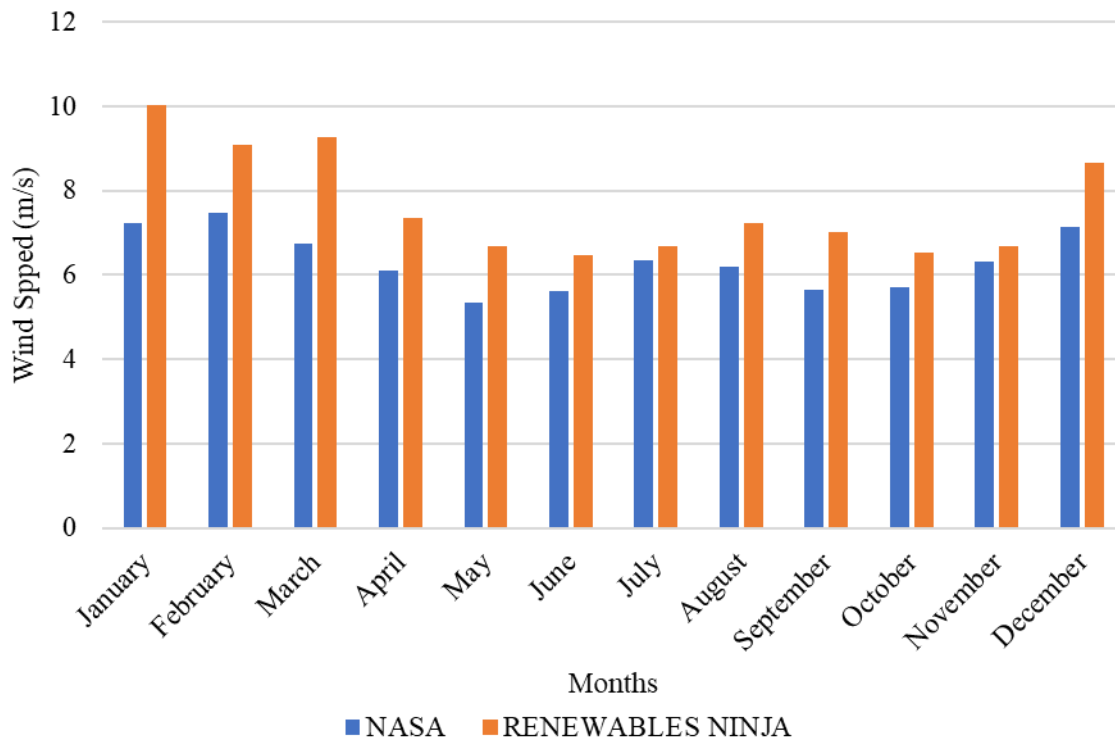


Figure 3-13 Monthly average wind speed at the study area. (Source: NASA POWER | Prediction Of Worldwide Energy Resources, n.d.; Pfenninger & Staffell, 2016; Staffell & Pfenninger, 2016)

Data (regarding wind speeds) from the POWER dataset is used to provide a more conservative approach with lower wind energy potential.

3.1.2.3 TEMPERATURE DATA

The monthly average temperature for 30 years (January 1984 – December 2013) was taken from POWER. RENEWABLES NINJA data was included in the MERRA-2 dataset for 2019.

Temperature data is of immense importance since it dramatically affects the performance of PV and WT. Based on *Figure 3-14*, both datasets have similar monthly averages. It is also clear that the temperature is the highest during the summer months, peaking at over 25°C. The average monthly temperature reached a low point of 12°C at the beginning of the year. The average yearly temperature from RENEWABLES NINJA and POWER databases was 19.07°C and 18.67°C, respectively.

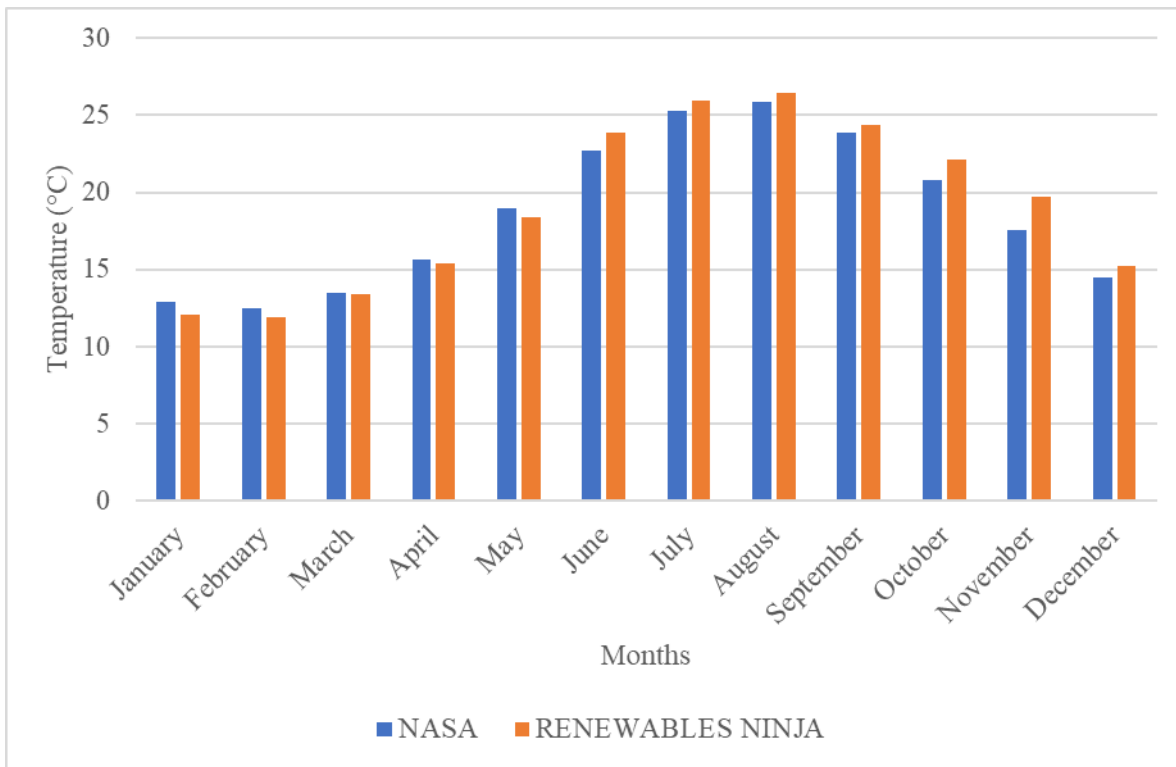


Figure 3-14 Monthly average temperature at the study area. (Source: NASA POWER | Prediction Of Worldwide Energy Resources, n.d.; Pfenninger & Staffell, 2016; Staffell & Pfenninger, 2016)

Data (regarding monthly average temperature) from POWER is used in this work due to the negligible variations between the two datasets.

3.1.2.4 BIOMASS DATA

Data for BA were collected from (O.I.I.E.K.E.I.I.E. - Home Page, n.d.), a Greek Payment Authority of Common Agricultural Policy Aid Schemes. It was found that the average land dedicated to olive and olive oil production in the municipality of Kissamos, where the bakery factory is located, for the years 2017, 2018 and 2019 is equal to 7,398.63 hectares. Correspondently, greenhouse tomatoes’ average land usage is equal to 112.64 hectares. The data relating to land usage per year is given in Table 3-3.

Table 3-3 BA data for the area of interest.

Factors	Land (hectare)			Reference
	2017	2018	2019	
Year				
Olive grove	7,357.26	7,385.24	7,453.4	O.I.I.E.K.E.I.I.E. - Home Page, n.d.
Greenhouse tomatoes	112.46	109.82	115.66	

In the municipality of Kissamos, land used for agricultural purposes is presented in Figure 3-15. Based on Figure 3-15, olive production is primarily located in the northern parts of the island. The

economically exploitable agricultural area is defined as a circle with a radius of 12.5 km around the manufacturing facility. Based on this assumption, more than 90 % of the olive-derived waste (i.e., olive pruning) from the municipality of Kissamos can be used for energy generation.

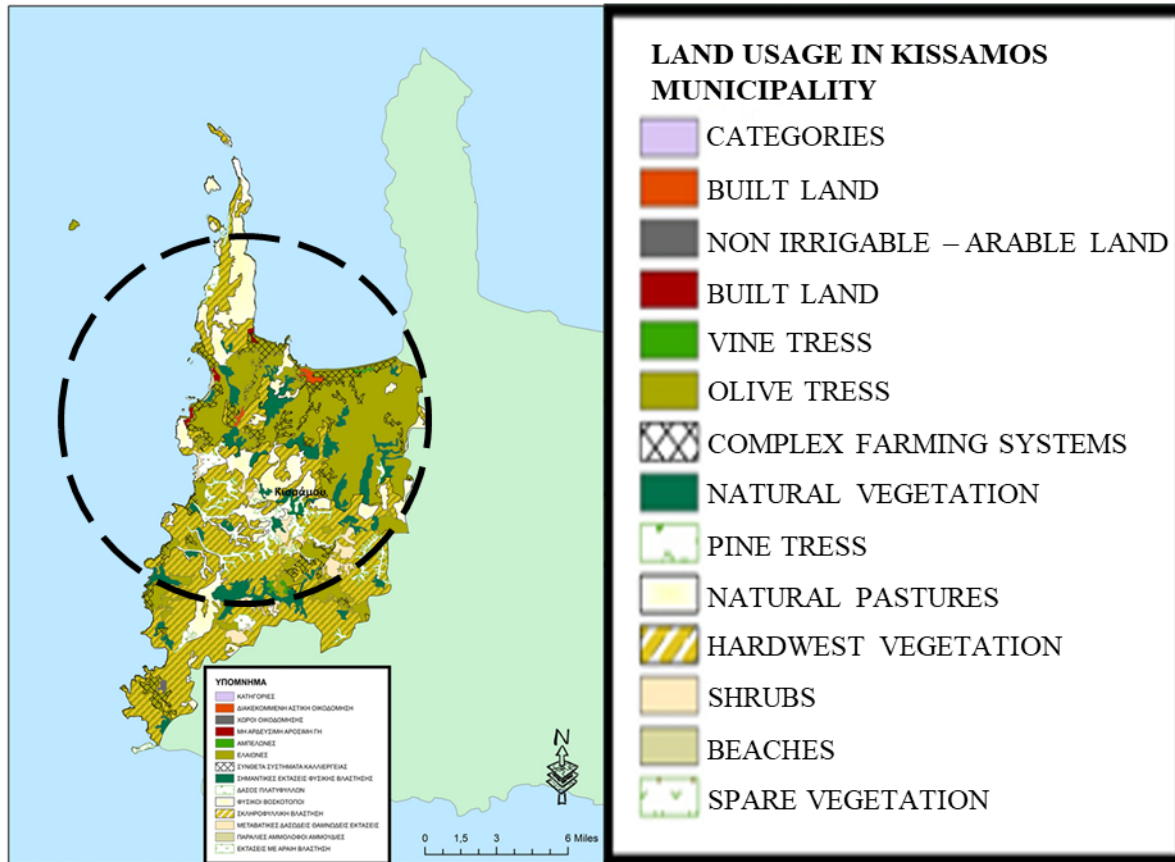


Figure 3-15 Land usage in the municipality of Kissamos for agricultural activities. Note: The circle represents a 12.5 km radius of economically exploitable land. (Source: 7η ΥΠΕ - Γεωγραφία Δήμων Νομού Χανίων, n.d.)

According to data from *Table 2-2* for olive pruning waste production, a yield of $1.5 \text{ tons} \cdot \text{ha}^{-1} \cdot \text{year}^{-1}$ is assumed. The average yearly olive pruning waste available for waste valorisation is presented in *Table 3-5*.

For the calculation of the gasification ratio a typical wood gasification ratio range of $2\text{-}3 \text{ Nm}^3 / \text{kg}_{\text{biomass}}$ is used (Aguado et al., 2021; Copa et al., 2020; Martínez et al., 2012). Assuming a composition of 20% CO , 21% H_2 , 44% N_2 , 12% CO_2 , and 3% CH_4 , the output fuels' density equals $1.07 \text{ kg}/\text{Nm}^3$. Therefore, the syngas yield is equal to $2.17\text{-}3.21 \text{ kg}_{\text{syngas}}/\text{kg}_{\text{biomass}}$. This gasification ratio value is very close to literature values obtained from (Aguado et al., 2021) and (Chambon et al., 2020), where the gasification ratio was found to be equal to 2.63 and $2.5 \text{ kg}_{\text{syngas}}/\text{kg}_{\text{biomass}}$, respectively. These parameters are presented in *Table 3-4*.

The gasification ratio refers to the mass of produced gas to the mass of the consumed biomass.

Table 3-4 Biomass for gasification properties.

<i>Parameters</i>	Value	Unit	Reference
<i>Carbon content</i>	45 – 50	% dry mass	See Table 2-4
<i>Lower heating value (LHV)</i>	4.5 – 6	MJ/Nm ³	Ribó-Pérez et al., 2021
<i>Gasification ratio</i>	2.17 – 3.21	kg of gas/kg of biomass	Ribó-Pérez et al., 2021

According to a recent study conducted on the island of Crete, the cost of woody biomass acquisition is in the range of 70 to 90 €/ton_{biomass} (Σαββάκης et al., 2018). Moreover, according to a research paper conducted in another region of Greece, the total cost of olive pruning ranges from 44.46 to 58.16 €/dry t (Kougioumtzis et al., 2019); however, the more conservative approach is used in this study. The total cost is greatly affected by the efficiency of the collection process, and therefore the optimization of the supply chain (e.g., gradual experience accumulation) can further reduce the cost of the olive pruning collection. Furthermore, fuel costs can greatly affect the final cost of the olive pruning collection process.

Additionally, a cost of transportation equal to 0.25 €/(km × ton) is found in a study conducted in 2018 (Σαββάκης et al., 2018). During that year, according to (Υπ. Ανάπτυξης, Ανταγωνιστικότητας, Υποδομών, Μεταφορών Και Δικτύων - Παρατηρητήριο Τιμών Υγρών Κανσίμων, n.d.) the price of diesel ranged from 1.306 to 1.473 €/litre with an average cost of 1.386 €/litre. In 2022 the prices have dramatically increased, with an average diesel price of 1.764 €/litre, with a maximum reported value of 1.969 €/litre and a minimum of 1.487 €/litre. An increase of 27.3 % in the average diesel price is observed, and thus an increase of 30 % in the transportation costs found in the literature is considered. According to *Figure 3-15*, the average distance travelled to harvest and store OTP in the Municipality of Kissamos varies from of 5 to 25 km, with an average value of 12.5 km, thanks to the mountainous terrain.

In *Table 3-5*, three scenarios with different land utilization percentages are employed to evaluate the energy potential of OTP gasification. The gasification ratio of olive pruning is assumed to be equal to 2.2 kg_{syngas}/kg_{biomass}. The composition of syngas produced from this process is presented in *Table 3-9*. The Lower heating value (LHV) is approximately equal to 5.45 MJ/kg. The annual syngas production varies from 2.27 to 9.08 million Nm³/year. As the LHV of syngas is equal to 5.45 MJ/kg, the value of syngas energy potential varies from 13.31 to 53.23 TJ, which corresponds to an energy potential of 3,696.23 to 14,784.94 MWh/year. The energy potential MJ/year of the ith waste stream is calculated using *Equation 13*.

$$EP_i = LHV_i \times GR_i \times MOSW_i \quad (13)$$

Where EP_i MJ/year is the energy potential of the ith waste stream; LHV_i MJ/kg_{gas} is the LHV of the produced gas; GR_i kg_{gas}/kg_{biomass} is the gas yield of the waste valorisation technology, and $MOSW_i$ kg_{biomass}/year is the annual WG of the ith waste stream. It is important to note that some waste to energy technologies such as AD can only convert volatile solids to biofuels, therefore it is important determine the total solids per kg_{biomass} and then determine the volatile solids as a %TS. This correction must be applied to accurately compute the energy potential.

Table 3-5 Gasification of olive pruning - energy potential for the area of study.

Metrics	Land utilization (%)			Unit
	10	25	40	
Land	739.86	1,849.66	2,959.45	ha
LHV of gas	5.5	5.5	5.5	MJ/kg
Pruning waste mass	6.86	12.12	17.37	tons
Annual syngas potential	2.27	5.67	9.08	million Nm ³ /year
Energy value	3,730.14	9,325.36	14,920.58	MWh/year

WG in the municipality of Kissamos is moderate, thanks to the relatively small number of inhabitants. The total number of inhabitants in 2011 was 10,790. The total MSW generated in 2015 equaled 5,716 tons, according to a study conducted in 2016 (Χατζηγιάβνη, 2016). This study also projected MSW generation for 2020 and 2025, respectively. It was also found that on the island of Crete, MSW generation per capita was equal to 586 kg · year⁻¹, a value 16 % higher than the European average. It was also found that 59 % of the total MSW generation accounts for biodegradable waste, 39.15 % of which is biowaste (e.g., food waste, fruits, and vegetables), and 19.94 % is paper. Table 3-6 shows MSW generation projections for 2020 and 2025.

Table 3-6 MSW generation data for the area of interest.

Factors	MSW generation (tons/year)			Reference
	2015	2020	2025	
Year				
MSW	5,716	6,008	6,314	Χατζηγιάβνη, 2016

Furthermore, according to Regional Waste Management Planning of Crete (Χατζηγιάβνη, 2016), the cost of using AD for biogas production utilizing the organic fraction of MSW is in the range of 80 to 125 €/ton.

A methane yield of 310 NmL_{CH₄}g⁻¹VS_{added} is considered for evaluating the energy potential of MSW energy valorisation via AD, which is presented in Table 3-7. Additionally, the annual generation of MSW is assumed to be equal to 6,130.4 tons, with an average biowaste percentage of 40 %. The fraction of technically exploitable MSW is assumed to be 50 %. The TS and VS are also assumed to be 32 % and 90 %, respectively. The LHV of MSW was determined, based on the composition of the produced biogas, as 21.50 MJ/kg. Annual energy potential of 708.07 MWh/year is found for the AD of MSW. The energy values related to the AD of MSW are given in Table 3-7.

Table 3-7 AD of MSW - energy potential for the area of study.

Metrics	Value	Unit
Annual average exploitable waste amount	3,065.2	tons/year
Average organic fraction	40	%
Annual biowaste amount	1,226.08	tons
LHV of biogas from MSW	21.5	MJ/kg
Annual biogas potential	109,464.42	Nm ³ /year
Energy value	708.07	MWh/year

Based on the proximity of the greenhouse tomatoes, it is assumed that most of the greenhouse tomato residues are economically exploitable. Assuming an average yield of $15 \text{ tons} \cdot \text{ha}^{-1} \cdot \text{year}^{-1}$ tomato-related waste, an average TS, VS, and a methane yield of 6.5 (%TM), 87 (%TS), and $300 \text{ NmL}_{\text{CH}_4} \text{g}^{-1} \text{VS}_{\text{added}}$, respectively. The total methane potential is demonstrated in Table 3-8.

Based on the case study, the cost of tomatoes was assumed to be 5 €/ton. The cost is low because waste tomatoes are unfit for the market and cannot be sold.

Likewise, three greenhouse land-use scenarios were considered, and their findings are presented in Table 3-8. The total energy potential via utilizing the waste valorisation technology of AD for biogas production from greenhouse tomato residues fluctuates from 26.75 to 107.02 MWh/year. A significant decrease compared to the available energy potential of OTP gasification.

Table 3-8 AD of tomato related waste - energy potential for the area of study.

Metrics	Land utilization (%)			Unit
	10	25	40	
Land	11.26	28.16	45.06	ha
LHV of gas	21.5	21.5	21.5	MJ/kg
Tomato waste mass	168.97	422.43	675.88	tons
Annual biogas potential	2,866.58	7,166.44	11,466.30	Nm ³ /year
Energy value	26.75	66.89	107.02	MWh/year

The total annual fuel production of gasification and AD are presented in Table 3-9.

Table 3-9 Total annual fuel production per technology.

Metrics	Type of fuel						Unit
	Syngas			Biogas			
Land usage	10	25	40	10	25	40	%
LHV	5.5	5.5	5.5	21.5	21.5	21.5	MJ/kg
Annual fuel production	2,441.55	6,103.87	9,766.20	121.67	126.32	130.98	tons/year

The total annual energy (TAP) potential is calculated using *Equation 14*.

$$TAP = \sum_{i=1}^u EP_i \quad (14)$$

Where $TAP \text{ MJ/year}$ is the total annual energy potential of all waste to energy technologies and waste streams.

The cost of biomass was found using *Equation 15*.

$$C_{biomass} = \frac{\sum_{i=1}^u [(C_{1,i} + C_{2,i} \times D_{1,i}) \times MOWS_i]}{\sum_{i=1}^u MOWS_i} \quad (15)$$

Where $C_{1,i} \text{ €/ton}$ is the cost of collection and storage for 1 ton of the i^{th} waste; $C_{2,i} \text{ €} \cdot \text{km}^{-1} \cdot \text{ton}^{-1}$ is the cost of transporting 1 ton of the i^{th} waste for 1 km; $D_{1,i} \text{ km}$ is the average distance travelled for the i^{th} waste stream, and the annual average WG of OTP, MSW and tomatoes is given by OTP_{mass} , MSW_{mass} , TOM_{mass} , respectively. The costs calculated using *Equation 15* are presented in *Table 3-10*. The cost varies from 70.92 to a maximum of 112.59 €/ton. The input parameters used to calculate the mean biomass cost are also provided in *Table 3-10*.

Table 3-10 Mean cost and input parameters of biomass.

Metrics		Input cost parameters						Unit
Economic parameters	$C_{1,OTP}$	70			90			€/ton
	$C_{1,TOM}$	5						€/ton
	$C_{2,OTP} \ \& \ C_{2,TOM}$	0.325						€/(ton × km)
	$D_{1,OTP} \ \& \ D_{1,TOM}$	12.5						km
	$C_{1,MSW} + C_{2,MSW} \times MSW_{mass}$	80			125			€/ton
		Land utilization scenarios						–
Economic parameters	Technology selection	Gasification			Gasification + AD			–
	Land utilization	10	25	40	10	25	40	%
	Low cost	74.06	74.06	74.06	75.72	72.58	70.92	€/ton
	Average cost	84.06	84.06	84.06	94.15	88.03	84.78	€/ton
	High cost	94.06	94.06	94.06	112.59	103.47	98.63	€/ton

The average values are close to those proposed in the literature for woody biomass (Braumakis et al., 2021; Pantaleo et al., 2015; Ribó-Pérez et al., 2021).

Because HOMER Pro software can only use one form of biofuel in a generator, it is necessary to model a gas mix equivalent to the biogas and syngas produced by the AD and gasification, respectively. The reference system design is shown in *Figure 3-16 a)*, whereas the HOMER Pro software equivalent system is presented in *Figure 3-16 b)*.

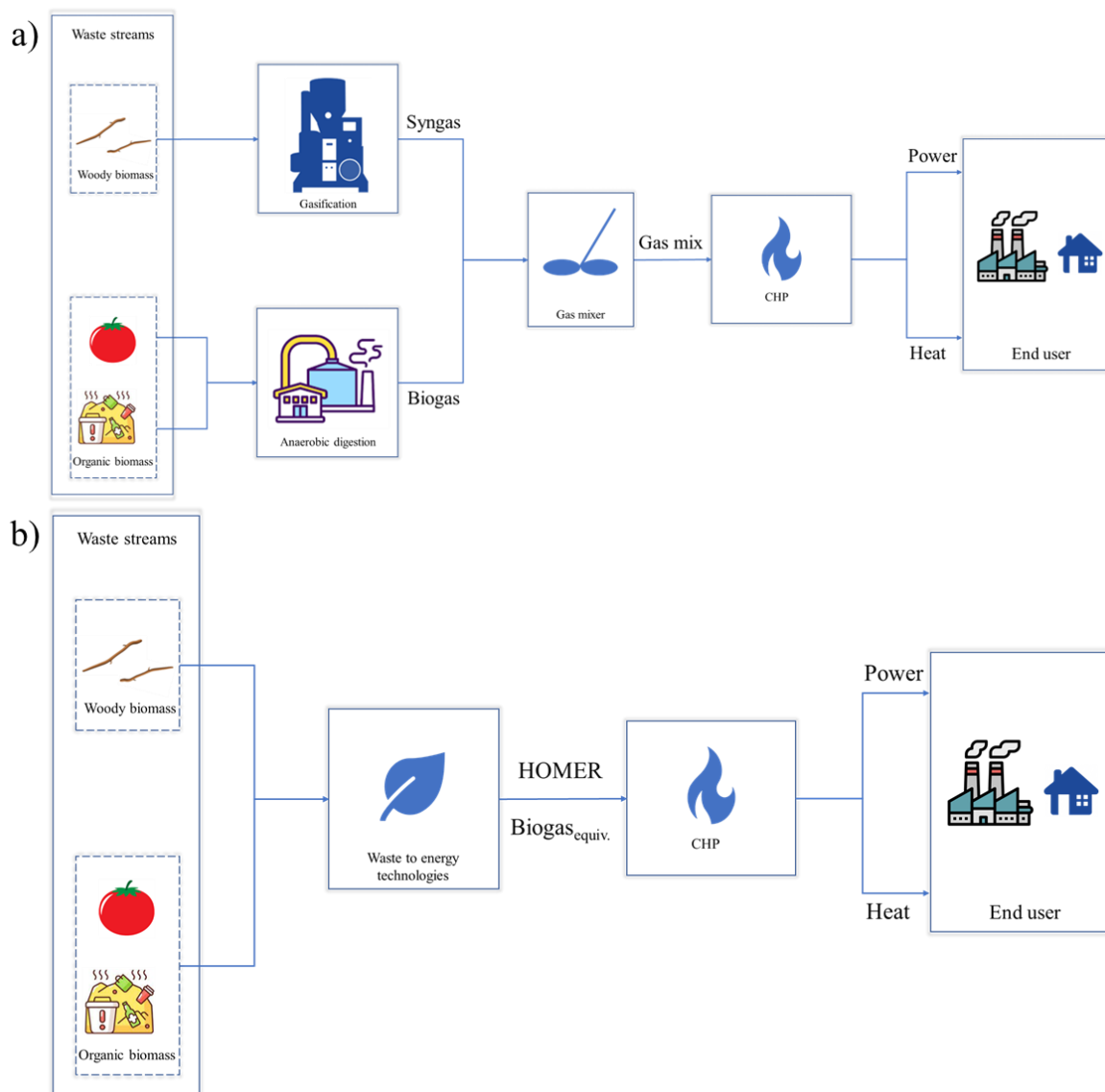


Figure 3-16 a) Schematic diagram of the reference waste to energy system b) schematic diagram of the HOMER equivalent waste to energy system.

Because HOMER Pro software assumes gasification as the waste-to-energy method and biogas as the result of the biomass valorisation, a gasification ratio comparable to the two subprocesses (AD and gasification) must be computed. The gasification ratio equivalent is computed using *Equation 19*, assuming that the two system's total annual energy output potential is equal, and that the composition of the gas mix is known and constant in time. In total, the biogas production from AD ranges from 112,331 to 120,930 Nm^3 , whereas the annual syngas production varies from 2,268,886 to 9,075,546 Nm^3 . The composition of the gas mix fuel used in HOMER Pro software varies from 95 to 99 %vol of syngas, with the rest being biogas. The fuel mix used in the CHP unit will vary depending on the land utilization scenario. However, biogas has a greater LHV value in comparison to syngas. The composition of the produced syngas and biomethane is shown in *Table 3-11*.

Table 3-11 Chemical characteristics of the produced gases.

<i>Fuel specification</i>	Natural gas	Syngas	Unit	Comments
	Value			
CH_4	65	3	%vol	N/A
H_2	0	21	%vol	N/A
CO_2	29	12	%vol	N/A
CO	0	20	%vol	N/A
N_2	0	44	%vol	N/A
H_2O	6	0	%vol	N/A
Density	1.08	1.07	kg/Nm ³	Measurement at 1.013 bar and 273 K
Molar mass	24.27	24.1	g/mol	N/A
LHV	21.50	5.45	MJ/kg	Own approximation was used to calculate the LHV based on the composition of the fuel mixture

The physicochemical characteristics of the gas fuel mixtures that is used in the CHP unit are provided in *Table 3-12*. The gas mix composition is a function of the land usage scenario. For example, 100 %vol syngas is present when gasification is the only waste to energy technology.

Table 3-12 Fuel characteristics used in the CHP unit.

<i>Fuel specification</i>	Gas mix				Unit	Comments
	95.28 %vol syngas	97.99 %vol syngas	98.69 %vol syngas	100 %vol syngas		
CH_4	5.9	4.2	3.8	3.0	%vol	N/A
H_2	20	20.6	20.7	21.0	%vol	N/A
CO_2	12.8	12.3	12.2	12.0	%vol	N/A
CO	19.1	19.6	19.7	20.0	%vol	N/A
N_2	41.9	43.1	43.4	44.0	%vol	N/A
H_2O	0.3	0.1	0.1	0	%vol	N/A
Density	1.0764	1.0762	1.0762	1.0761	kg/Nm ³	N/A
LHV	6.21	5.78	5.66	5.45	MJ/kg	Own approximation was used to calculate the LHV based on the composition of the fuel mixture

The new fuel mixtures used in the CHP unit have similar characteristics to the produced syngas, as seen in *Tables 3.11* and *3.12*, as a result of the higher concentration of syngas in the gas mixtures.

3.2 SYSTEM MODELLING METHODOLOGY

In this section, all the system components were added to the HRES developed in HOMER Pro, along with cost and performance characteristics. Additionally, all the constraints considered in this study are analyzed in this section.

3.2.1 PV MODULE

A PV system is employed to convert solar energy to supply electrical power during the daytime. The component used in this study is the LONGI Solar LR4-60HPH. The PV techno-economic specifications are presented in *Table 3-13*.

Table 3-13 Technical and economic parameters of solar PV.

Factors	Value	Unit	Reference
Size (Step size: 80 kW)	0 – 240	kW_p	
Capital cost (CAC)	750 – 1500	€/kW _p	Sifakis et al., 2021
Replacement cost (RC)	750 – 1500	€/kW _p	Sifakis et al., 2021
O&M Cost	10	€/kW _p /year	Sifakis et al., 2021
Module efficiency	20.6	%	Sifakis et al., 2021
Affected by temperature	YES		
Temperature co-efficient	-0.35	%/°C	Solar Permit Package Software SolarDesignTool, n.d.
Derating factor	88	%	
Operation temperature	43	°C	
Lifetime	25	years	Sifakis et al., 2021

The capital and the investment cost of the PV range from 750 to 1,500 €/kW_p because the economy of scale has been considered. Larger PV installations cost less per kW_p compared to smaller installations. However, solar PV capacity farms higher than 100 kW_p, according to Greek law, are required to build a substation, which increases the CAC and RC.

The maximum RES production for one medium voltage grid-connection line is equal to 300 kW_p. Therefore, because WT are limited by law to a maximum of 60 kW_p, a maximum of 240 kW_p of solar PV is considered. The industrial site has three medium voltage connections with the grid; however, in this study, RES production is limited to the capacity of one, even though the theoretical maximum is equal to 900 kW_p of installed RES.

The different costs, including the construction costs of a power substation, based on installed power of solar PV, are presented in *Table 3-14*. The cost of the bi-directional inverter was integrated on the solar PV cost.

Table 3-14 Solar PV economy of scale.

Capacity (kW _p)	Capital (€)	Replacement (€)	O&M (€/year)
1	1,400	1,400	10
10	9,000	9,000	100
50	40,000	40,000	500
100	75,000	75,000	1,000
200	300,000	300,000	2,000
400	600,000	600,000	4,000

The panel slope is set to 35.47 ° with an azimuth (degrees West of South) equal to 0 °. These values were automatically calculated by HOMER Pro software as the optimum values for the study area's

location. Due to the study area being in the northern hemisphere, an azimuth of 0° is the optimal value.

3.2.1.1 PV MODULE MATHEMATICAL MODEL

Assuming that the PV module is affected by the ambient temperature, HOMER Pro software calculates the output of the PV array using *Equation 16*.

$$P_{PV} = Y_{PV} \times f_{PV} \times \left(\frac{\bar{G}_T}{\bar{G}_{T,STC}} \right) [1 + \alpha_p \times (T_c - T_{c,STC})] \quad (16)$$

where Y_{PV} is the rated capacity of the PV array (power output in standard test conditions (STC) – radiation of $1 \text{ kW}/\text{m}^2$, a cell temperature of 25°C , and no wind); f_{PV} is the derating factor; \bar{G}_T is the solar radiation incident in the current time step of the simulation; $\bar{G}_{T,STC}$ is the solar radiation incident during STC; α_p is the temperature coefficient of power; T_c is the PV cell temperature in the current time step of the simulation, and $T_{c,STC}$ is the PV cell temperature under STC.

3.2.2 WIND TURBINE

WT are used to convert the wind's kinetic energy into electrical energy. The economic and technical parameters of the wind turbine used in this thesis are presented in *Table 3-15*.

Table 3-15 Technical and economic parameters of WT.

Factors	Value	Unit	Reference
<i>Model name</i>	V – Twin 10		
<i>Size considered</i>	0 – 6	Units	
<i>Rated capacity</i>	10	kW	
<i>Electrical bus</i>	AC	AC or DC	
<i>CAC</i>	2,000	€/kW _p	Terlouw & Bauer, 2021
<i>RC</i>	2,000	€/kW _p	Terlouw & Bauer, 2021
<i>O&M Cost</i>	32	€/kW _p /year	Herenčić et al., 2021; Terlouw & Bauer, 2021
<i>Cut-in wind speed</i>	4	m/s	Terlouw & Bauer, 2021
<i>Rated wind speed</i>	12 – 19.5	m/s	Terlouw & Bauer, 2021
<i>Cut-out wind speed</i>	19.5	m/s	Terlouw & Bauer, 2021
<i>Hub height</i>	22.5	m	Terlouw & Bauer, 2021
<i>Lifetime</i>	25	years	Terlouw & Bauer, 2021

According to (Terlouw & Bauer, 2021), the novel wind turbine (V-Twin 100) that is now being developed by Renewable Energy Systems & Technology UG (REST) has a targeted CAC of $1,500 \text{ €/kW}_p$. However, a more conservative approach was adopted with a capital and a RC equal to $2,000 \text{ €/kW}_p$. Lastly, in this diploma thesis, a scaled-down version (10 kW_p) of this novel turbine is used due to regulatory restrictions on wind power installations. Lastly, the total available WT energy potential is limited to 60 kW_p by the Greek legislation by Law 4546/2018 paragraph 2

article 50. Therefore, 6 WT with a nominal capacity of 10 kW_p each is the maximum limit of the wind turbine installation.

3.2.2.1 WIND TURBINE MATHEMATICAL MODEL

Calculating the WT power output HOMER Pro software requires a 3-step process. Initially, it calculates the wind speed at hub height for every time step. By default, HOMER Pro software uses the logarithmic law to convert the input wind speed to hub height wind speed, using *Equation 17*.

$$U_{hub} = U_{anem} \times \left(\frac{\ln\left(\frac{z_{hub}}{z_0}\right)}{\ln\left(\frac{z_{anem}}{z_0}\right)} \right) \quad (17)$$

Where U_{hub} is the wind speed at the hub height of the wind turbine used in the simulation; U_{anem} is the wind speed at the anemometer height; z_{hub} is the hub height of the wind turbine; z_{anem} is the anemometer height, and z_0 is the surface roughness length.

After calculating the wind speed at hub height, HOMER Pro software refers to the WT power curve to calculate the expected power output at standard temperature and pressure conditions. The power curve of the WT used in this study is provided in *Figure 3-17*.

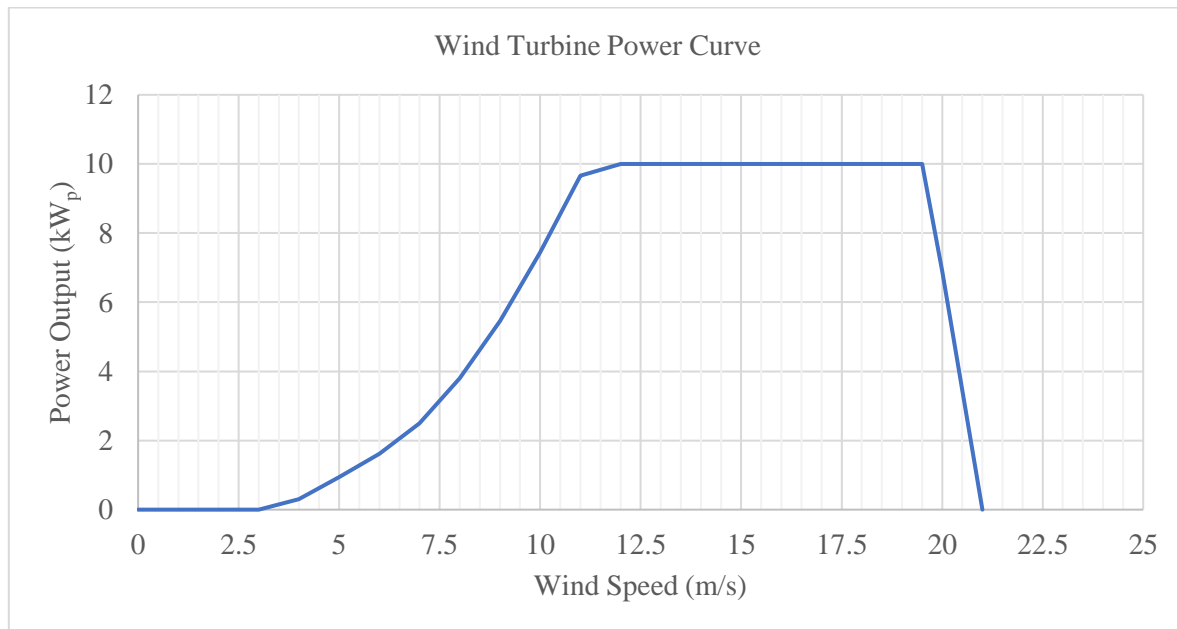


Figure 3-17 Power curve of the Generic 10kW wind turbine. (Source: Terlouw & Bauer, 2021)

The power output is zero if the wind speed at hub height exceeds the usable speed range defined by the WT. This assumes that wind speed higher than cut-out and lower than cut-in leads to zero power production.

After calculating the expected output at STC, a density correction is applied using *Equation 18*.

$$P_{WTG} = \begin{cases} \left(\frac{\rho}{\rho_0}\right) \times P_{WTG,STP} & \text{if } v_{cut-in} \leq U_{hub} \leq v_{cut-out} \\ 0 & \text{otherwise} \end{cases} \quad (18)$$

Where P_{WTG} is the WT true power output; $P_{WTG,STP}$ is the power output at STC; ρ is the actual air density, and ρ_0 is the air density under STC.

3.2.3 GENERATOR

A generator provides the industrial site with electrical energy and heat. This is achieved by utilizing heat with a heat recovery system. Generators utilizing biomass can be an excellent alternative to conventional fuels, such as diesel. The produced gas from gasification and AD can be used as a substitution for diesel. According to (Riley et al., 2020), the initial cost of investment and the O&M cost of a micro turbine biogas-fueled CHP varies from 1,100 to 3,200 €/kW_{el} and 0.008 to 0.02 €/kWh, respectively.

In the generator tab in the HOMER Pro, it is essential to include the capital, replacement, and O&M cost of the gasifier, anaerobic digester, and the CHP unit, the combination of which results in the generator.

According to the recent literature the capital investment for a gasification plant ranges from 1,338 to 3,636 €/kW (Chambon et al., 2020; Indrawan et al., 2020; Ribó-Pérez et al., 2021). The replacement cost ranges between 80-90% of the capital investment cost. According to (Braumakis et al., 2021; Ribó-Pérez et al., 2021), O&M costs can be approximately as 2 % of the initial investment cost. Moreover, following (Indrawan et al., 2020), a 1 kW gasifier requires a total syngas flow of more than 3 m³_{syngas}/h. Lastly, according to (Chambon et al., 2020), the O&M cost of a gasification plant varies from 0.008 and 0.011 €/kW/hour.

Moreover, according to (Sigarchian et al., 2015), the CAC of a biogas engine with a digester system is equal to 1,500 €/kW, with replacement and O&M costs equal to 1,200 €/kW and 0.1 €/kW/hour, respectively.

According to (Chambon et al., 2020), a BG has a fuel curve slope equal to 3.45 kg_{gas mix}/hr/kW_{output} and a fuel curve intercept coefficient of 0.4 kg_{gas mix}/hr/kW_{output}. However, in this diploma thesis, because the fuel is a gas mix containing biogas (~5%vol), a fuel curve slope equal to 1.375 kg_{gas mix}/hr/kW_{output} and a fuel curve coefficient of 0.2 kg_{gas mix}/hr/kW_{output} are assumed to approach the electrical (~40 %) and thermal (~50 %) efficiency of the CHP unit provided by (Terlouw & Bauer, 2021).

Additionally, it is assumed that a CHP plant has a nominal electrical output of 240 kW_{el}. A 50 % scaled-down version of this CHP plant is considered in the simulation. The techno-economic parameters used to model the BG (which includes a gasifier, a digester, and an internal combustion biogas engine) are presented in *Table 3-16*.

As stated by (Yin et al., 2020), the heat-to-power ratio of gas-fired CHP units ranged from 0.8 to 1.0. For biomass CHP units the values vary from 2.3 to 4.0. A more conservative approach is used in this diploma thesis, and therefore, the heat recovery ratio used is equal to 25 %. Additionally, a

30 % minimum load ratio was assumed for the generator, as stated by (Chambon et al., 2020; Yimen et al., 2018, 2021).

The economic and technical parameters of the HOMER Pro generator used in this thesis are presented in *Table 3-16*.

Table 3-16 Technical and economic parameters of the generator with gasification and AD.

Factors	Value		Unit	Reference
	Gasification	Gasification + AD		
Size considered (Step: 120 kW)	0 – 240	0 – 240	kW _{el}	
CAC	5000	6500	€/kW	Braimakis et al., 2021; Chambon et al., 2020; Ribó-Pérez et al., 2021; Riley et al., 2020; Sigarchian et al., 2015
RC	3050	4250	€/kW	Braimakis et al., 2021; Chambon et al., 2020; Ribó-Pérez et al., 2021; Riley et al., 2020; Sigarchian et al., 2015
O&M Cost	0.11	0.12	€/h/kW	Braimakis et al., 2021; Chambon et al., 2020; Ribó-Pérez et al., 2021; Riley et al., 2020; Sigarchian et al., 2015
Main fuel	Gas mix	Gas mix		
Fuel curve slope	1.375	1.375	kg _{gas mix} /hr /kW _{output}	Terlouw & Bauer, 2021
Fuel curve intercept coefficient	0.2	0.2	kg _{gas mix} /hr /kW _{output}	Terlouw & Bauer, 2021
Minimum load ratio	30.0	30.0	%	Chambon et al., 2020; Yimen et al., 2018, 2021
Heat recovery	25	25	%	
Schedule	Optimized	Optimized		
Lifetime	150,000	150,000	hours	Chambon et al., 2020

For the modelling of a BG, a biomass resource must be used. The daily available biomass ranges from 3.04 to 17.37 tons/day. This is the sum of all available waste streams in the area of study. The variation is the result of different land utilization scenarios. Because different waste-to-energy technologies are used, an equivalent gasification ratio must be calculated. To calculate the equivalent gasification ratio, every technology's total annual energy potential had to be first identified. The total annual potential ranges from 15.92 to 56.04 TJ/year. Assuming a range of LHV values between 5.45 and 6.21 MJ/kg_{gas mix}, the resulting gasification ratio varies from 1.02 to 2.20 kg_{gas mix}/kg_{biomass} and is a function of the total annual WG. Each value used in the HOMER Pro simulation represents a land usage scenario. The equation used to calculate the gasification ratio is presented in *Equation 19*.

$$GR_{eq} = \frac{TAP}{\overline{LHV} \times (\sum_{i=1}^u MOWS_i)} \quad (19)$$

Where GR_{eq} (kg_{gas mix})/(kg_{biomass}) is the gasification ratio used in the HOMER Pro software; TAP MJ/year is the total annual energy potential; \overline{LHV} MJ/(kg_{gas mix}) is the LHV of the gas mix, and the sum of every WG (kg_{biomass})/year.

The carbon content used in this work is 44 %, according to the biomass resources' physicochemical characteristics. This value is on par with values used by (Ribó-Pérez et al., 2021).

The schedule of the generator was set to be optimized based on the electrical, thermal demand, and the economics of the other power sources.

3.2.3.1 BIOGAS GENERATOR MATHEMATICAL MODEL

A generator uses fuel to produce heat and electricity. HOMER Pro offers a variety of options regarding generator types (e.g., fuel cells, internal combustions engines). Characteristics such as the fuel consumption, the fuel curve and the minimum and maximum electrical output are required for the modelling of the system component. HOMER Pro assumes the fuel curve is a straight line that intercepts y-axis. *Equation 20* is used to calculate the generator's fuel consumption at any given time step.

$$F = F_0 \times Y_{gen} + F_1 \times P_{gen} \quad (20)$$

Where F_0 *kg/hour/kW* is the fuel curve intercept coefficient; Y_{gen} *kW* is the rated capacity of the generator; F_1 *kg/hour/kW* is the fuel curve slope, and P_{gen} *kW* is the electrical output of the generator.

The electrical efficiency is defined as the electrical energy coming out of the generator divided by the total chemical energy of the fuel going in. *Equation 21* shows the is used to calculate the electrical efficiency at any given time step.

$$\eta_{gen} = \frac{3.6 \times P_{gen}}{\dot{m}_{fuel} \times LHV} \quad (21)$$

Where \dot{m}_{fuel} *kg/hr* is mass flow rate of the fuel².

Because $\dot{m}_{fuel} = F$ the efficiency equation is given in *Equation 22*.

$$\eta_{gen} = \frac{3.6 \times p_{gen}}{(F_0 \times +F_1 \times P_{gen}) \times LHV} \quad (22)$$

Where p_{gen} is the relative output ($p_{gen} = P_{gen}/Y_{gen}$) of the generator.

3.2.4 CONVERTER

A converter allows the energy flows between AC and DC electrical components of the system. Conversion of the current is essential for the electrical load in every application. Generally, most electrical loads in the industry use AC to be powered. In this study, a generic converter comprising a rectifier and an inverter is used to perform bi-directional AC-DC conversion. Conversion to DC is

² The factor 3.6 arises from the conversion of kWh to MJ (Note 1 kWh = 3.6 MJ)

considered only if the system uses BAT as a storage solution or if the electric load is DC and power generation is AC.

As abovementioned, the economic parameters of the converter are integrated into the PV cost parameters, and therefore, the cost values presented in *Table 3-17* are set to zero.

Table 3-17 Technical and economic parameters of the converter.

Component	Costs			Lifetime (years)	Inverter Efficiency (%)	Parallel with AC generator
	Capital (€/kW)	Replacement (€/kW)	O&M (€/kW/year)			
Converter	0	0	0	10	95	YES

The efficiency of the rectifier was set to 90 % and the relative capacity equal to 100 %. Furthermore, the optimal sizing of the converter will be found from the capacity optimization performed by the HOMER Pro optimizer.

3.2.5 GRID

According to (Terlouw & Bauer, 2021), electricity prices in the study area vary from 0.10 to 0.20 €/kWh. However, considering the recent energy price increases, a range of 0.20 to 0.30 €/kWh is more realistic. A simple rate of 0.25 €/kWh is assumed. An annual net metering option for the HRES is enabled, and the sellback price is considered constant and equal to zero. The calculation of the grid's CDE is shown in *Equation 23*.

$$CDE = F_{PE} \times F_D \times F_{FF} \quad (23)$$

Where $CDE \text{ kg } CO_{2eq}/kWh$ is the carbon dioxide emissions (CDE) of the grid per unit of produced power; F_{PE} is the primary energy factor and is used to convert the final to primary energy, and is equal to 2.9; F_D is the diesel factor and equals $0.989 \text{ kg } CO_{2eq}/kWh$ (Sifakis et al., 2021), and F_{FF} is the fossil fuels' factor of the grid. In studies conducted in Crete where the RES penetration is equal to 21.5 % the fossil fuels' factor equals 78.5 % (Tial Kio et al., 2021). Therefore, the CDE of the grid per unit of energy is equal to $2.25 \text{ kg } CO_{2eq}/kWh$.

3.2.6 BOILER

Because of the existence of thermal loads in this study, a boiler must be included to meet any unmet thermal loads that the generators are unable to meet the needs. It is also important to note that HOMER Pro software considers serving thermal loads as of secondary importance compared to electric loads. This means a generator will not be dispatched to meet only a thermal load. Therefore, the boiler provides the required thermal energy whenever the electric load is met from other sources and the thermal load is unmet. HOMER Pro also assumes that a boiler is a pre-existing component of the system while also being able to serve any thermal load. The fuel used in the boiler is diesel. The efficiency of the boiler is set to 85 %.

Diesel prices constantly fluctuate, but for the Prefecture of Chania, a price of 1.555 €/litre , including value added tax (VAT), in bulk is considered. This is the latest price (May 5th, 2022) for diesel provided by the Greek Ministry (Υπ. Ανάπτυξης, Ανταγωνιστικότητας, Υποδομών, Μεταφορών Και Δικτύων - Παρατηρητήριο Τιμών Υγρών Καυσίμων, n.d.). During the same period last year, diesel price in the Prefecture of Chania was 0.977 €/litre (including VAT). An increase of 59 % is observed. This sharp price increase is an aftermath of the European energy crisis that dramatically increased energy and fuel prices inside the EU.

3.2.7 GENERAL

In this study, a nominal discount rate of 8 % is assumed. The expected inflation rate is set to 2 %, however; these variables are sensitive and hard to predict. Additionally, the projects lifetime is equal to 25 years. The social cost of CDE is assumed to be equal to 82.76 €/tonCO_{2eq} (TRADING ECONOMICS / 20 Million INDICATORS FROM 196 COUNTRIES, n.d.). The price was retrieved on June 10th. Lastly, no annual capacity shortage is allowed in this system.

3.3 ECONOMIC MODEL

In this diploma thesis, three main economic indexes are used to evaluate and rank the hybrid energy systems proposed by the HOMER Pro software; these include the total net present cost (NPC), the levelized cost of electricity (LCOE), and the initial CAC. HOMER Pro ranks the systems based on the NPC of the proposed system. NPC is a reliable economic parameter, whereas LCOE is arbitrary to some extent. The annualized CAC of each component is given by *Equation 24* (Haghighat Mamaghani et al., 2016).

$$C_{acap} = C_{cap} \times CRF \quad (24)$$

where *CRF* is the capital recovery factor calculated by *Equation 25* (Haghighat Mamaghani et al., 2016; Tazay, 2020).

$$CRF = \frac{i \times (1 + i)^K}{(1 + i)^K - 1} \quad (25)$$

Where *K* and *i* are the expected system lifetime and the annual real interest rate, respectively.

The total annualized cost (TAC) for all the system components is calculated using *Equation 26* (Haghighat Mamaghani et al., 2016).

$$TAC = C_{acap} + \sum_{j=1}^m C_{OM,j} + C_f + \sum_{j=1}^m C_{R,j} \quad (26)$$

Where *m* is the total number of all system components; *C_{OM,j}* is the annual O&M cost for the *jth* component; *C_f* is the total annual fuel cost, and *C_{R,j}* is the annual RC of the *jth* component. NPC is calculated using *Equation 27* (Haghighat Mamaghani et al., 2016; Tazay, 2020).

$$NPC = \frac{TAC}{CRF} \quad (27)$$

The levelized cost of electricity is a metric that presents the average cost of used generated electrical energy from the proposed energy solution. The total electrical energy generation of the proposed HRES is calculated by *Equation 28* (Haghighat Mamaghani et al., 2016).

$$E_{total} = E_{prim,AC} + E_{prim,DC} + E_{def} + E_{grid,sales} \quad (28)$$

where $E_{prim,AC}$ is the load served for the primary AC load; $E_{prim,DC}$ is the load served for the primary DC load; E_{def} is the load served for the deferrable load, and $E_{grid,sales}$ is the energy sold to the grid. The equation for the LCOE is presented in *Equation 29* (Haghighat Mamaghani et al., 2016; Tazay, 2020).

$$LCOE = \frac{TAC}{E_{total}} \quad (29)$$

Similarly, the levelized cost of thermal energy (LCOTE) can be calculated using *Equation 30*.

$$LCOTE = \frac{AC_{boiler}}{TE_{boiler}} \quad (30)$$

Where $TE_{boiler} kWh/year$ is the annual thermal output of the boiler and $AC_{boiler} €/year$ is the annualized cost of the boiler.

3.4 SCENARIO CONCEPTUALISATION

The commercially available grid simulation software HOMER Pro has been employed to simulate, optimize and sort alternative HRES configurations. These HRES configurations have been previously conceptualized. These systems include PV, WT, a boiler, a combined heat and power unit and a gasification/AD unit. Storage via BAT or flywheels is not tested due to the increased investment cost and the relatively high grid stability in the study area. The scenarios employed in this diploma thesis are presented in *Table 3-18*.

Two scenario categories were formulated, modelled, and compared to the current energy state of the industry. These scenarios aim to optimize the HRES without the use of an energy storage solution while also investigating if the use of AD can reduce the NPC of the energy system. Due to high solar and wind potential, PV and WT are considered in every scenario. In addition, each scenario reflects a grid-connected system due to the industry's high energy consumption and the increased volatility of RES. Lastly, every scenario is simulated using a different BA.

Table 3-18 Different HRES configurations analyzed in HOMER Pro software.

Scenario ID	Hybrid System combinations	BA ³ (%)		
		1	PV + Wind + Grid + Boiler + CHP + Gasification	10
2	PV + Wind + Grid + Boiler + CHP + Gasification + AD			

In total, six scenarios are evaluated. The results of the optimal system are selected manually, and a sensitivity analysis is executed to determine the effects of variations in the system control variables. A summary of the characteristics of each HRES system evaluated is presented in *Table 3-19*. An important note is that the biomass price (BP) used is the average BP presented in *Table 3-10*.

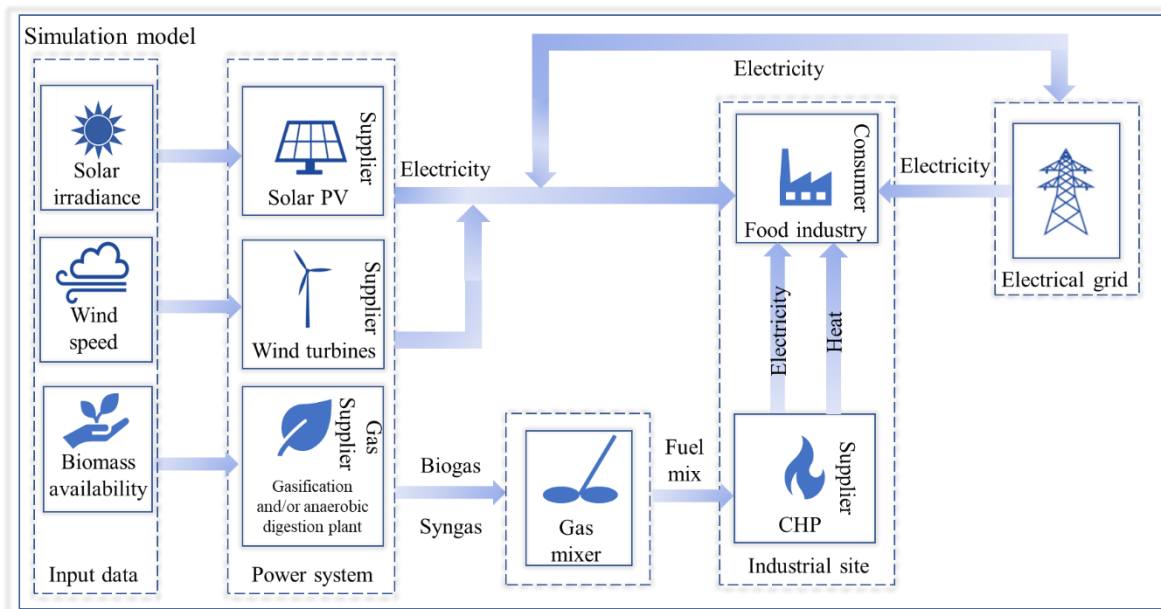


Figure 3-18 Schematic diagram of the proposed HRES.

Scenarios 1-3 are the scenarios with gasification as the only waste-to-energy technology used. A similar pattern is used for scenarios 4-6; however, these scenarios utilize the biogas production from AD in parallel with syngas from gasification.

³ Biomass availability refers to OTP and tomato waste, MSW waste availability is considered constant and equal to 50 % of the total MSW generation

Table 3-19 Scenarios.

ID	Components							Biomass characteristics				Gas mix composition and characteristics			HOMER Pro generator		
	PV	WT	GRID	BOILER	GENERATOR	GASIFIER	AD	BA (%)	BP (€ /ton)	WG (tons /day)	GR ($kg_{gas\ mix} / kg_{biomass}$)	Syngas (%vol)	Biogas (%vol)	LHV (MJ/kg)	CAPEX (€ /kW _p)	REPEX (€ /kW _p)	O&M (€/(kW _p × hr))
1	✓	✓	✓	✓	✓	✓	✗	10	84.06	3.04	2.20	100	0	5.45	5,000	3,050	0.11
2	✓	✓	✓	✓	✓	✓	✗	25	84.06	7.60	2.20	100	0	5.45	5,000	3,050	0.11
3	✓	✓	✓	✓	✓	✓	✗	40	84.06	12.16	2.20	100	0	5.45	5,000	3,050	0.11
4	✓	✓	✓	✓	✓	✓	✓	10	94.15	6.86	1.02	95.28	4.72	6.21	6,500	4,250	0.12
5	✓	✓	✓	✓	✓	✓	✓	25	88.03	12.12	1.41	97.99	2.01	5.78	6,500	4,250	0.12
6	✓	✓	✓	✓	✓	✓	✓	40	84.78	17.37	1.56	98.69	1.31	5.66	6,500	4,250	0.12

3.5 SIMULATION SOFTWARE (HOMER Pro)

HOMER (Hybrid Optimization of Multiple Energy Resources) software is currently one of the most predominantly used microgrid software globally. It was created by the U.S. National Renewable Energy Laboratory (*HOMER Pro - Microgrid Software for Designing Optimized Hybrid Microgrids*, n.d.). The programming language used to create the software HOMER Pro is Visual C++. Currently, researchers and professionals are using this tool in the energy sector. It is used to model, design, assess, and optimize grid-connected and off-grid energy systems. It is also widely used to formulate and assess micro-grid, bigger energy systems (e.g., island grid), as well as HRESs.

HOMER Pro software models the behaviour of an energy system, and it provides valuable information about the life cycle cost of this energy system. It is a software tool that helps to understand these systems and quantifies the effects of uncertainty or changes on input variables. It allows the user to compare design alternatives by analyzing them in technical and financial terms.

Small-scale energy systems that generate electricity and heat can be modelled to meet the required energy carriers (electric, thermal, hydrogen, or a combination of these). This software includes a large combination of electricity and heat generation systems and energy storage solutions, allowing the user to choose whether this system is connected to the grid or stand-alone. Some of the components that HOMER Pro software can model are:

- Solar PV;
- WT;
- Storage technologies;
- Converter;
- Boiler;
- Hydro;
- Reformer;
- Electrolyzer;
- Hydrogen tank;
- Hydrokinetic;
- Grid

The technological cost and availability of the energy resources have a significant impact on the users' final decision. Usually, due to many of technological options and possible system configurations, the decision is a complex problem, something that HOMER Pro software, through optimization algorithms and sensitivity analysis, aims to simplify. The core capabilities of the HOMER Pro software are simulation, optimization, and sensitivity analysis. The relationship between these core capabilities is shown in *Figure 3-19*.

HOMER Pro software generates an output file with extensive analysis capabilities based on the input parameters. These analysis and visualization tools give the end-user important information on various aspects to evaluate the developed energy system. An example of input and output parameters used in HOMER Pro software is presented in *Figure 3-20*.

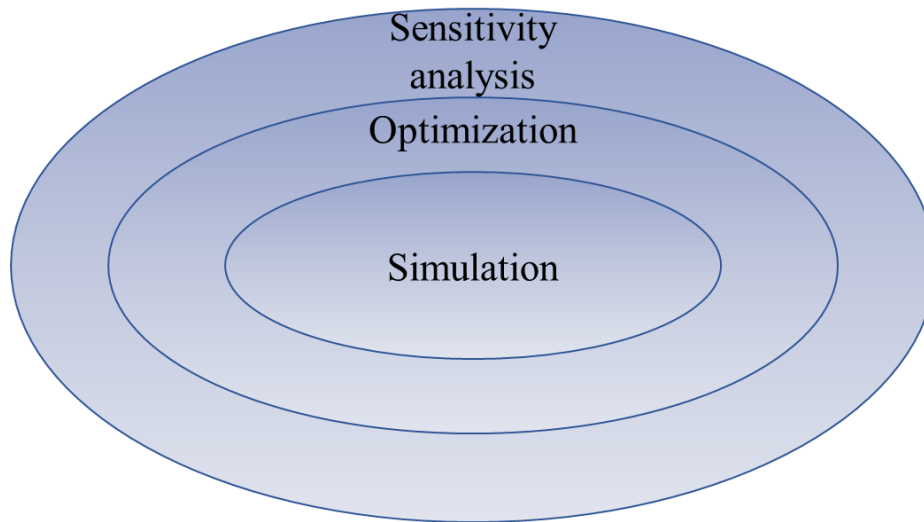


Figure 3-19 Core capabilities of the HOMER Pro software. (Source: Ram et al., 2021)

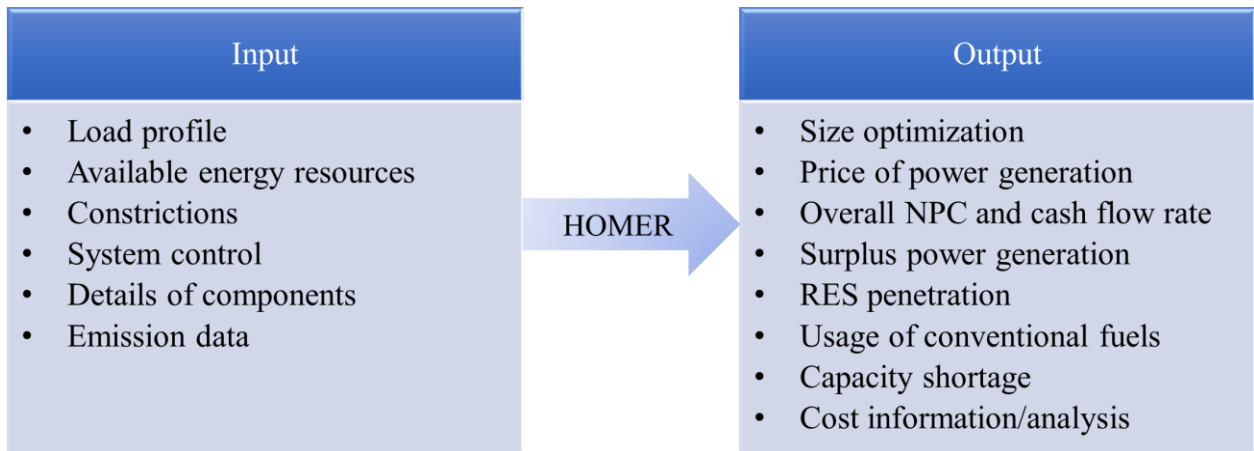


Figure 3-20 Input and output variables in HOMER Pro software. (Source: P. Kumar & Vallabhbai, 2016; Ram et al., 2021)

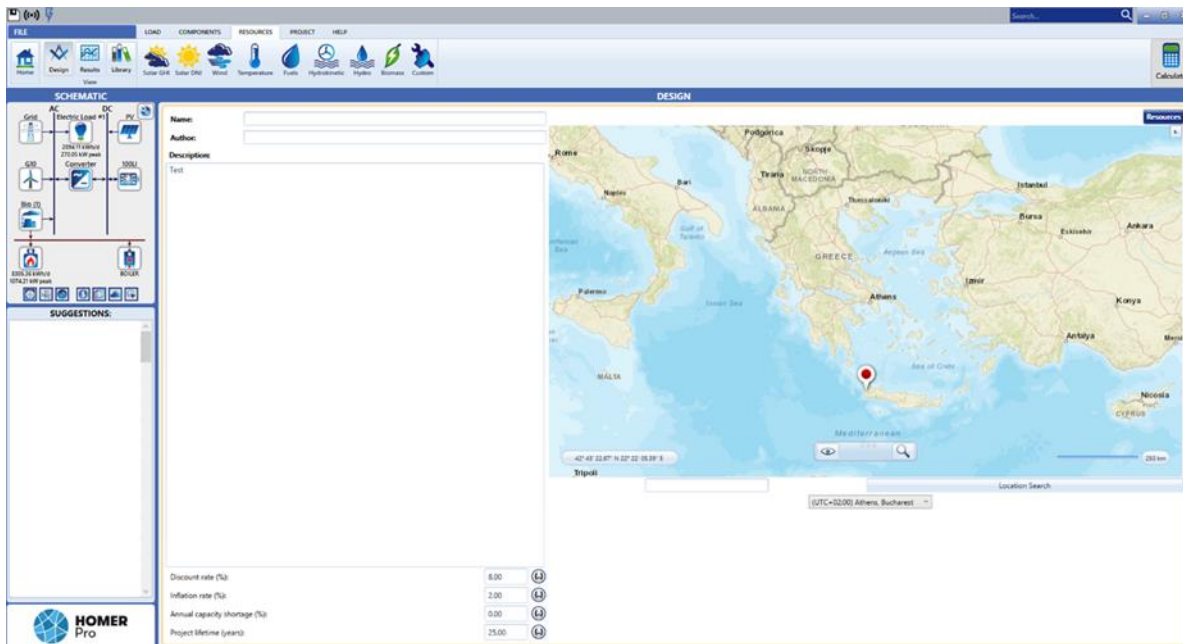


Figure 3-21 Main screen of the HOMER Pro software.

Undoubtedly, HOMER is one of the most used microgrid simulation and optimization software, with users ranging from energy professionals, researchers, policymakers, and students. It can be used for techno-economic analysis with fully customizable projects. It can provide a wide range of HRES components, thus offering the user an extensive library of available tools. An overview of the advantages and limitations of HOMER are presented in Table 3-20.

Table 3-20 Advantages and disadvantages of the HOMER Pro software. (Source: P. Kumar & Vallabhkhair, 2016; Ram et al., 2021)

Software	Advantages	Disadvantages
HOMER	HOMER Pro is freely accessible	Use of imperial units only
	Easy to understand	Daily average time series cannot be imported
	Results in graphical and tabular form	Multiobjective problems cannot be modelled in HOMER Pro. It only allows single objective function for minimizing NPC
	Can handle hourly data	Does not consider depth of discharge in BAT
	Ability to perform sensitivity analysis	Unable to analyze thermal systems
	Off-grid and grid connected power systems modelling capabilities	Does not consider intra-hour variability
	Economic impact of the emissions	Fluctuation in bus voltage is not considered
	Can consider selling or purchasing electricity, to or from, the grid	
Computationally inexpensive		

3.6 LIMITATIONS AND ASSUMPTIONS

As with every research project, software limitations appeared, and logical assumptions were made during this diploma thesis. Some of the most important assumptions made are presented in the following section:

- HOMER Pro software assumes that the gasification ratio remains constant in time; however, it greatly depends on the biomass characteristics, the efficiency of the process, and the load of the gasifier;
- HOMER Pro software assumes the boiler can serve any thermal load that the generator cannot, as well as that the boiler is an existing infrastructure and therefore has no initial cost;
- The boiler uses diesel to meet any unmet thermal loads in case of biomass shortage;
- A fuel mixer is not considered in the simulation;
- The gasifier and the anaerobic digester have a lifetime equal to the generators’;
- The chemical composition of AD is constant and identical for the digestion of tomatoes and MSW;
- of MSW generation is available for energy valorisation;
- Constant daily production of biomass is assumed for the whole duration of the study;
- The heat generated from the CHP unit can be used in the industrial facility (CHP produces heated water to almost 80 °C, whereas the industry requires hot air with temperatures higher than 150 °C);
- The study does not account for changes in electrical and thermal demand with time because of the changes in the production system;
- Social factors (social acceptance) are not considered in the ranking of the systems.

3.7 METHODOLOGY SUMMARY

A summary of the methodological framework developed in this diploma thesis used to design and evaluate a hybrid energy system is presented in *Figure 3-22*. The analytical flowchart is presented in *Appendix C*.

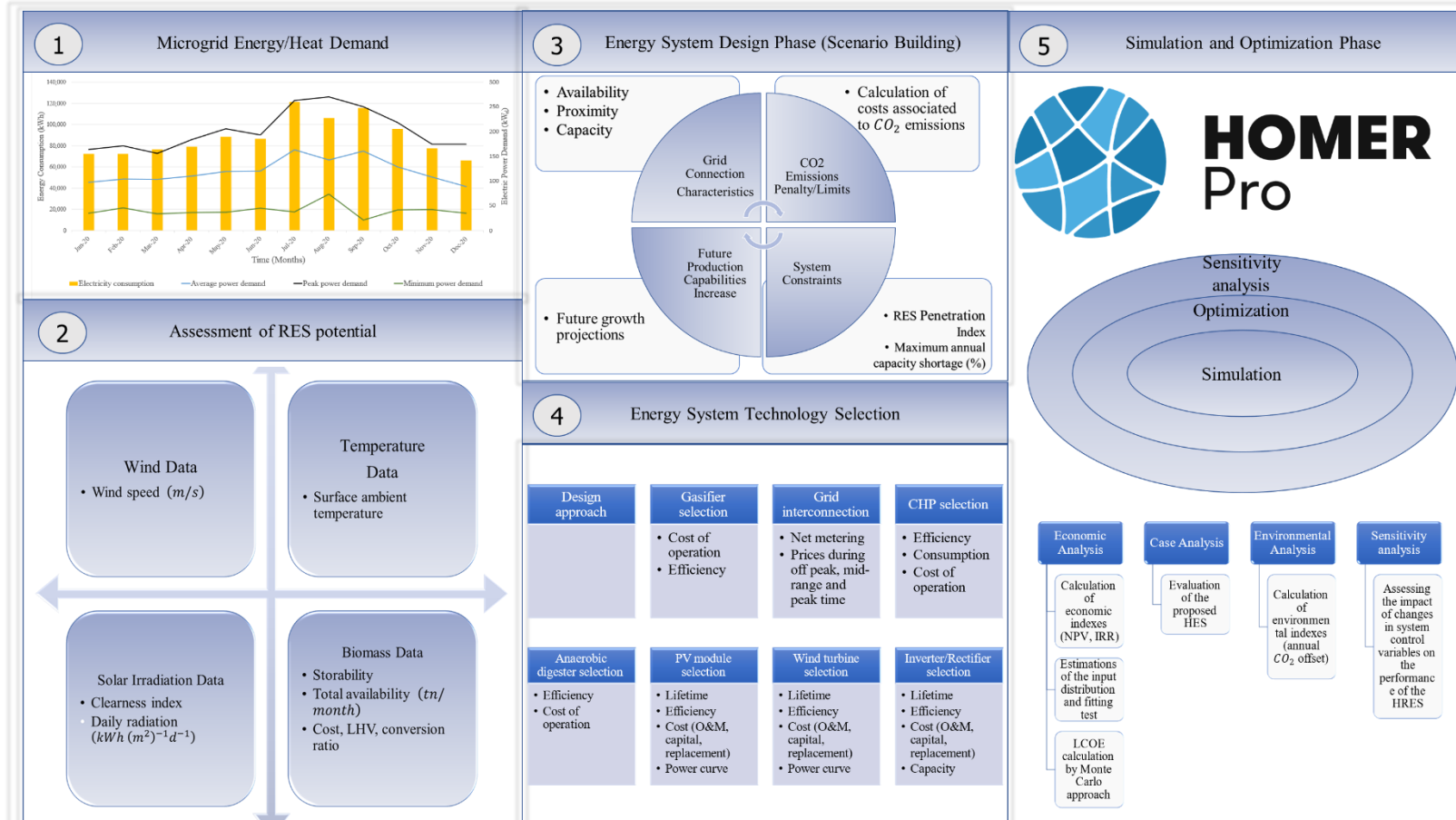


Figure 3-22 Summary of the proposed methodological framework developed.

CHAPTER 4

RESULTS

4.1 HOMER PRO RESULTS

This chapter will provide the details of the studied HRES for the bakery industry located in Crete. This section describes the technical and economic aspects of all the tested configurations. A techno-economic analysis is conducted to determine the optimal system's technology selection, design, and sizing. The optimization of the system has been investigated using the HOMER Pro software. The ranking of the proposed systems is done based on objective parameters such as the NPC of the system. A high renewable fraction is desired along with a lower CDE compared to the baseline system. Section 4.1.1 contains the key findings used to determine the most favorable HRES. Additionally, it provides the results of the baseline energy system. Afterward, an analytical presentation of the optimal energy system is provided in Section 4.1.2. Lastly, the results of the sensitivity analysis are presented in Section 4.1.3.

4.1.1 BASELINE CASE AND SUGGESTED SCENARIOS

To identify the optimal system, the baseline system has to be first described. Therefore, an assessment of the current energy system must precede. The existing energy system consists of a grid connection and internal combustion engines to provide the necessary electricity and heat to the facility. The internal combustion engines utilize diesel for heat production with no generator for further utilizing the combustion of diesel. In HOMER Pro, the set of internal combustion engines is substituted for a boiler. The schematic diagram of the baseline energy system is presented in *Figure 4-1*.

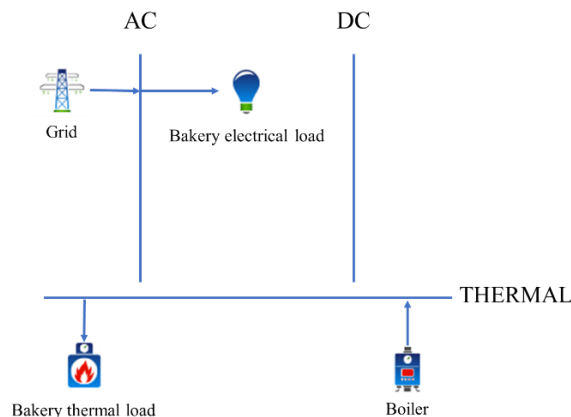


Figure 4-1 Schematic diagram of the baseline system.

The costs of electricity and thermal supply, assuming an energy price of 0.25 €/kWh and a diesel price of 1.555 €/L, for the bakery industry are presented in *Table 4-1*. In the baseline system, 362,4 tons of diesel are consumed to meet the thermal needs of the bakery industry.

Table 4-1 Cost of the baseline case.

Component	Annual energy generation (kWh/year)	C_{ANN} (€/year)	Lifetime (years)	C_{NPC} (€)
Grid electricity	1,056,350	264,087	25	3,413,995
Boiler	3,031,458	563,595	25	7,285,895
Carbon tax	–	276,067	–	3,568,865
Total	–	1,103,750	25	14,268,756

Table 4-1 provides the results obtained from the economic analysis of the baseline system. More importantly, the NPC of the system was found equal to 14.268 million €, where 51 % of the costs are related to diesel purchasing. Apart from the grid and diesel-related costs, emissions penalties for the production of CO₂ are also included. The annual CDE of the system are equal to 3,335.7 tCO_{2eq}. The annualized cost for CDE is equal to 276,067 €, and the total NPC of the CDE for the projects' lifetime was found to be 3,568,865 €, underlying the importance of CDE to the economic performance of the system. In the baseline system, the LCOE and LCOTE are equal to 0.4362 and 0.1859 €/kWh, respectively.

The economic results of the energy system simulations for every scenario, are presented in *Figure 4-2*. More notably, the NPC, initial capital, and CDE are presented for the current energy supply system as well as for the six developed scenarios.

What stands out in *Figure 4.2 a)* is that all the developed hybrid systems offer better economic and environmental performance compared to the current energy supply system. The most interesting aspect of the graph is that the lowest NPC appears in scenarios 1-3, where gasification is the only waste-to-energy technology employed and equals 10,611,356 €. The best-case scenario decreases the NPC by 25.63 % compared to the baseline energy system. By adding AD in the HRES, the decrease of NPC, compared to the baseline system, ranges from 17.92 to 21.87 %. Different BA leads to different BPs, so a different NPC is found. When a combination of gasification and AD is used (scenarios 4-6), it can be seen that in *Figure 4-2 a)*, there is a clear trend of decreasing NPC for increased land usage. This is caused thanks to lower BPs due to higher BA. CAC is higher for scenarios that incorporate AD in the energy system equalling 1.36 million €, whereas, for gasification-only systems, the cost is 13 % lower.

Figure 4-2 (b) provides the LCOE and the carbon avoidance of the current supply and the developed scenarios. The implementation of AD reduces GHG emissions while also providing better economic performance compared to the baseline system; however, it leads to higher energy-related costs compared to the HRESs with gasification only. There was a significant difference between the LCOE of the baseline system and the simulated HRESs. In scenarios 1-3, the LCOE is 0.1533 €/kWh, a 64.86 % decrease compared to the current baseline system. Additionally, scenarios 4-6 have a LCOE equal to 0.2266, 0.1965, and 0.189 €/kWh, respectively. Interestingly, no significant reduction regarding the LCOTE was found between the baseline system and the HRESs of every scenario, a somewhat disappointing result. A possible explanation for this result may be the small decrease of the boiler contribution to the total thermal energy generation. CDE avoidance peaked in scenarios with gasification only in accordance with data from *Figure 4-2 b)*.

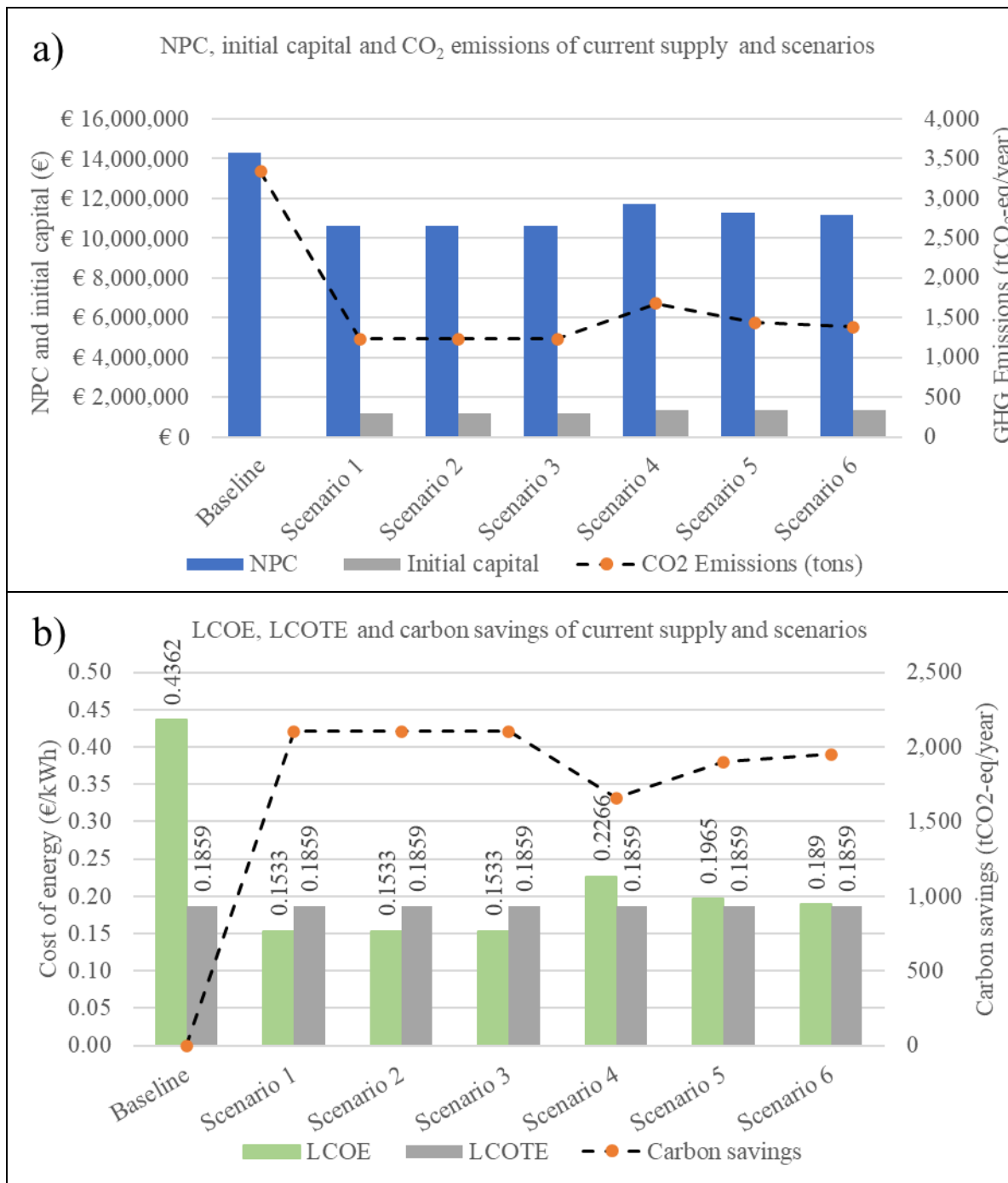


Figure 4-2 a) NPC, initial capital, and CDE of current supply and scenarios b) LCOE, LCOTE and carbon savings of current supply and scenarios.

Using gasification to produce syngas is beneficial for the cost of the HRES while also providing environmental benefits. The use of gasification (scenarios 1-3) provides average annual carbon savings equal to approximately 2,100 tons. Similarly, by adding AD to the technologies employed in the HRES (scenarios 4-6), the decrease in annual CDE ranged from 1,658 to 1,951 tons.

Some valuable remarks regarding electricity generation and the LCOE of every scenario can be derived from *Figure 4-3 a)*. This figure reveals that the electricity generation is dominated by the BG and solar PV for the scenarios incorporating gasification. These two technologies contribute more than 70 % to total energy generation. The energy and the levelized cost of production from WT and solar PV remain unchanged throughout all scenarios. The marginal generation cost of the BG ranges from a minimum of 0.236 €/kWh (scenarios 1-3) to a maximum of 0.31 €/kWh (scenario 4). This can be attributed to the lower BPs in scenarios with OTP-only waste. Additionally, biomass cost dramatically affects the energy production of the BG. BA does not affect the design of the optimal HRES because even in the case of 10 % land utilization, the available feedstock is more than enough to meet the generator's needs. By adding AD, grid purchases increase, and the overall contribution of the BG is reduced.

Regarding *Figure 4-3 b)* some important remarks can be drawn regarding the total thermal generation of every component as well as the renewable fraction of every scenario. This figure shows that the boiler generates most of the thermal energy while the BG only produces a small fraction of the required thermal energy demand. The generator serves almost 5 % of the total thermal load in gasification-only scenarios. By adding AD, the percentage drops to almost 4 %. The renewable fraction is maximized in scenarios 1-3, where it equals 87.9 %. For scenarios incorporating AD, the renewable fraction is decreased, ranging from 71.8 to 82.4 %. The increase in BPs and consequently the decreased average energy output from the BG are the causes of this decline.

Figure 4-3 c) can provide useful remarks concerning every scenario's total annual diesel and biomass consumption. This figure reveals that biomass consumption in gasification-based scenarios is lower than in AD-gasification scenarios. Biomass utilization peaked in scenario 5 with an average biomass consumption of 376 tons/year. Increased biomass consumption in scenarios that include AD but with lower energy generation is caused because the gasification ratio is smaller than the gasification-only counterparts. This is caused because of the assumption that all biomass is utilized from one waste to energy technology equivalent to AD and gasification. The utilization of a biomass resource leads to a reduction in diesel consumption. In scenarios 1-3, diesel consumption dropped by 5 %, which translates to 18,042 litres. Scenarios incorporating both waste-to-energy technologies result in smaller reductions in diesel consumption, ranging from 3.3 to 4.4 % compared to the baseline system.

Table 4-2 summarizes the preliminary results of the simulation from both an energy and economic perspective. As shown in *Table 4-2* the optimal HRES configuration for every scenario consists of the same components, namely the architecture PV/BG/WT is the optimal. Additionally, it can be observed that the sizing of the components is the same across every scenario. What is interesting about the data in this table is that the capacity factor of the BG is higher for the gasification-only scenarios, suggesting a better utilization profile. Additionally, gasification-only scenarios result in lower annual O&M costs compared to scenarios where a combination of AD and gasification is present. The results, shown in *Table 4-2*, indicate a 33.9 % drop in annual O&M costs compared to the baseline energy system.

Table 4-2 Optimization results.

Specification category	Specification	Unit	Best HRES per scenario					
			1	2	3	4	5	6
System architecture	PV	<i>kW</i>	240	240	240	240	240	240
	Wind turbine	<i>quantity</i>	6	6	6	6	6	6
	BG	<i>kW</i>	120	120	120	120	120	120
	Converter	<i>kW</i>	271	271	271	271	271	271
	Dispatch strategy	LC or CC	CC	CC	CC	CC	CC	CC
Cost	LCOE	<i>€/kWh</i>	0.1533	0.1533	0.1533	0.2266	0.1965	0.1890
	LCOTE	<i>€/kWh</i>	0.1859	0.1859	0.1859	0.1859	0.1859	0.1859
	NPC	<i>million €</i>	10.611	10.611	10.611	11.712	11.261	11.148
	Total annual O&M cost	<i>€/year</i>	729,557	729,557	729,557	800,791	765,861	757,125
	Initial CAC	<i>million €</i>	1.180	1.180	1.180	1.360	1.360	1.360
Electrical power production	PV array	<i>kWh/year</i>	436,731	436,731	436,731	436,731	436,731	436,731
	Wind turbine	<i>kWh/year</i>	183,151	183,151	183,151	183,151	183,151	183,151
	BG	<i>kWh/year</i>	419,816	419,816	419,816	229,620	333,115	354,933
	Grid purchases	<i>kWh/year</i>	142,782	142,782	142,782	332,978	229,483	207,665
	Total electricity production	<i>kWh/year</i>	1,182,480	1,182,480	1,182,480	1,182,480	1,182,480	1,182,480
	Unmet load	<i>kWh/year (%)</i>	0 (0)	0 (0)	0 (0)	0 (0)	0 (0)	0 (0)
	Excess electricity	<i>kWh/year (%)</i>	0 (0)	0 (0)	0 (0)	0 (0)	0 (0)	0 (0)
Thermal power production	BG	<i>kWh/year</i>	150,905	150,905	150,905	99,007	129,721	134,013
	Boiler	<i>kWh/year</i>	2,880,553	2,880,553	2,880,553	2,932,450	2,901,736	2,897,444
	Total thermal production	<i>kWh/year</i>	3,031,458	3,031,458	3,031,458	3,031,458	3,031,458	3,031,458
Fuel consumption	Diesel consumption	<i>L/year</i>	344,399	344,399	344,399	350,604	346,932	346,418
	Biomass consumption	<i>tons/year</i>	307	307	307	356	376	363
Capacity factor	PV array	%	20.8	20.8	20.8	20.8	20.8	20.8
	Wind turbine	%	34.8	34.8	34.8	34.8	34.8	34.8
	BG	%	39.9	39.9	39.9	21.8	31.7	39.9
	Converter	%	17.5	17.5	17.5	17.5	17.5	17.5

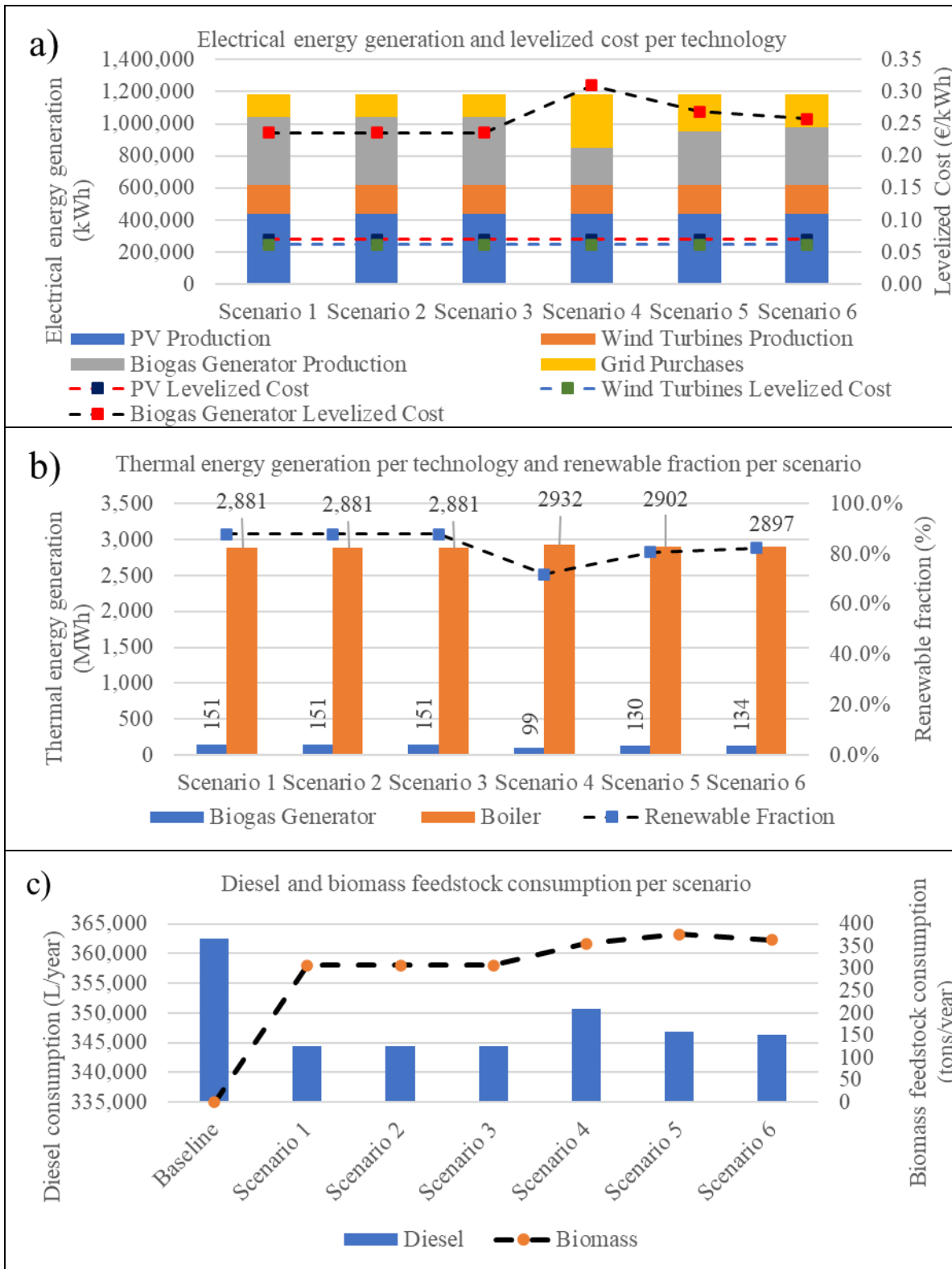


Figure 4-3 a) Electrical energy production for every scenario and levelized cost per technology, b) thermal energy production per technology and renewable fraction for every scenario, and c) diesel and biomass consumption per scenario.

4.1.2 OPTIMAL SYSTEM ARCHITECTURE

The optimal design of the HRES for the current study consists of different components. The most optimal HRES to meet the load demands of the industrial facility comprises of a $240 kW_p$ PV array, a $120 kW_p$ biogas generator (gasifier only), $60 kW_p$ WT, and a $271 kW$ converter. This system is the best configuration simulated, presenting the lowest NPC across all simulations. The optimal system technology selection is based on Scenarios 1-3 where the valorisation of OTP waste for syngas production is used. The system architecture is summarized in *Table 4-3*.

Table 4-3 System architecture.

<i>Component</i>	Name	Size	Unit
<i>Generator</i>	Generic Biogas Genset (size-your-own)	120	<i>kW</i>
<i>PV</i>	Generic flat plate PV	240	<i>kW</i>
<i>Wind turbine</i>	Generic 10 kW	6	<i>quantity</i>
<i>Converter</i>	System converter	271	<i>kW</i>
<i>Boiler</i>	Generic Boiler	1	<i>quantity</i>
<i>Grid</i>	Grid	999,999	<i>kW</i>
<i>Dispatch strategy</i>	HOMER Cycle Charging	–	–

A comparison of scenario 1 with the current energy system shows that the transition to the optimal HRES system described in *Table 4-3* has a present worth equal to 3,657,401 €, indicating that the proposed HRES compares favourably as an investment option with the baseline system. The annual worth equals 282,916 €. Additionally, an internal rate of return (IRR) and the return on investment (ROI) of the transition equals 31.5 % and 27.9 %, respectively. The simple and discounted payback times equal 3.17 and 3.62 years, respectively. The relatively low payback times signify good economic performance.

A schematic diagram of the proposed HRES, containing all the components, is shown in *Figure 4-4 (left)*. Furthermore, in *Figure 4-4 (right)*, a comparison between the cumulative discounted cash flows is presented, highlighting that the optimal system offers better economic performance compared to the baseline case.

The results of the optimization process revealed that the proposed HRES requires an initial investment equal to 1.18 million €. Additionally, regarding the environmental performance of the system, in total $2,103 tCO_{2eq}$ are prevented from being released into the atmosphere annually, signifying great environmental performance.

The results, as shown in *Table 4-4*, indicate that the optimal HRES offers competitive economic performance despite the high initial investment cost of the installation. More specifically, the best optimized HRES offers a NPC equal to 10.611 million € and a competitive LCOE equal to 0.1533 €/kWh, a decrease of 64.86 % compared to the baseline energy system. This indicates that electricity is cheaper by 0.2829 €/kWh, and the industry owners can save almost 300,000 € annually by implementing the proposed HRES, as electricity consumption for 2020 equaled 1,057 MWh. The annual savings regarding electricity consumption can increase as energy prices increase due to potential energy crises. Another critical finding is that LCOTE is not affected by HRES integration. Therefore, no economic benefit appears regarding thermal energy generation aside from fuel-related costs.

Table 4-4 Optimal system economics.

Metric	Value	Unit
NPC	10,611,360	€
Levelized cost of electricity	0.1533	€/kWh
Initial CAC	1,180,000	€

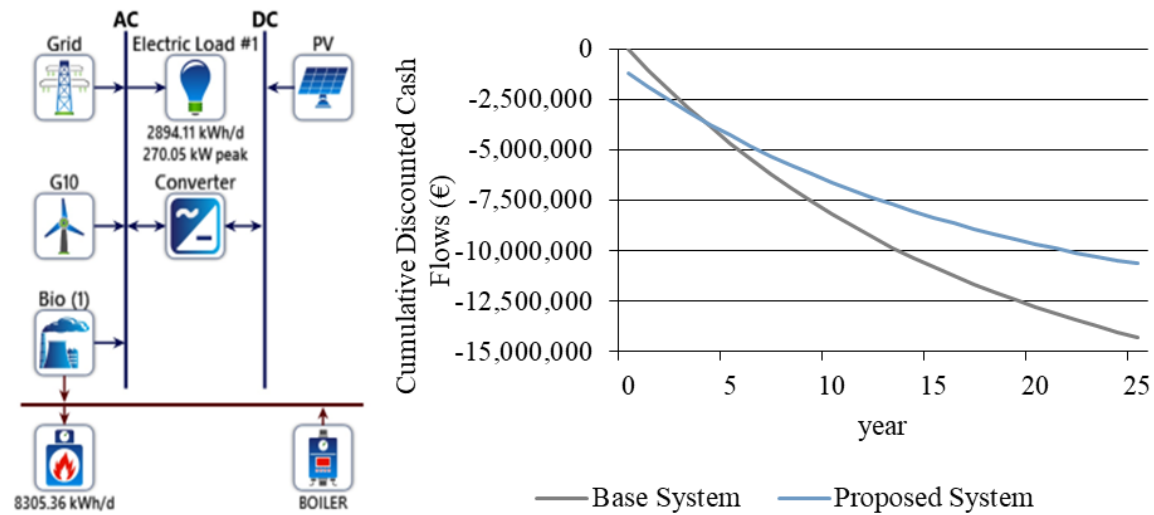


Figure 4-4 Schematic of the system (left), comparison of cumulative discounted cash flows (right).

4.1.2.1 COST SUMMARY

In Table 4-5, the capital, operating, replacement, and resource costs are presented for every component. What stands out in this table is that the biggest contributor to the initial investment cost is the generator with a gasification unit. In total, the BG has an NPC equal to 1.60 million €. The O&M costs of the generator are the highest, with a total NPC equal to 0.722 million €. The total NPC of the carbon tax equals 1.30 million €, contributing by more than 10 % to the total NPC. The resource-related costs are dominated by the generator and the boiler.

Figure 4-5 a) presents a cost summary of the optimized HRES for selected components. More specifically, it reveals that most of the costs are related to the generator, boiler, and carbon taxes. Almost 59 % of the total CAC was due to the biogas generator and the cost of CHP integration. Replacement costs appear to be zero because every system component has a lifetime higher than 25 years. What is interesting about the data in Figure 4-5 a) is that more than 68 % of the total NPC is directly connected to fuel costs. This can be justified by the fact that the thermal demand in this case study is higher compared to the electrical power demand. Another interesting result from this figure is that during the lifetime of this project, carbon tax costs represent a significant portion of the operating costs.

The cash flow for the HRES components over the project lifetime is presented in *Figure 4-5 b*). Additionally, what stands out in *Figure 4-5 b*) is the existence of an initial cost related to the system adaptation costs. The modification of the existing infrastructure (e.g., installing a heat exchanger and pipes) is required to operate a CHP unit, which results in a capital investment cost at the beginning of the project. This cost includes purchasing and installing the necessary equipment to utilize waste heat from the CHP unit. This figure also shows that the main source of costs throughout the years comes from the boiler and the BG. On the other hand, RES components (WT, PVs) have a small contribution to the total NPC of the HRES.

In *Figure 4-5 c*), cash flows by cost type over the project lifetime are presented. From the data in *Figures 4-5 b*) and *c*), it is apparent that during the lifetime of the project, the cash flows are constant and non-changing because every component has a lifetime higher or equal to 25 years. Another significant finding is that most of the costs on a yearly basis are mainly fuel-related. Lastly, in the final year of the study, a positive cash flow can be observed due to the remaining value of the BG (assuming linear depreciation).

Table 4-5 NPCs.

<i>Component</i>	Name	Capital	Operating	Replacement	Salvage	Resource	Total
<i>Wind turbine</i>	Generic 10 kW	€120,000	€24,821	€0.00	€0.00	€0.00	€144,821
<i>PV array</i>	Generic flat plate PV	€360,000	€31,026	€0.00	€0.00	€0.00	€391,026
<i>Generator</i>	Generic Biogas Genset	€600,000	€702,367	€0.00	-€27,531	€333,924	€1.61M
<i>Grid</i>	Grid	€0.00	€124,390	€0.00	€0.00	€0.00	€124,390
<i>Boiler</i>	Generic Boiler	€0.00	€0.00	€0.00	€0.00	€6.92M	€6.92M
<i>Carbon tax</i>	Carbon tax	€0.00	€1.32M	€0.00	€0.00	€0.00	€1.32M
<i>Fixed cost of CHP generator</i>	–	€100,000	€0.00	€0.00	€0.00	€0.00	€100,000
<i>Summary</i>	System	€1.18M	€2.20M	€0.00239	-€27,531	€7.26M	€10.6M

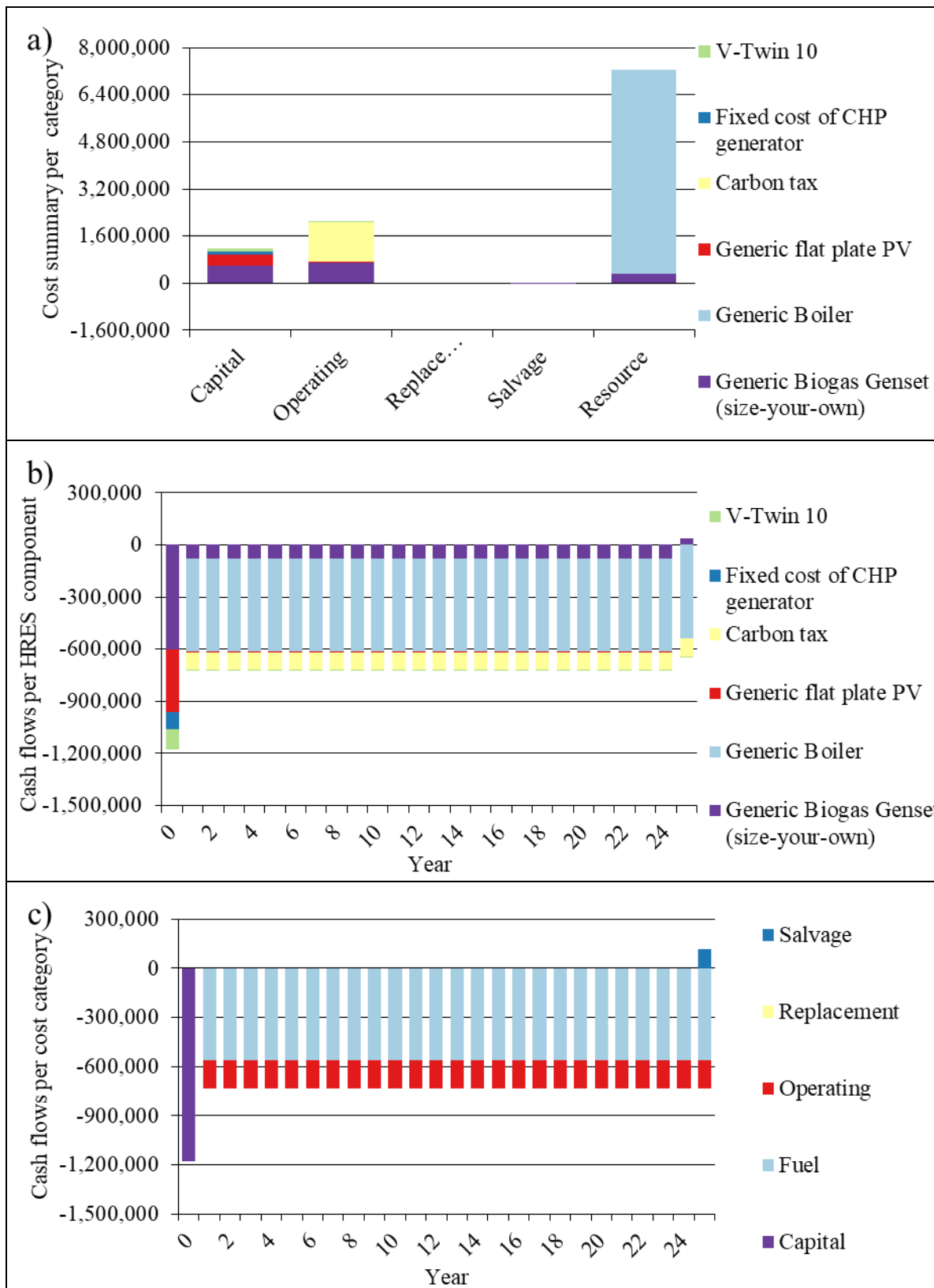


Figure 4-5 Cost flows of the optimal system.

4.1.2.2 ELECTRICAL DEMAND SUMMARY

The industrial site requires, on average, 2,894 kWh/day and has a peak of 270 kW_{el}. The monthly electrical power generation of each component comprising the optimal HRES is presented in Figure 4-6. Data from Figure 4-6 can be compared with the data in Figure 3-3, which shows that the monthly electricity generation matches (or even surpasses) the monthly electricity consumption.

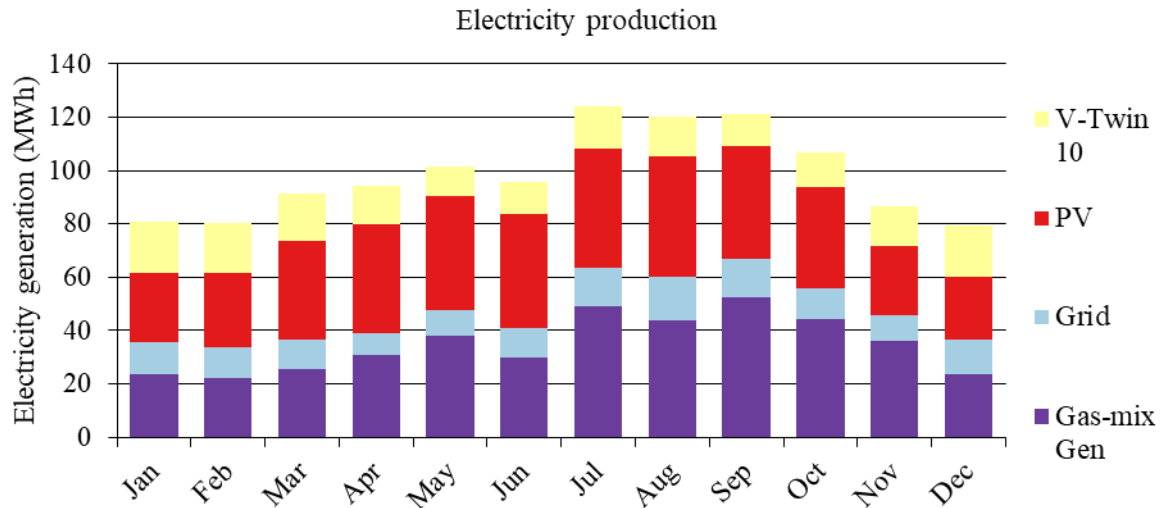


Figure 4-6 Monthly electrical energy production per technology.

Figure 4-6 and Table 4-6 clearly show the dominance of PV and biogas generator in electricity generation. More specifically, 36.9 % of the total electricity production comes from the 240 kW_p PV array. Additionally, the 120 kW_{el} BG operates throughout the year according to the load and the generation from non-dispatchable sources and produces 35.5 % of the total electricity demand. Lastly, 12.1 and 15.5 % of the total electricity production is purchased and produced from the grid and WT, respectively. Figure 4-6 reveals that wind energy production remains relatively unchanged throughout the year. In addition, grid electricity purchases reached a peak point during the summer when the energy demand peaked.

The average output of the WT equals 20.9 kW, whereas the solar PV average power output is equal to 49.9 kW or 1,197 kWh/day. The BG's mean electrical output is found to be 102 kW, with a 41.0 % mean electrical efficiency.

Shortages are not allowed, and therefore 0 kWh/year of unmet electric load appears in the proposed HRES.

Table 4-6 Electricity production summary.

Component	Name	Production (kWh/year)	Percent of total production (%)
Generator	Biogas Genset	419,816	35.5
	Generic flat plate PV	436,731	36.9
Wind turbine	V-Twin 10	183,151	15.5
Grid	Grid	142,782	12.1
Total	-	1,182,480	100

What can be clearly seen in *Figure 4-8 a)* is the general pattern of PV electricity production throughout the year. PV electricity production reached a peak during the summer. Additionally, a close inspection of the data shown in this figure shows that PV power production mainly took place between 06:00 and 18:00. It is also evident that more extended electricity production periods can be observed during the summer. Also, during the winter months, PV production is dramatically reduced, probably due to lower solar radiation striking the earth's surface and bad weather conditions (cloud coverage). The total number of operational hours for the PVs was 4,282; therefore, a PV array in the study area generates energy for 12 hours per day on average. The specific yield of the PV array was found equal to $1,820 \text{ kWh/kW}_p$, confirming the high solar potential in the study area. Moreover, the marginal cost of energy generation from solar PV is equal to 0.0693 €/kWh . This value is higher compared to other studies because, as abovementioned, for PV installations in Greece higher than 100 kW_p rated capacity, the construction of a substation is mandatory, thus increasing the marginal cost of energy generation.

Regarding WT, the power output throughout the year is illustrated in *Figure 4-8 b)*. What stands out in *Figure 4-8 b)* is the variability of wind turbine electricity production throughout the year. No specific pattern can be observed for wind power generation due to the volatile nature of wind; however, the highest reported value is equal to 60.5 kW . The average WT power output equaled 20.9 kW with a capacity factor equal to 34.8 %. The levelized cost of electricity regarding WT is equal to 0.0612 €/kWh . This value is considerably lower compared to values reported in the literature. This result may be explained by the fact that the CAC of WT used in this study is lower compared to the rest of the literature. Wind penetration is lower than the other technologies due to the lower total rated capacity of employed WT. This is a consequence of the Greek law limiting WT construction near populated areas.

Concerning BG, the general pattern of electric power output throughout the year is presented in *Figure 4-8 c)*. Energy generation periods are mainly located during the early and late hours of the day when electricity production from PV is zero. During the morning hours, when solar PV energy generation is low, the generator is used to cover part of the electric power demand of the facility. It is apparent from *Figure 4-8 c)* that the biogas generator was likely to deliver its maximum electrical output during the morning hours. The number of starts per year is equal to 517. This number is high due to this generator's high minimum load ratio. The generator operates at 39.9 % of its rated capacity, indicating that it can still generate electricity and heat if the industry's energy demands increase in the future. Lastly, during the summer, electricity generation from the generator peaks, a direct effect of the higher energy consumption during the summer months.

Figure 4-7 provides an example of the electrical power output of every component for a typical week (19th week). This figure shows that the BG operates during off-peak times when PV production is low. Additionally, it shows that excess electricity is produced during the daytime when PV power generation peaks.

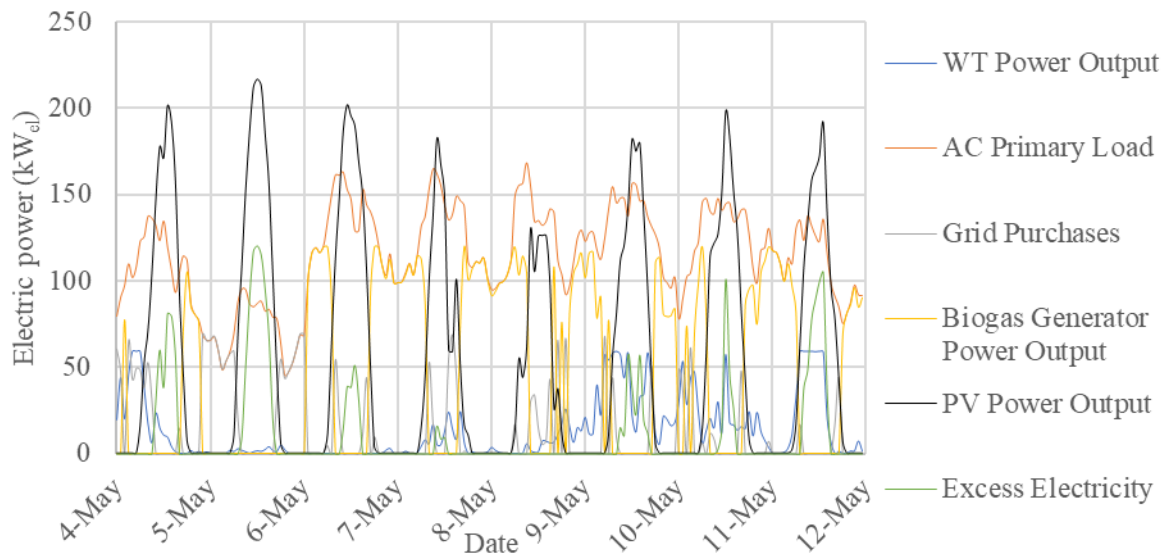
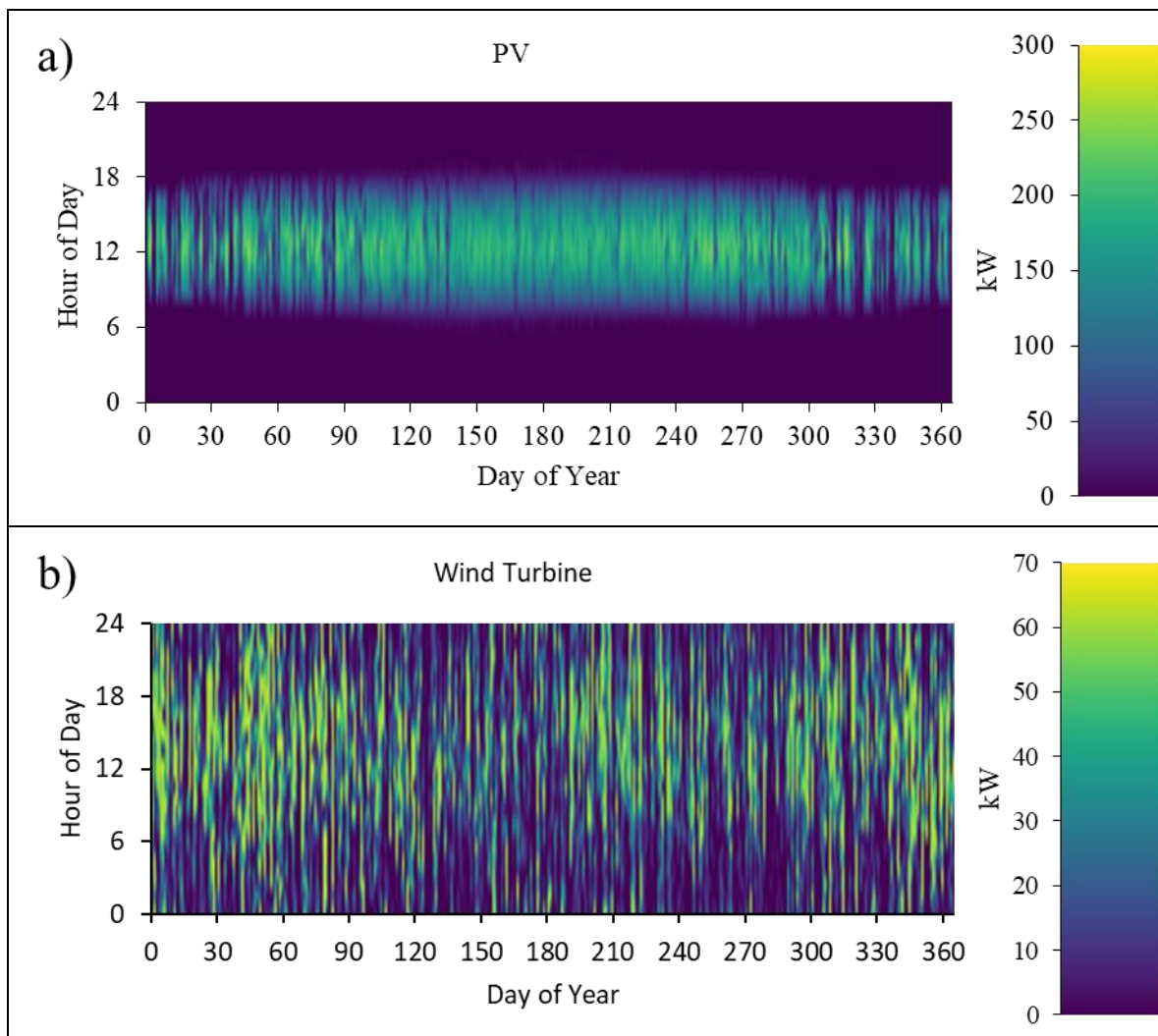


Figure 4-7 Hourly electrical power generation according to HOMER for a typical week (19th week)



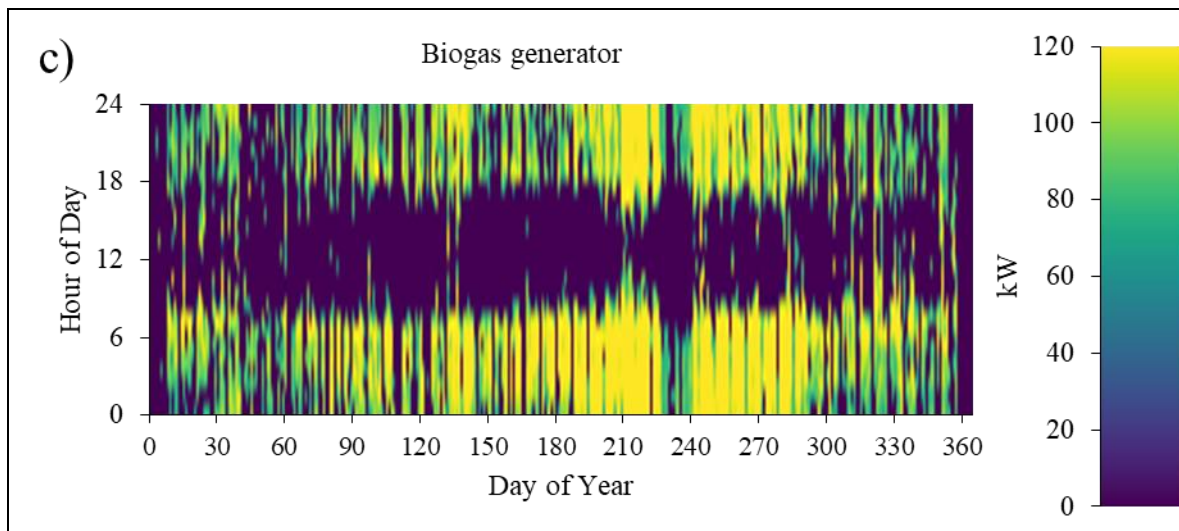


Figure 4-8 Data maps for electricity production of every component of the proposed HRES.

4.1.2.3 THERMAL DEMAND SUMMARY

The industrial site requires, on average, 8,294 kWh/day and has a peak of 1,074 kW_{th}. The monthly thermal power generation of each component comprising the optimal HRES is presented in Figure 4-9. Data from Figure 4-9 can be compared with the data in Figure 3-7, which shows that the monthly heat generation matches the monthly heat consumption.

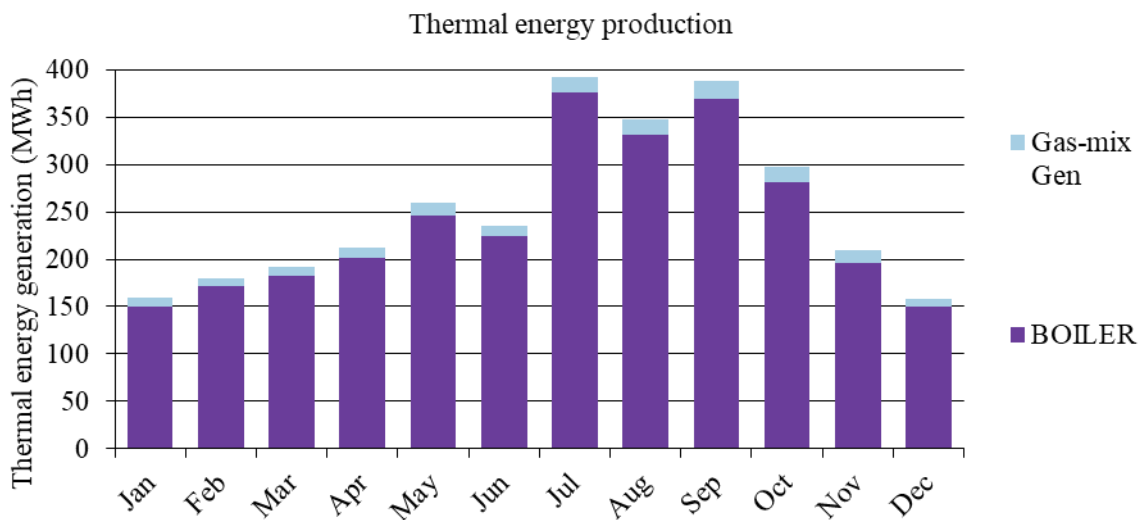


Figure 4-9 Monthly thermal energy production per technology.

It is evident from Figure 4-9 that thermal power generation is dominated by the boiler. According to Figure 4-9 and Table 4-7, only 4.98 % of the thermal energy is produced from the BG. It is apparent from Figure 4-9 that thermal energy production experiences phenomenal growth during the summer months. This is caused by the increased production needs during the summer period.

During the summer months, the contribution of the boiler is increased and reaches a peak during July when more than 95 % of the thermal energy consumption is supplied from the boiler.

Table 4-7 Thermal energy production summary.

<i>Component</i>	<i>Name</i>	<i>Production</i>	<i>Percent of total production</i>	<i>Unit</i>
<i>Generator</i>	Biogas Genset	150,905	4.98	<i>kWh/year</i>
<i>Boiler</i>	Generic Boiler	2,880,553	95.02	<i>kWh/year</i>
<i>Total</i>	-	3,031,458	100	<i>kWh/year</i>

Figure 4-10 provides an example of the thermal power output of every component for a typical week (19th week). This figure shows the small contribution of the BG regarding thermal power generation. This graph also indicates that the BG works supplementary with the boiler instead of aiming to replace it.

Figure 4-11 illustrates the thermal power output of the BG and boiler for one year. What stands out in Figure 4-11 a) and b) is the difference between the thermal energy production between the generator and the boiler. The boiler mainly produces thermal energy during peak thermal power demand hours, whereas the BG is utilized during off-peak hours. The mean output of thermal energy from the boiler is found to be $329 kW_{th}$, with a peak value higher than $1,000 kW_{th}$. The boiler works to provide the thermal energy when the BG cannot provide enough at full utilization. This is the case during the summertime when the BG reaches a peak thermal output of $41.5 kW_{th}$. During the daytime, when solar PV power output peaks, the CHP unit is not being utilized because it produces extra electricity that cannot be used from the industrial facility. Therefore, it is cheaper to resort to thermal power produced from the boiler. Additionally, the BG operates for 4,116 hours/year, whereas the boiler operates for 8,305 hours/year. Therefore, a significant result is that the generator works supplementary rather than replacing the boiler entirely.

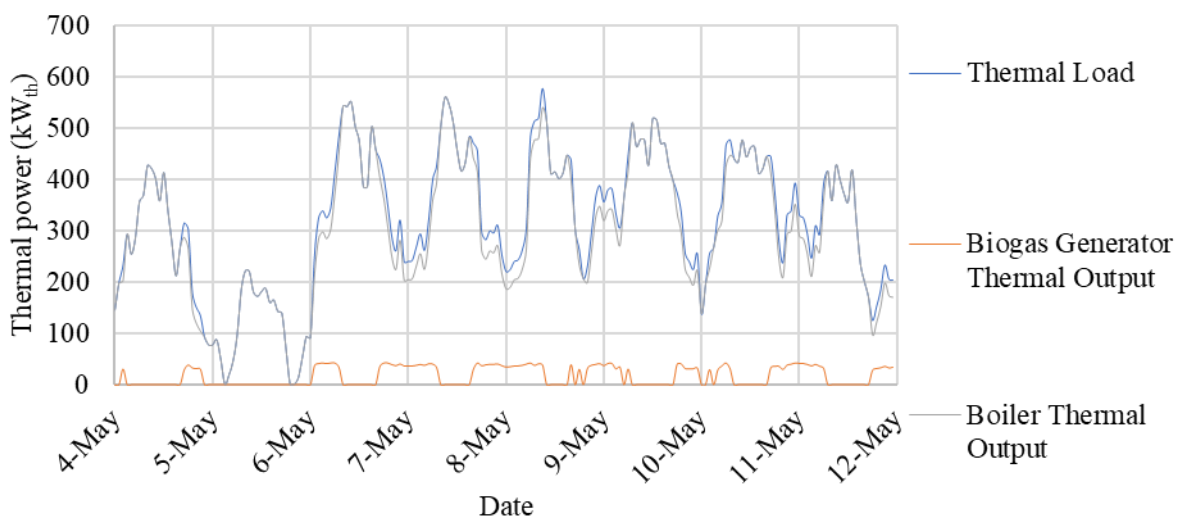


Figure 4-10 Hourly thermal power generation according to HOMER for a typical week (19th week).

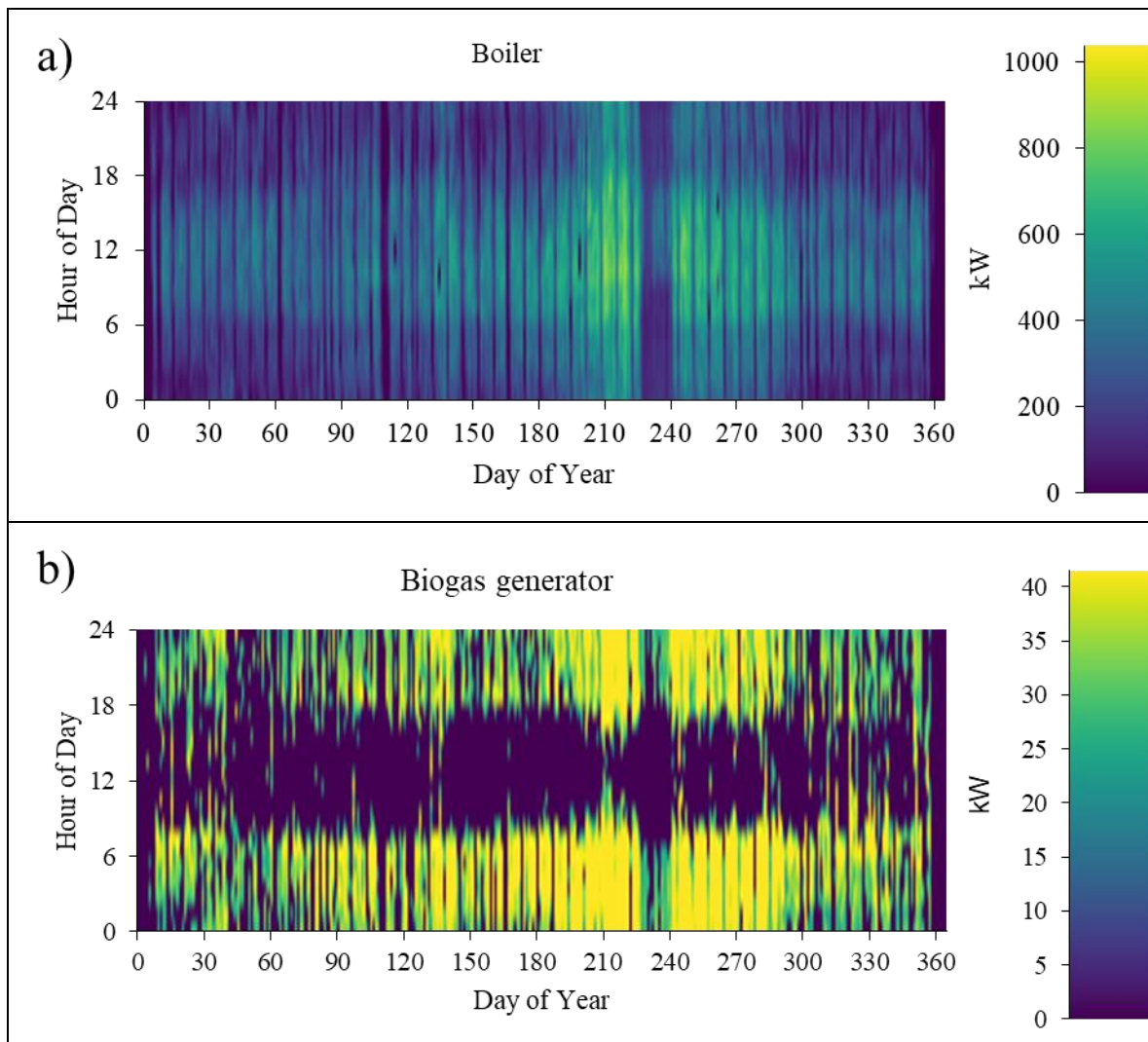


Figure 4-11 Data maps for thermal energy production of every component of the proposed HRES.

4.1.2.4 FUEL SUMMARY

During a year, a total of 307 tons of biomass feedstock, to produce the gas mix used by the CHP, are consumed to meet part of the electric and thermal needs of the industry. Diesel consumption is reduced compared to the baseline energy system at just 344,399 litres, a 4.98 % drop in diesel consumption. The biogas and diesel consumption patterns are the same as the thermal output of the BG and boiler, respectively.

Table 4-8 reveals that the average feedstock consumed per day is equal to 0.842 tons, which is lower than the daily available biomass feedstock with 10 % land utilization of olive trees. The most striking result to emerge from the data presented in Table 4-8 is that the utilization of more land does not provide any economic benefit. Interestingly, just 3 % of land utilization of the olive-derived waste can serve the needs of the generator of this system.

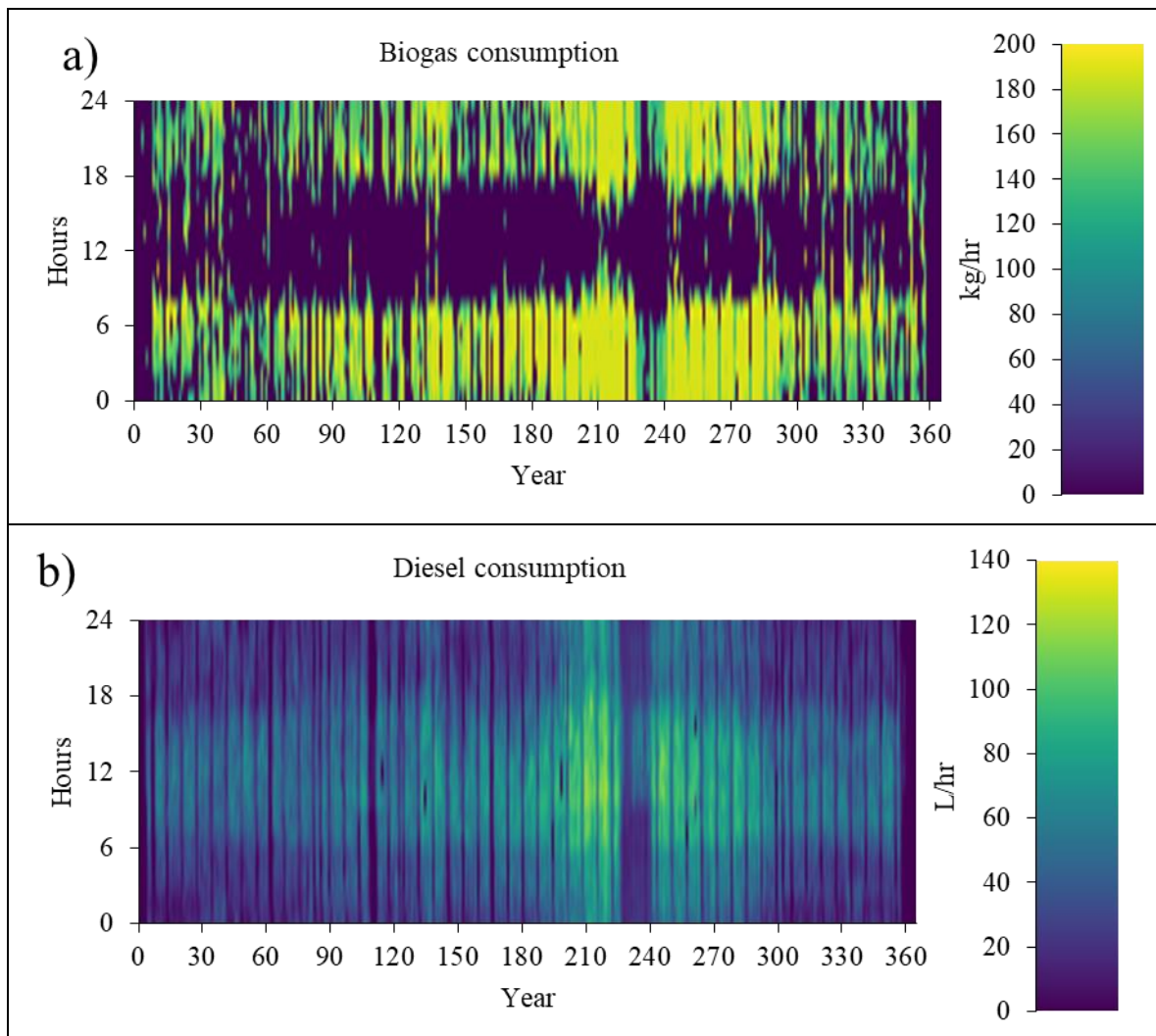


Figure 4-12 Data maps for biogas and diesel consumption.

Table 4-8 Fuel consumption summary.

	Quantity	Value	Unit
Biogas	Total feedstock consumed	307	tons/year
	Average feedstock per day	0.842	tons/day
Diesel	Total fuel consumed	344,399	L/year
	Average fuel per day	944	L/day

4.1.2.5 GRID

Table 4-9 presents an overview of the monthly net energy purchases. This table shows that the annual energy purchased from the grid is 142,782 kWh and the annual energy sold to the grid is 104,294 kWh.

What stands out in *Table 4-9* is the negative values during the Spring months. This is a result of the HRES generating more energy than the actual energy consumption of the industrial facility. This happens when non-dispatchable RES components such as PVs and WT produce more energy than the industrial facility's energy needs.

Table 4-9 Grid monthly summary.

<i>Month</i>	Energy purchased (kWh)	Energy sold (kWh)	Net energy purchased (kWh)	Peak load (kW)	Energy charge	Demand charge	Total
<i>January</i>	12,116	11,006	1,110	68.9	€0.00	€0.00	€0.00
<i>February</i>	11,899	8,739	3,160	68.8	€0.00	€0.00	€0.00
<i>March</i>	11,048	13,308	-2,260	68.9	€0.00	€0.00	€0.00
<i>April</i>	8,157	12,966	-4,809	69.1	€0.00	€0.00	€0.00
<i>May</i>	9,372	8,673	699	69.1	€0.00	€0.00	€0.00
<i>June</i>	11,075	9,368	1,707	69.1	€0.00	€0.00	€0.00
<i>July</i>	14,336	3,729	10,606	103	€0.00	€0.00	€0.00
<i>August</i>	16,354	9,542	6,813	97.3	€0.00	€0.00	€0.00
<i>September</i>	14,263	3,735	10,528	85.8	€0.00	€0.00	€0.00
<i>October</i>	11,243	6,750	4,494	83.3	€0.00	€0.00	€0.00
<i>November</i>	9,600	6,632	2,967	68.6	€0.00	€0.00	€0.00
<i>December</i>	13,319	9,846	3,474	68.9	€0.00	€0.00	€0.00
<i>Annual</i>	142,782	104,294	38,489	103	€9,622	€0.00	€9,622

The trend of energy purchases and sales from or to the grid throughout a year is shown in *Figure 4-13*. From data presented in *Figure 4-13 a)*, most energy purchases happen in the morning and evening when PV energy generation is at its lowest. The highest reported value of electrical load received from the grid is equal to 103 kW_{el} , and it occurred during July. The results, as shown in *Table 4-9* and *Figure 4-13 a)*, indicate that the optimal HRES lowered grid dependency considerably.

On the contrary, energy sales to the grid occur more frequently during the daytime, when electricity demand is at its highest. During the summer, when the energy requirements of the industrial plant increase, the frequency and overall amount of energy purchases from the grid also peak.

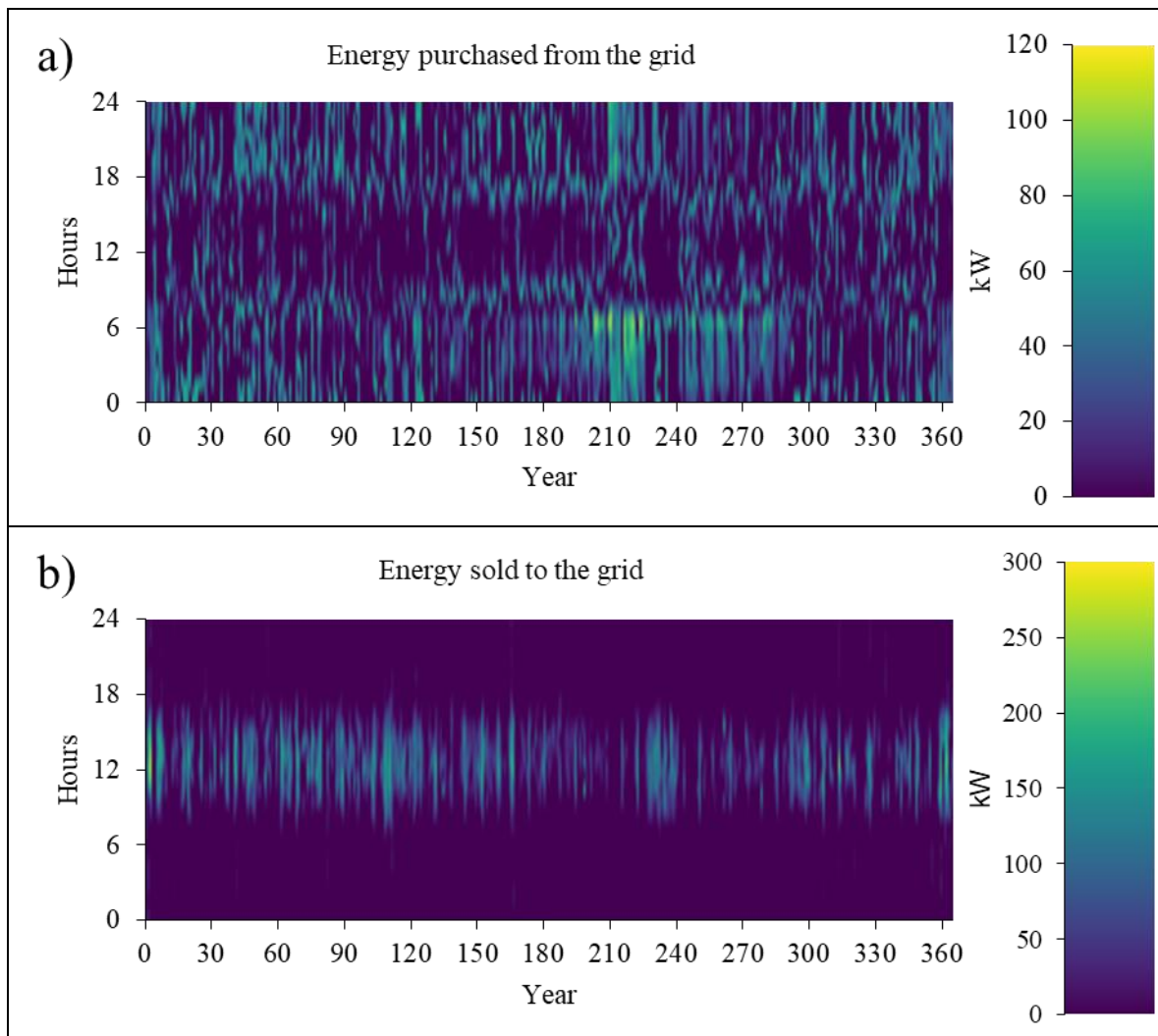


Figure 4-13 Data maps for energy purchases and sales from or to the grid.

4.1.3 SENSITIVITY ANALYSIS

To investigate the effects of different factors on the performance, a sensitivity analysis was performed. The LCOE, LCOTE, IRR, CDE, renewable fraction, and the contribution of the BG to the energy mix are the metrics that have been used to assess the impact of specific uncertainties on the best-case scenario. The sensitivity analysis was performed on the optimal energy system proposed by HOMER Pro. This optimal system consists of $240 kW_p$ of PVs, $60 kW_p$ of WT and a generator (gasifier-included) with a capacity of $120 kW_p$.

Due to the nature of renewable energy systems, uncertainties are always present. The cost of energy, diesel, CE, biomass, and the average daily electrical and thermal load significantly impact the HRES' economic and environmental performance. These are the system control variables that significantly affect the system outputs and operating costs. The system control variables and their relative variation from the baseline scenario are presented in *Table 4-10*.

The impact of these parameters is assessed in the following subsections.

Table 4-10 List of sensitivity analysis variables.

<i>Sensitivity variable</i>	Range of value values (step size 10%)	Unit
<i>BP</i>	[-50%, 50%]	€/kWh
<i>Average daily energy and heat demand</i>	[-50%, 50%]	kWh/day
<i>Grid energy price</i>	[-50%, 50%]	€/ton
<i>Carbon emissions penalty</i>	-100% and [-50%, 50%]	€/tCO _{2eq}
<i>Diesel fuel price</i>	[-50%, 50%]	€/litre

4.1.3.1 SENSITIVITY ANALYSIS FOR BIOMASS PRICE

The connection between the economic performance of the suggested HRES and the price of biomass is shown in *Figure 4-14*. The LCOE witnessed an upward trend, whereas the IRR index dropped for increased BPs. As observed, a 50 % decrease in the BP results in a 1.8 % increase in IRR and an 11.35 % drop in the LCOE. Similarly, an increase in biomass prices drives energy generation costs while simultaneously lowering the IRR of the proposed HRES. The results, as shown in *Figure 4-14*, indicate that the optimal HRES proposed offers better economic performance than the baseline system. The current discount rate employed in this study is lower than the IRR index, which indicates better economic performance.

Figure 4-15 presents the effects of changes in BP concerning the CDE and the renewable fraction. Similar patterns involving the CDE, and the renewable fraction may be seen in *Figure 4-15*. The CDE exhibited an upward trend, whereas the renewable fraction decreased following the rising of BPs. The CDE varied from 1,169 to 1,319 tons, whereas the renewable fraction ranged from 84.8 to 90.2 %, indicating better environmental performance for lower BPs. Increased CDE indicates higher grid dependability, and as *Figure 4-15* illustrates the renewable fraction decreases as BPs increase.

Figure 4-16 illustrates the effects of variations in the BP concerning the total contribution of the BG. What stands out in this figure is that increased BP results in lower overall usage of the BG and, therefore, more grid purchases occur. Reduced use of BGs increases reliance on the grid and boilers to supply the necessary electrical and thermal energy, thus resulting in a higher overall environmental impact of the proposed HRES.

Table 4-11 Summary of the results in BP sensitivity analysis.

Metric	% Change of reference scenario	Cost of biomass (€/ton)	Levelized Cost Of Electricity (LCOE)	Internal Rate of Return (IRR)	CO ₂ Emissions (tons)	Renewable Fraction (%)	BG electricity production (%total)	BG thermal energy production (%total)
	-50%	42.03	0.1359	33.3%	1,169	90.2%	37.8%	5.34%
	-40%	50.44	0.1392	32.9%	1,180	89.8%	37.4%	5.28%
	-30%	58.84	0.1427	32.6%	1,192	89.4%	37.0%	5.21%
	-20%	67.25	0.1461	32.2%	1,204	89.0%	36.5%	5.14%
	-10%	75.65	0.1495	31.9%	1,217	88.5%	36.1%	5.07%
	0%	84.06	0.1533	31.5%	1,233	87.9%	35.5%	4.98%
	10%	92.47	0.1568	31.1%	1,248	87.4%	35.0%	4.90%
	20%	100.87	0.1602	30.8%	1,261	86.9%	34.5%	4.82%
	30%	109.28	0.1638	30.4%	1,278	86.3%	33.9%	4.73%
	40%	117.68	0.1677	30.0%	1,298	85.6%	33.2%	4.62%
	50%	126.09	0.1716	29.6%	1,319	84.8%	32.4%	4.51%

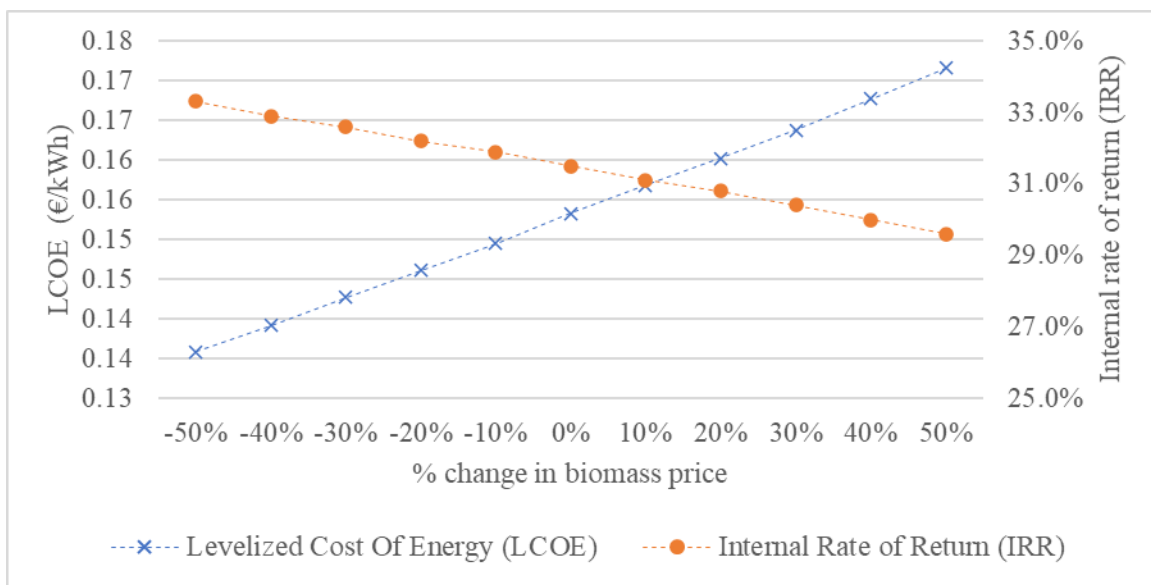


Figure 4-14 The effect of the BP on LCOE and IRR.

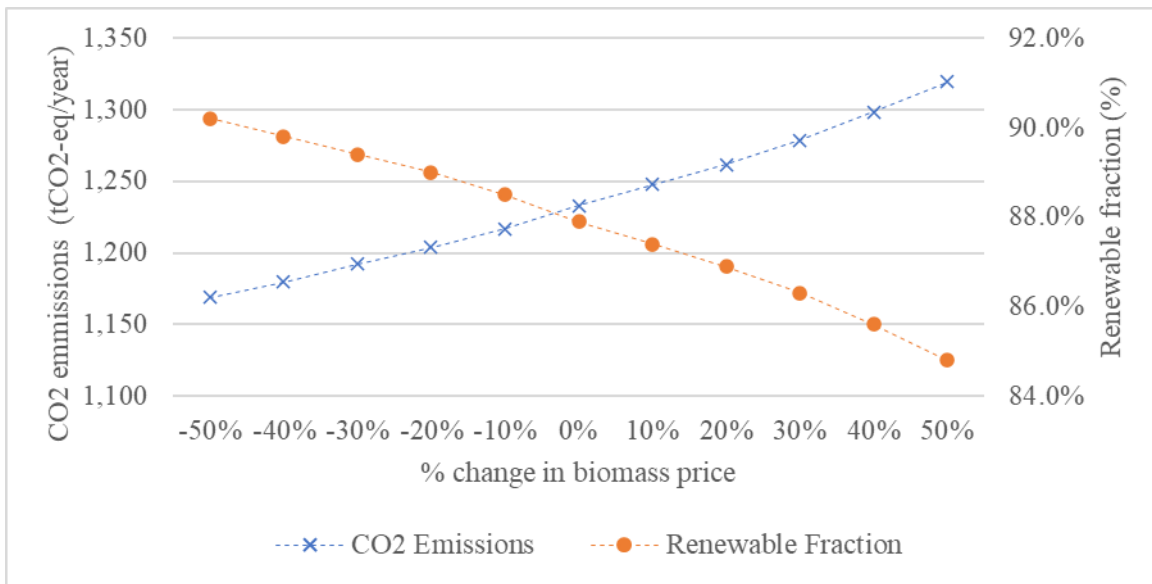


Figure 4-15 The effect of the BP on CO₂ emissions and the renewable fraction.

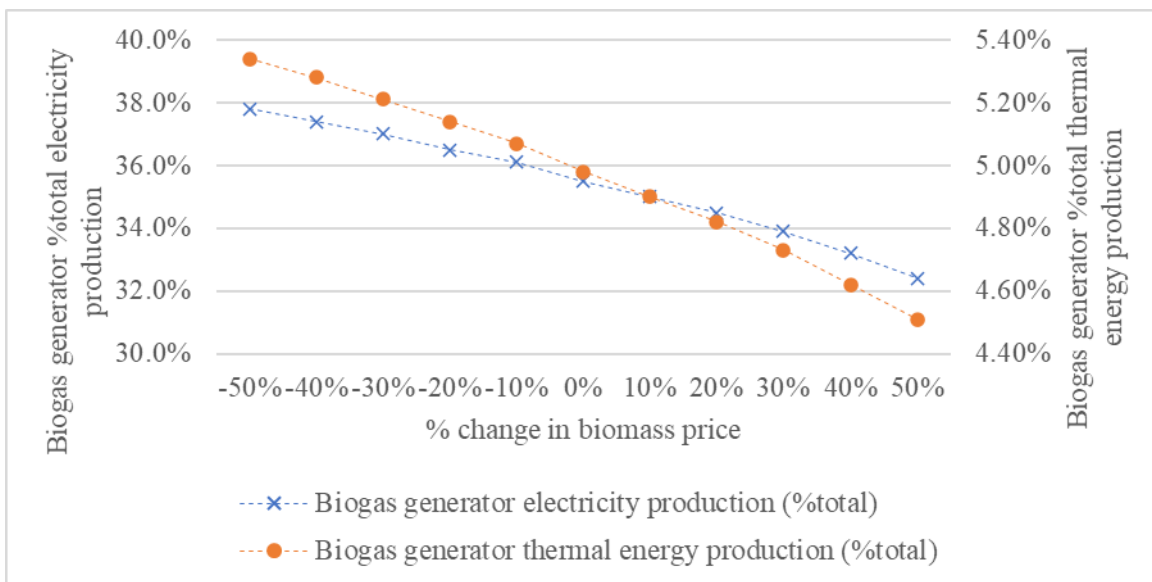


Figure 4-16 The effect of the BP on biogas electricity/heat contribution (%total generation).

4.1.3.2 SENSITIVITY ANALYSIS FOR AVERAGE DAILY ENERGY AND HEAT DEMAND

The daily average energy and heat demand is the following variable whose effect on the system's economic and environmental performance has been analyzed. This sensitivity analysis was conducted to assess the effects of possible variations in the production capabilities of the system. Another possible cause that could drastically affect the average load is the use of energy efficiency measures. The profile has been considered identical, but the data has been scaled up and down by 50 % with a constant step of 10 %.

The graph presented in *Figure 4-17* shows the effects of changes in the average daily energy and heat consumption on the system's economic performance. What stands out in these results is that a 50 % decrease in energy and heat consumption results in higher energy-related costs and lower economic performance (IRR). Furthermore, a local minimum of the LCOE can be found for a 10 % load decrease due to the sizing of the generator. This result is somewhat counterintuitive. This outcome may be explained by the fact that a reduction in electric and thermal power generation diminishes the benefits provided by the HRES over the baseline system. A decrease in load would have a negative impact on the investment. As it can be seen in *Figure 4-17*, IRR varies between 15.8 and 41.4 %, indicating that the investment is offering economic benefits even in unfavorable conditions. A high IRR for an increase in the average daily load is indicative of a robust system that ensures good economic performance if production capacities are expanded.

The sensitivity analysis's results of the average electricity and heat consumption in terms of CDE and the system's share of renewable energy are shown in *Figure 4-18*. It can be observed that the renewable fraction increases for a slight reduction in energy demand, but it remains over 80% for changes in the daily average of the electric and thermal load of $\pm 50\%$. It is also evident that increases in energy demand led to higher CDE. Interestingly, the renewable fraction peaks for a 10 % load decrease, suggesting that the system's components are oversized. Increased load demand results in higher CDE. This is an expected outcome. These relationships may partly be explained by the fact that the system is sized for the base-case load; therefore, increases in the average daily load result in more grid and boiler dependence to compensate for any unmet load by the non-dispatchable components.

Figure 4-19 illustrates the underutilization of the BG for lower average daily energy usage. This is caused because the PV and WT have a more competitive marginal energy generation cost and can meet most of the electric load. As shown in *Figure 4-19*, the BG electricity contribution (%total) varies greatly between 5.1 and 43.7 %, showing that load decreases render the BG an ineffective component due to its underutilization. The thermal load contribution (%total) of the BG varies from 1.07 to 5.57 %. Additionally, it can be observed that for an increase of more than 20 %, the contribution of the BG remains relatively unchanged, indicating a high-capacity factor.

Table 4-12 Summary of the results in average daily electricity and thermal energy consumption sensitivity analysis.

% Change of reference scenario	Metric		Levelized Cost Of Electricity (LCOE)	Internal Rate of Return (IRR)	CO ₂ Emissions (tons)	Renewable Fraction (%)	BG electricity production (%total)	BG thermal energy production (%total)
	Average daily energy consumption ($\frac{kWh}{day}$)	Average daily heat consumption ($\frac{kWh}{day}$)						
-50%	1447.06	4152.68	0.1569	15.8%	840	80.3%	5.1%	1.07%
-40%	1736.47	4983.22	0.1561	19.1%	936	81.3%	11.3%	2.08%
-30%	2025.88	5813.75	0.1538	22.4%	993	84.0%	18.9%	3.16%
-20%	2315.29	6644.29	0.1508	25.8%	1,053	86.3%	25.8%	3.99%
-10%	2604.70	7474.82	0.1486	29.0%	1,121	88.0%	31.7%	4.65%
0%	2894.11	8305.36	0.1533	31.5%	1,233	87.9%	35.5%	4.98%
10%	3183.52	9135.90	0.1575	33.9%	1,354	87.6%	38.7%	5.25%
20%	3472.93	9966.43	0.1626	36.1%	1,498	86.6%	41.0%	5.43%
30%	3762.34	10796.97	0.1683	38.1%	1,662	85.2%	42.5%	5.52%
40%	4051.75	11627.50	0.1746	39.9%	1,843	83.5%	43.4%	5.57%
50%	4341.17	12458.04	0.1818	41.4%	2,046	81.4%	43.7%	5.55%

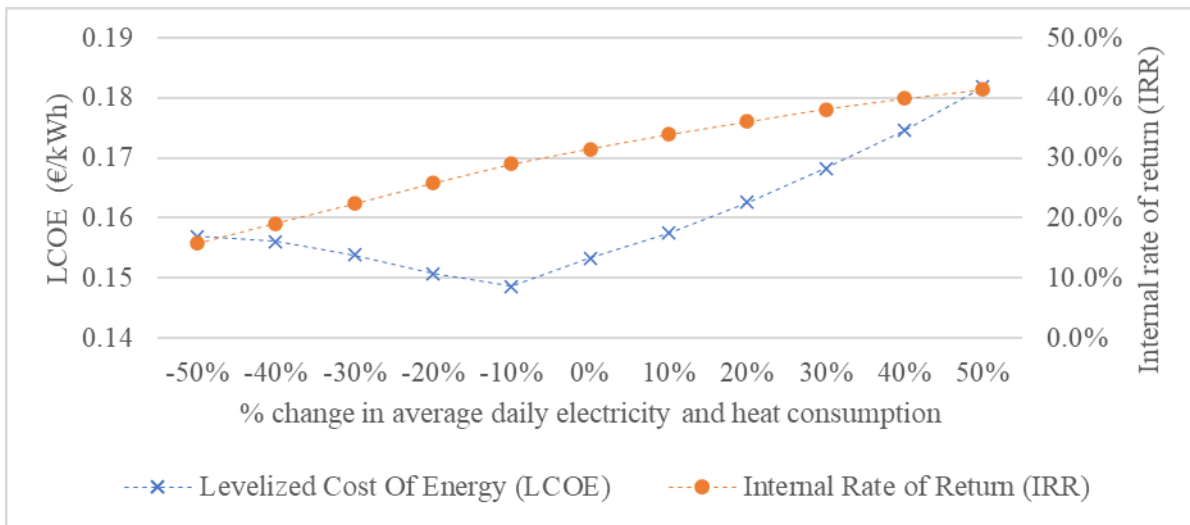


Figure 4-17 The effect of the electric and thermal demand on LCOE and IRR.

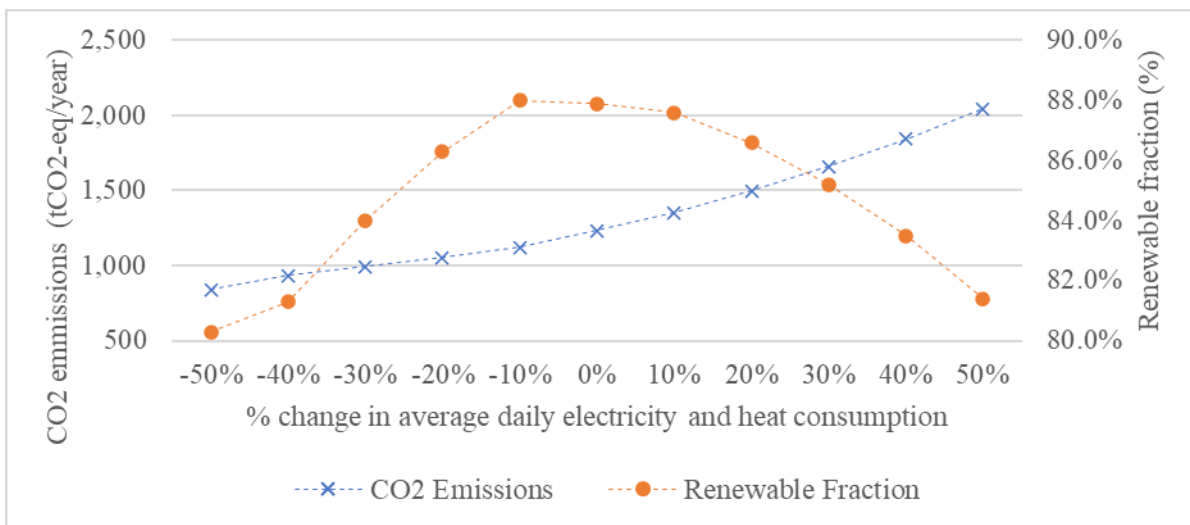


Figure 4-18 The effect of electric and thermal demand on CDE and the renewable fraction.

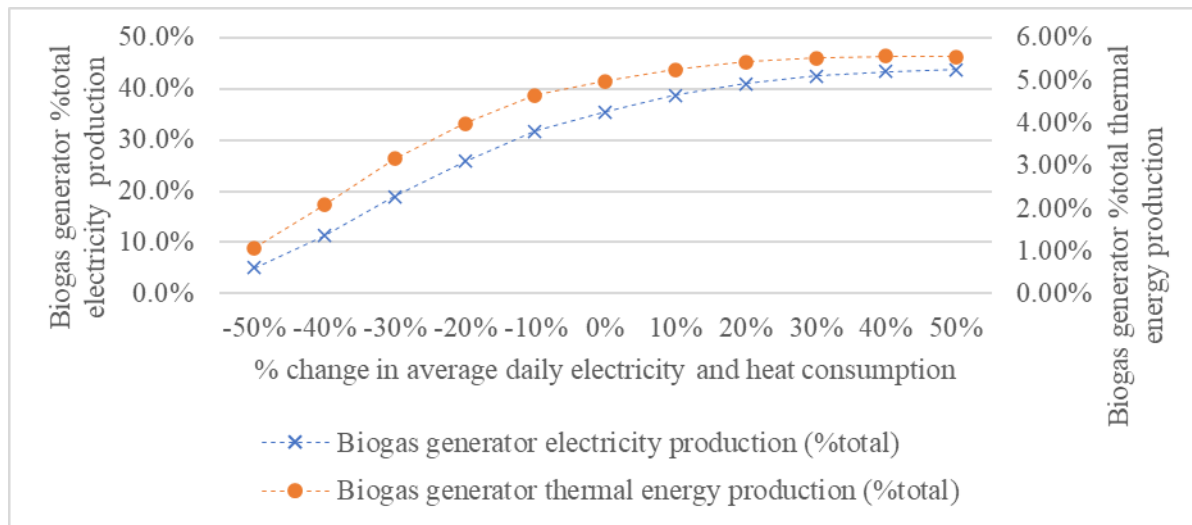


Figure 4-19 The effect of electric and thermal demand on biogas electricity/heat contribution (%total generation).

4.1.3.3 SENSITIVITY ANALYSIS FOR GRID ENERGY PRICE

The grid power price is the variable whose impact on the economic and environmental performance of the system has been evaluated. Electricity price is one of the most critical factors in the economic sustainability of the proposed HRES. Recent events have demonstrated that energy prices are highly volatile and can rise considerably because of energy poverty.

Figure 4-20 presents an overview of the economic effects of grid energy price fluctuations. LCOE varies from a minimum of 0.147 €/kWh for a power price equal to 0.375 €/kWh, to a maximum of 0.2163 €/kWh for a power price reduction of 50 %. The IRR index varies from 13.3 to 43.4 %. It is evident that higher grid prices result in better economic performance due to better utilization of the HRESs components underlying that grid dependence is disadvantageous. A 50 % decrease in grid prices can result in a 41 % higher cost of electricity, which dramatically reduces the economic feasibility of the proposed HRES. On the contrary, a 50 % increase in electricity prices offers an increase of 11.9 % in the IRR while also resulting in a 4.1 % decrease in the LCOE. Interestingly, a reduction greater than 50 % on the grid power prices renders the investment unfavorable due to a low IRR index.

Figure 4-21 depicts the results of the sensitivity analysis of the grid power price in terms of CDE and the system's share of renewable energy. What is interesting about the data in *Figure 4-21* is that lower grid prices result in dramatically lower renewable fraction; therefore, the system's CDE is almost doubled. This results in lower environmental benefits by using the proposed HRES. Lowered grid costs result in insufficient or zero BG utilization, forcing the system to rely more on the grid to supply all the required electrical demand. The renewable fraction varies from a minimum of 52.4 % for a 50 % decrease in power price to a maximum of 93.1 % for a grid power price equal to 0.375 €/kWh, underlying the importance of grid power price in the renewable fraction of the system.

Figure 4-22 demonstrates the effects of fluctuations in the grid power price on the BG's overall contribution (%total) to energy generation. As Figure 4-22 indicates, a decrease of more than 40 % in grid prices makes the use of the generator economically unfavorable, and as a result, no energy is produced from the generator. On the contrary, for higher grid prices, the contribution of the BG increases dramatically. The data from this figure demonstrates the strong connection between the grid power price and the contribution of the BG.

Table 4-13 Summary of the results in energy price sensitivity analysis.

Metric % Change of reference scenario	Energy price (€/kWh)	Levelized Cost Of Electricity (LCOE)	Internal Rate of Return (IRR)	CO ₂ Emissions (tons)	Renewable Fraction (%)	BG electricity production (%total)	BG thermal energy production (%total)
-50%	0.125	0.2163	13.3%	2,224	52.4%	0.0%	0.00%
-40%	0.150	0.1891	18.6%	1,784	68.2%	15.8%	2.13%
-30%	0.175	0.176	22.3%	1,567	76.0%	23.6%	3.22%
-20%	0.200	0.1651	25.7%	1,402	81.9%	29.5%	4.07%
-10%	0.225	0.1578	28.8%	1,296	85.7%	33.2%	4.63%
0%	0.250	0.1533	31.5%	1,232	87.9%	35.5%	4.98%
10%	0.275	0.1493	34.2%	1,183	89.7%	37.3%	5.26%
20%	0.300	0.1461	36.8%	1,146	91.0%	38.6%	5.47%
30%	0.325	0.146	39.0%	1,120	91.9%	39.5%	5.63%
40%	0.350	0.1465	41.2%	1,101	92.6%	40.2%	5.75%
50%	0.375	0.147	43.4%	1,084	93.1%	40.8%	5.85%

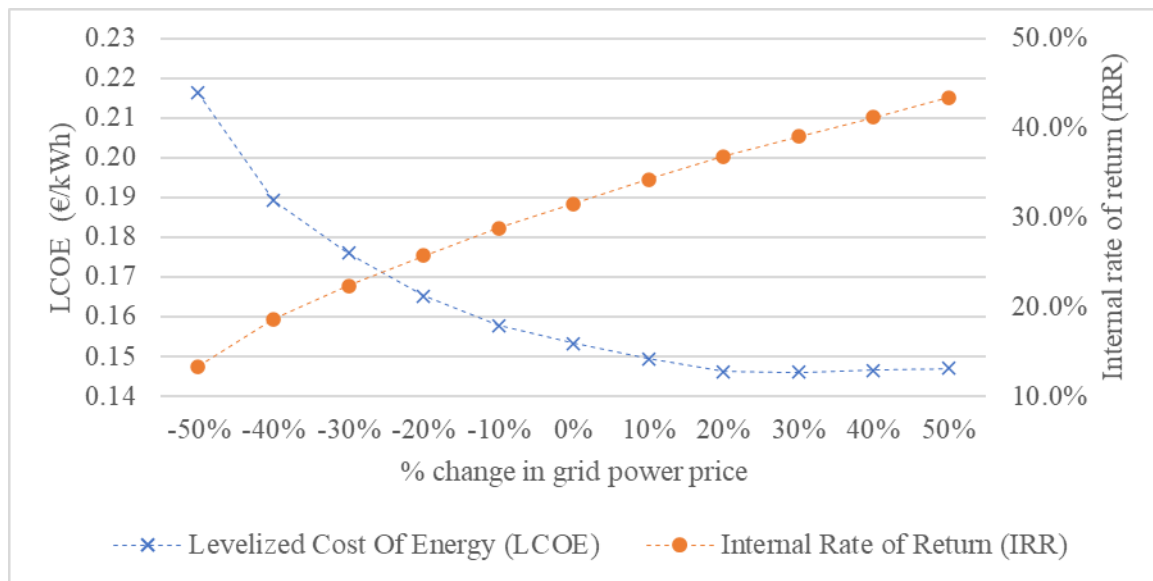


Figure 4-20 The effect of grid energy price on LCOE and IRR.

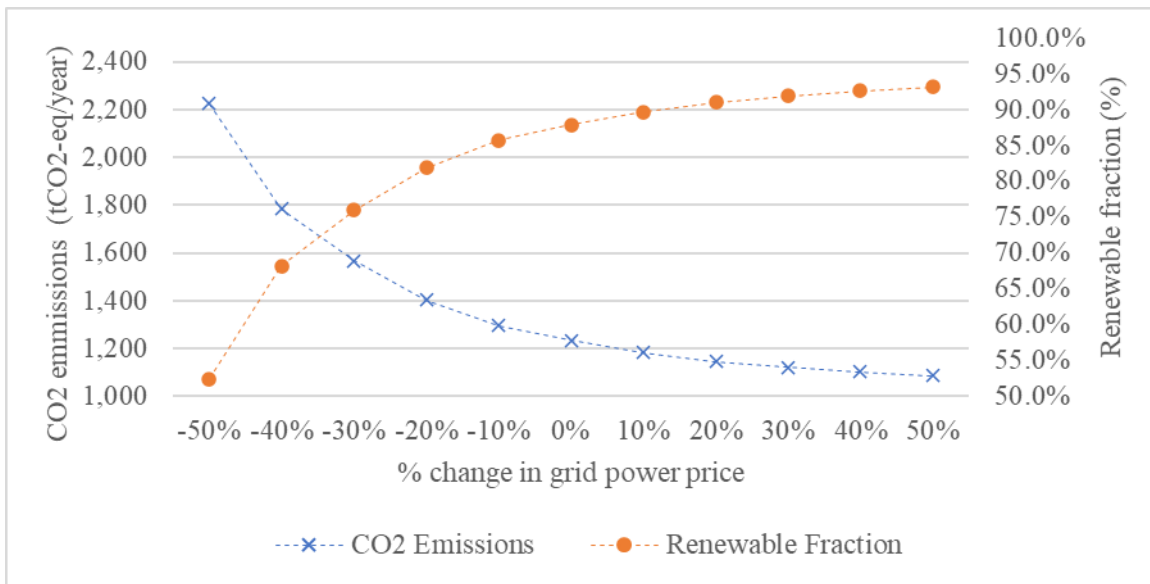


Figure 4-21 The effect of grid energy price on CDE and the renewable fraction.

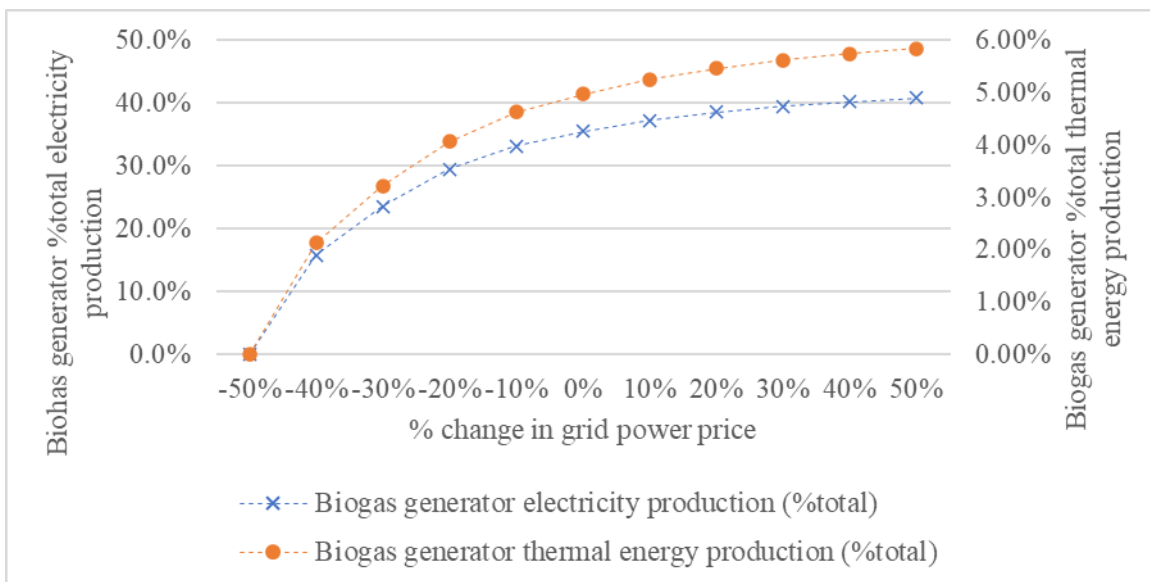


Figure 4-22 The effect of grid energy price on biogas electricity/heat contribution (%total generation).

4.1.3.4 SENSITIVITY ANALYSIS FOR CARBON EMISSIONS PENALTY

In Greece, there are currently no CDE penalties in effect, but their implementation is anticipated in the future. Therefore, it is important to investigate the effects of this variable on the economic and environmental performance of the optimal system. In this study, as a baseline scenario, a CDE of 82.76 €/tCO_{2eq} is considered; however, the relative variation from the baseline scenario is ±50 % with 10 % steps. To study the economic performance of the system using present-day CDE penalty costs, a scenario with no CDE penalties is also examined.

Figure 4-23 depicts the impact of variations in the CDE penalty on the system's economic performance. The results from this analysis clearly show that CDE penalties significantly impact every economic metric used to identify the system's economic performance. A 50 % increase in CDE penalties led to a LCOE of 0.1673 €/kWh, whereas the LCOE equaled 0.1327 €/kWh for a CDE penalty reduction of 100 %. The cost of energy is decreased because the grid purchases, a carbon-intensive source of energy generation, are mostly unaffected. Regarding the IRR index, a linear correlation was found between the IRR index and the CDE penalty. The IRR ranges from a minimum of 16.6 % for no CDE penalties to a maximum of 38.5 %. The economic advantage of reducing CDE is negated by lowering the CDE penalty. This finding indicates the system's robust performance in future scenarios where high CDE penalties are implemented. Considering potential future rises in carbon taxes, the recommended HRES is a future-proof approach because increased emissions penalties result in improved economic performance.

Figure 4-24 presents the findings of the sensitivity analysis of CDE penalties in terms of CDE and the system's renewable energy contribution. This figure shows that CDE linearly increase while the renewable fraction linearly decreases for increases in CDE penalties. These are counterintuitive results, indicating higher CDE emissions for higher CDE penalty costs. The annual CDE emissions range from 1,163 to 1,266 tCO₂, while the renewable fraction ranges from 86.7 to 90.4 %. These results indicate that CDE penalties have small effects on the environmental performance of the optimal HRES.

Figure 4-25 shows the output of BGs (%total) as a function of the carbon tax. The most interesting aspect of this graph is that increased CDE penalties result in lower overall usage of the BG, indicating higher dependence on the grid and boiler to supply the required energy to the industrial facility. Due to the increased emissions produced by BG's energy output, it has been discovered that higher CDE penalties result in decreased generator use.

Table 4-14 Summary of the results in carbon emission penalties sensitivity analysis.

Metric	Carbon emissions penalties (€/tCO ₂)	Levelized Cost Of Electricity (LCOE)	Internal Rate of Return (IRR)	CO ₂ Emissions (tons)	Renewable Fraction (%)	BG electricity production (%total)	BG thermal energy production (%total)
-100%	0.00	0.1327	16.6%	1,163	90.4%	38.0%	5.38%
-50%	41.38	0.1415	24.3%	1,195	89.3%	36.8%	5.19%
-40%	49.66	0.1436	25.8%	1,202	89.0%	36.6%	5.15%
-30%	57.93	0.1458	27.2%	1,210	88.7%	36.3%	5.11%
-20%	66.21	0.1481	28.7%	1,216	88.5%	36.1%	5.07%
-10%	74.48	0.1506	30.1%	1,224	88.2%	35.8%	5.03%
0%	82.76	0.1533	31.5%	1,233	87.9%	35.5%	4.98%
10%	91.04	0.1559	32.9%	1,240	87.7%	35.2%	4.94%
20%	99.31	0.1587	34.3%	1,247	87.4%	35.0%	4.90%
30%	107.59	0.1615	35.7%	1,254	87.2%	34.8%	4.86%
40%	115.86	0.1644	37.1%	1,261	86.9%	34.5%	4.83%
50%	124.14	0.1673	38.5%	1,266	86.7%	34.3%	4.79%

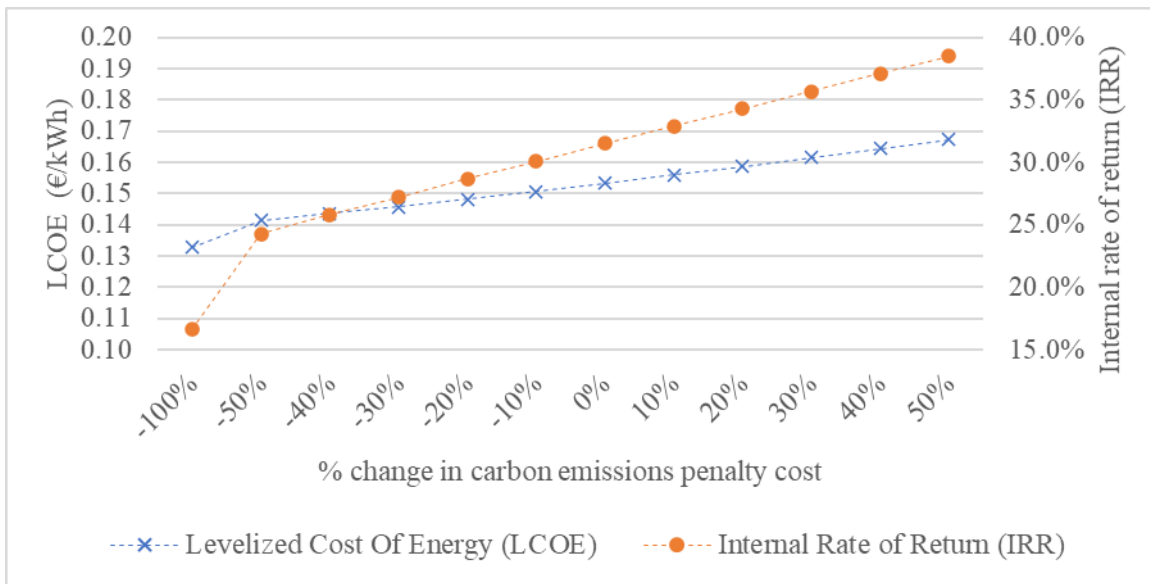


Figure 4-23 The effect of CDE penalties on LCOE and IRR.

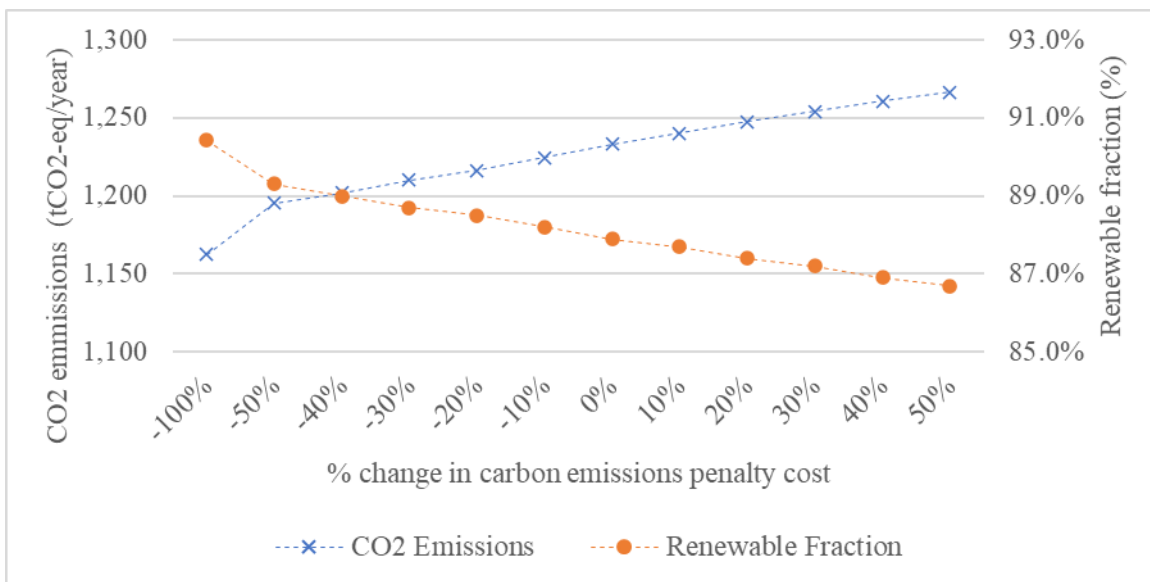


Figure 4-24 The effect of CDE penalties on CDE and the renewable fraction.

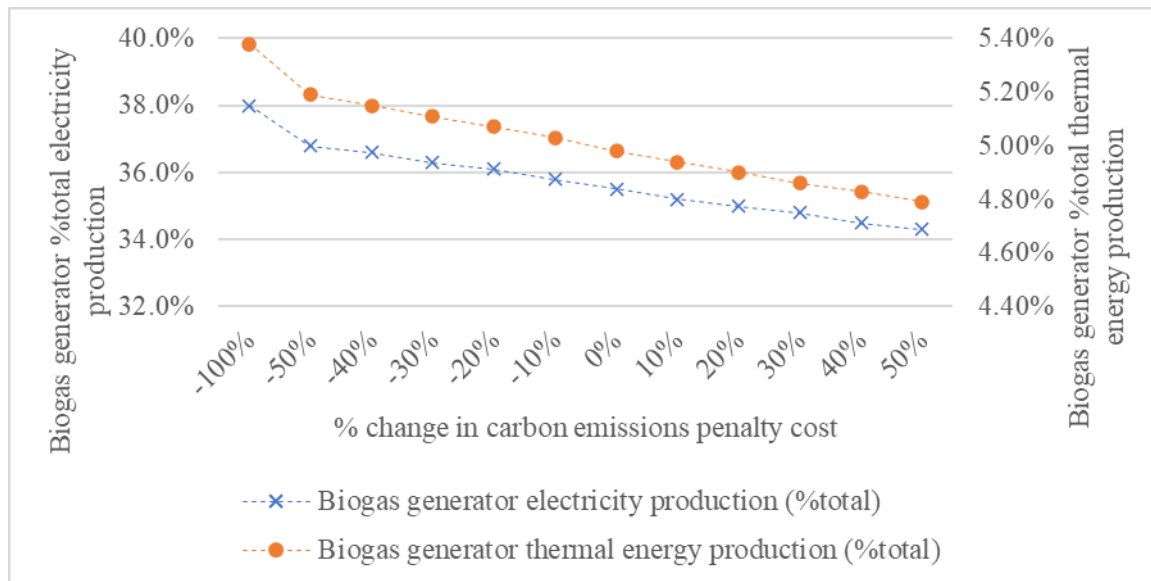


Figure 4-25 The effect of CDE penalties on biogas electricity/heat contribution (%total generation).

4.1.3.5 SENSITIVITY ANALYSIS FOR DIESEL PRICES

The price of diesel is the following variable whose effect on the system's economic and environmental performance has been analyzed. Due to the projected HRES's heavy reliance on diesel, the diesel price is one of the most important economic factors. Recent events have revealed the extreme volatility of fuel prices. Therefore, it is one of the most key factors regarding the economic sustainability of the HRES.

What stands out in *Figure 4-26* is the general pattern of the LCOE, LCOTE, and IRR as a function of diesel prices. This figure reveals that the LCOE tends to linearly decrease as diesel prices increase. In contrast, as diesel costs increase, the IRR and LCOTE increase linearly. This finding was unexpected, and it suggests that rising diesel prices result in a more promising economic performance of the proposed HRES. A possible explanation for this might be that by increasing the diesel prices, both the baseline system and the proposed HRES offer higher NPC's; however, due to the higher dependence of the baseline system on diesel, the HRES offers an economic advantage. Overall, a reduction in diesel price diminishes the benefits provided by the HRES over the baseline system. Concerning the LCOTE, the range of values observed in this study is between 0.0930 and 0.2789 €/kWh, underlying the strong dependence of the LCOTE on diesel prices.

Figure 4-27 depicts the results of the sensitivity analysis of diesel prices in terms of CDE and the system's share of renewable energy. It can be observed that the renewable fraction increases for a slight increase in diesel price, remaining over 84 % for changes in diesel price of ± 50 %. It can also be observed that increases in diesel prices led to lower CDE, indicating better environmental performance for increased diesel prices.

The output of BG's (percent of total) as a function of the diesel price is depicted in *Figure 4-28*. Overall, diesel prices affect the BG's contribution to total energy generation. As can be observed

from Figure 4-28, both the thermal and electrical power generation is increased for high diesel prices. BG electricity production (%total) varies from a minimum of 32 % to a maximum of 38 %. A minor increase in thermal energy generation (%total) can be observed. A possible explanation might be that higher diesel prices lead to lower boiler usage. Therefore, the BG produces a more sizeable portion of the total electrical and thermal energy.

Table 4-15 Summary of the results in diesel prices sensitivity analysis.

Metric % Change of reference scenario	Diesel price (€/litre)	Levelized Cost Of Electricity (LCOE)	Levelized Cost Of Thermal Energy (LCOTE)	Internal Rate of Return (IRR)	CO ₂ Emissions (tons)	Renewable Fraction (%)	BG electricity production (%total)	BG thermal energy production (%total)
-50%	0.778	0.1734	0.0930	29.5%	1,331	84.4%	32.0%	4.44%
-40%	0.933	0.1693	0.1115	29.9%	1,309	85.2%	32.8%	4.56%
-30%	1.089	0.1649	0.1301	30.3%	1,285	86.1%	33.7%	4.69%
-20%	1.244	0.1609	0.1487	30.7%	1,265	86.8%	34.4%	4.80%
-10%	1.400	0.1571	0.1673	31.1%	1,249	87.3%	34.9%	4.89%
0%	1.555	0.1533	0.1859	31.5%	1,233	87.9%	35.5%	4.98%
10%	1.711	0.1492	0.2045	31.9%	1,215	88.6%	36.1%	5.08%
20%	1.866	0.1453	0.2231	32.3%	1,199	89.1%	36.7%	5.17%
30%	2.022	0.1416	0.2417	32.7%	1,187	89.5%	37.1%	5.24%
40%	2.177	0.1377	0.2603	33.1%	1,173	90.0%	37.6%	5.32%
50%	2.333	0.1342	0.2789	33.4%	1,163	90.4%	38.0%	5.38%

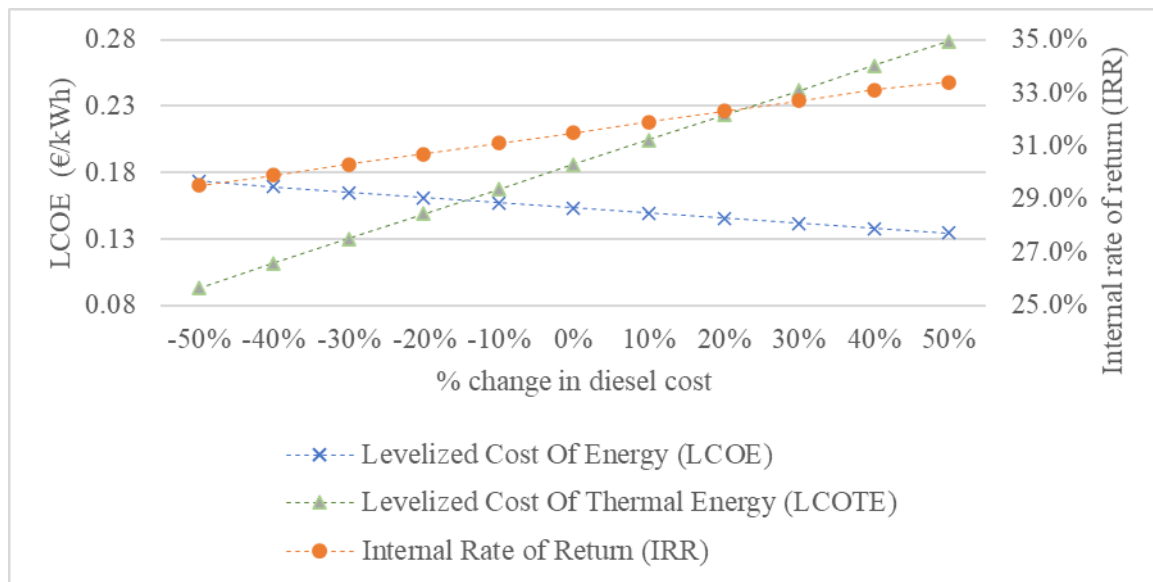


Figure 4-26 The effect of diesel price on LCOE and IRR.

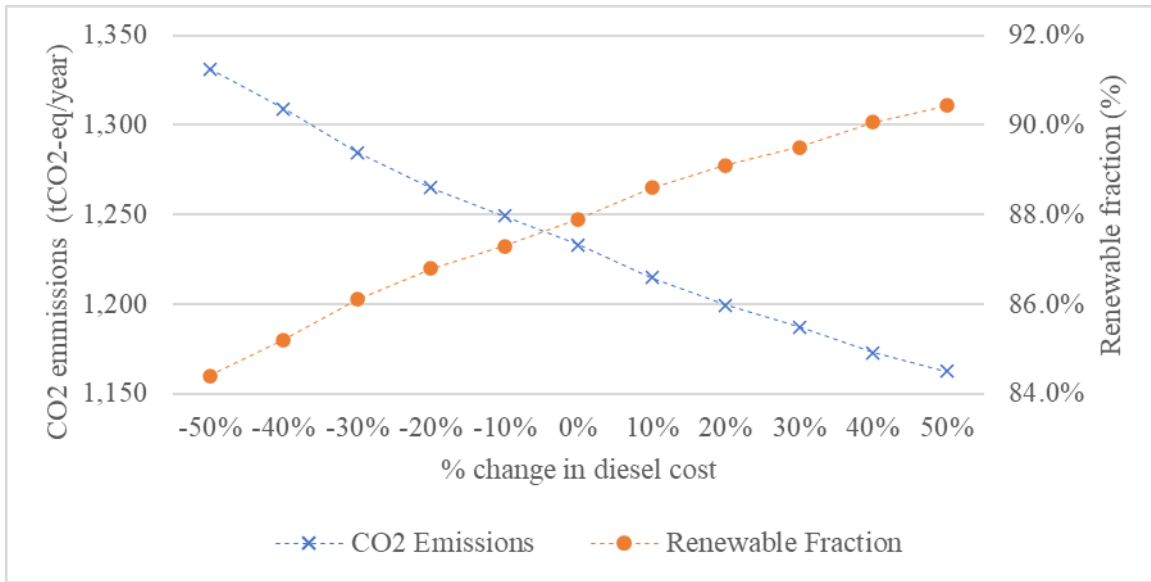


Figure 4-27 The effect of diesel price on CDE and the renewable fraction.

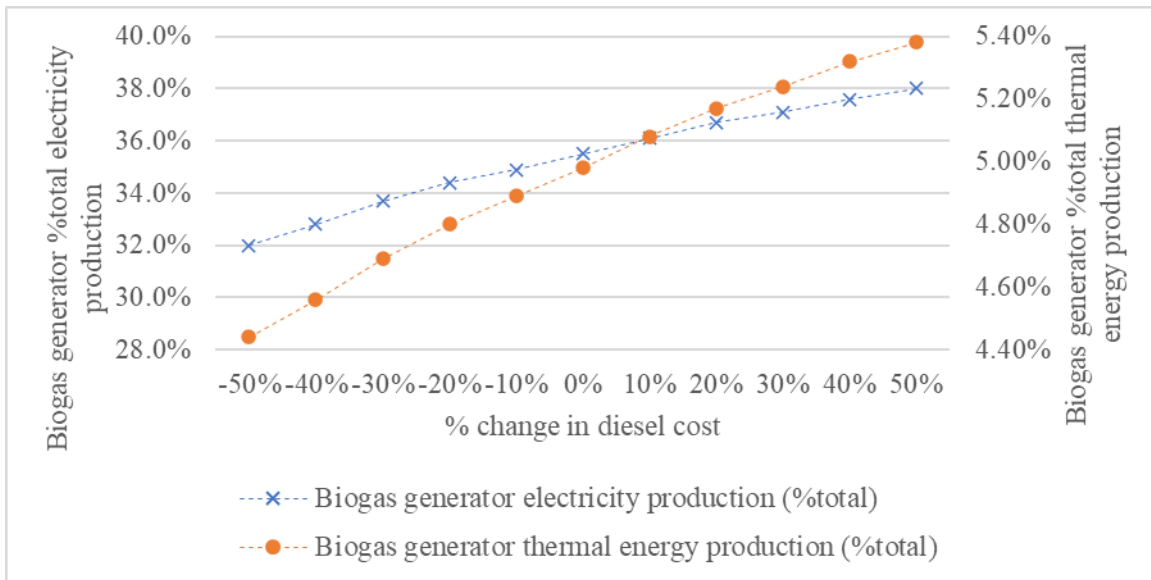


Figure 4-28 The effect of diesel price on biogas electricity/heat contribution (%total generation).

Altogether these results provide important insights into the operational aspects of the best optimal HRES to achieve an optimal balance between LCOE, GHG emissions, and RES penetration. Overall, these results indicate that the proposed HRES could help meet the bakery industry's electrical and thermal power demand at a lower LCOE than the current energy solution. No significant reduction in LCOTE was found compared to the baseline system; however, the optimal system reduced diesel dependence by 5 %.

The findings from the sensitivity analysis demonstrated that dramatic changes in operational aspects (system control variables) of the HRES still result in an economically and environmentally advantageous investment.

CHAPTER 5

DISCUSSION

5.1 RESULTS DISCUSSION

The results that are presented above clearly show that the proposed HRES could help to meet the electric and thermal power demand of the industrial facility while also providing better LCOE and a lower environmental footprint compared to the current energy supply. Every scenario included in this study used a waste-to-energy system that included either gasification or a combination of gasification and AD to utilize locally accessible biomass energy sources. This diploma thesis demonstrates that HRES that take advantage of locally available energy resources can be economically and technically superior compared to current energy solutions. In contrast to prior research, a complete evaluation of the electrical and thermal demand occurred concurrently with a detailed evaluation of the biomass potential in the study area. Actual data on energy consumption were used to produce a more accurate and realistic energy assessment. This work advances the literature that aids the green energy transition in the food industry while also supporting concepts such as industrial symbiosis and circular economy.

The first step during the energy modeling is an electricity/heat consumption analysis based on the real energy consumption data. The thermal load profile was generated using the available energy and diesel consumption data, assuming that the industrial processes require electricity and thermal energy. An assessment of the available RES potential followed, where climate conditions data from various sources were used to provide more realistic results. To assess the POWER dataset's quality, data from the MERRA-2 dataset were used. BA was assessed using real data provided by the Greek Payment Authority of Common Agricultural Policy for the years 2017, 2018, and 2019. A literature review was conducted to determine the RES potential, using up-to-date conversion rates and costs. It was found that the available OTP waste could meet the needs of the industrial facility. Furthermore, a high solar and wind potential was identified in the area of study. Based on the locally available energy resources, the technology planning was conducted where all scenarios were built. In this work, a novel approach to model more than two waste-to-energy technologies was used to take advantage of multiple waste streams. As abovementioned in this diploma thesis, two similar energy systems were modeled and analyzed. The main difference between the two systems is the set of employed waste-to-energy technologies. Additionally, three land utilization scenarios were used to determine the effect of BA in the technology selection phase. It was found that the use of AD is economically unfavorable due to the required increased initial investment as well as the increased O&M costs of the system.

The optimization results suggested the addition of a 120 kW_p BG that utilizes OTP waste via gasification in combination with 240 kW_p and 60 kW_p of PVs and WT respectively. Due to the installment of a 120 kW_p generator, a system adaptation cost of 100,000 € was considered. This cost includes the necessary equipment (pipes, heat exchanger etc.) as well as the installment costs.

The proposed HRES resulted in a 65 % decrease of LCOE with an IRR equal to 31.5 %. Furthermore, a 63 % decrease in CDE was found that demonstrates the environmental impact of the proposed system. Concerning the LCOTE, no significant differences between the initial LCOTE and the optimal systems were evident. However, this result has not previously been described in the literature.

A sensitivity analysis was conducted to determine the effects of different factors on the system's performance. It was found that the biggest contributing factor to the economic performance of the system is the average daily electricity and heat consumption. It was found that a decrease in the average daily energy demand resulted in lower economic performance, whereas an increase led to better economic performance. This provides convincing evidence that the proposed HRES is a robust energy solution that takes into consideration future expansion capabilities. Furthermore, it was found that in case of a 50 % increase in daily energy consumption, the HRES can provide more than 80 % of the annual electricity demand using RES and almost 6 % of the total thermal energy requirements. Additionally, due to the current energy crisis, the effect of grid and diesel prices was evaluated to determine the economic feasibility, in the case of extreme energy and diesel price fluctuations, of this system. It was found that fluctuations in grid energy prices can greatly affect the economics of the system.

Local industries with significant thermal and electric power consumption could be the main beneficiaries from the adoption of the research conducted. These results provide further support for the hypothesis that locally available waste could help realize the green energy transition in the food industry. The main expected benefits are summarized below.

Firstly, local WG will be redirected from landfills, thus reducing the environmental impact of the local communities and industries. Secondly, this study is a clear demonstration of a circular economy model that offers significant economic benefits in the industrial sector. Lastly, proving that the creation of an energy system using a decentralized approach is feasible and economically competitive with the current energy supply.

The main barriers to implementing the primary research outcomes of this study are the high investment cost (>1 million €), social acceptance of the proposed system, and the considerable risk of investment due to the volatility of the prices of the components.

To overcome the primary limitations of this work, additional research is needed. The three primary ones are the failure to consider the increase in electric and thermal power demand over time due to production increase capabilities; social factors such as social acceptance of the system are not considered for the selection of the optimal system, and the software limitations discussed in Section 3.6.

One of the more significant findings to emerge from this study is that waste-to-energy technologies can be implemented in the current energy supply of the food industry. It was found that a HRES comprising of PVs, WT, a gasifier, and a BG can greatly contribute to the electrical and thermal needs of the case study by reducing the energy-related costs and GHG emissions. Overall, this study strengthens the idea that HRES can realize the green energy transition in the food industry, taking advantage of newly developed waste-to-energy systems. Lastly, these findings have significant implications for the understanding of how the system control variables affect the economic performance of the HRES.

5.2 RESULTS COMPARISON WITH RELEVANT LITERATURE

There are only a few research articles with case studies that require both electrical and thermal energy. Additionally, another limitation during the literature review was the lack of research articles regarding the techno-economic analysis of HRESs using HOMER Pro in industries. What is more, most of the related studies are in Asia, presenting a gap in techno-economic analyses of HRESs conducted in Europe. However, these results further support the implementation of HRES areas with high available biomass potential. In this study, a reduction of 65 % in the LCOE was found. It is encouraging to compare this finding with that found by (Rajbongshi et al., 2017; Ribó-Pérez et al., 2021; Sigarchian et al., 2015), who found a similar decrease in the LCOE. In a study conducted by (Yimen et al., 2021), it was found that gasification offered better results compared to AD, and the implementation of a gasifier on a HRES resulted in a 40 % decrease in the LCOE. This study's renewable fraction for the optimal HRES equaled 87.9%. These results corroborate the findings of a great deal of the previous work conducted by (Ahmad et al., 2018; Bhattacharjee & Dey, 2014; Malik et al., 2020) on HRESs. The CO₂ reduction observed in this study was found to be 63 %, lower than that of previously reported values (Jahangir & Cheraghi, 2020; R. Kumar & Channi, 2022). A possible explanation of this might be that the presence of a thermal load led to this difference. Lastly, the payback time found in this study equaled 3.17 years. This finding is similar to that of (Vendoti et al., 2021), who proposed a HRES with a payback time of 4.43 years.

Table 5-1 Results comparison with relevant literature. Note: (N/E: Not Examined, N/G: Not Given)

<i>Reference</i>	LCOE (%reduction)	LCOTE (%reduction)	CDE (%reduction)	Renewable fraction (%)	Payback time
<i>This study</i>	65	0	63	87.9	3.17
Rajbongshi et al., 2017	55.86	N/E	N/G	N/G	N/G
Ribó-Pérez et al., 2021	50 – 94	N/E	N/G	N/G	N/G
Sigarchian et al., 2015	19.35 – 55	N/E	N/G	N/G	N/G
Yimen et al., 2021	29 – 40	N/E	N/G	N/G	N/G
Ahmad et al., 2018	N/G	N/E	N/G	88	N/G
<i>Bhattacharjee & Dey, 2014</i>	N/G	N/E	N/G	92	N/G
Malik et al., 2020	N/G	N/E	N/G	83	N/G
<i>Jahangir & Cheraghi, 2020</i>	N/G	N/E	99	99	N/G
<i>R. Kumar & Channi, 2022</i>	N/G	N/E	99.9	100	N/G
Vendoti et al., 2021	N/G	N/E	N/G	N/G	4.43

CHAPTER 6

CONCLUSION

The present research aimed to develop a HRES to meet the needs of a local bakery industry. This study aims to examine the operational aspects of the optimal system to achieve high-RES penetration while also reducing the LCOE and the ecological footprint of the system. Two different waste-to-energy combinations of technologies are considered. Additionally, three land utilization scenarios are examined. In total, six scenarios were developed and evaluated. The proposed HRES consisted of technologies such as gasification, PV, WT, and CHP units.

The findings of the optimized system are assessed and presented. These findings show that locally available biomass and waste can help realize the green transformation of the industrial sector. The findings presented in this work suggest that the proposed optimal HRES can lower the energy-related costs of the industrial system while also offering better economic performance compared to the current energy supply. These findings have significant implications for the development of HRESs in the food sector.

The present study appears to be the first study to utilize a combination of waste-to-energy technologies in HOMER Pro. As concerning the optimal set of waste-to-energy technologies, the optimization results showed that the gasification-only system offered better economic performance compared to the counterpart system that uses a combination of gasification and AD. By adding AD to the energy generation mix, the reduction of the LCOE ranges from 48.05 to 56.67 % compared to the current energy supply. However, a gasification system led to an almost 65 % decrease in energy-related costs. A system comprising a gasifier also provided higher annual carbon savings compared to the systems comprising a combination of gasification and AD. The sensitivity analysis of the system control variables led to a better understanding of the system on possible input variable changes. The results of the sensitivity analysis showed a robust energy system with increased flexibility to meet the needs of the industrial facility even in extreme scenarios (diesel and electricity price increases).

The findings were validated with relevant research articles. It was found that the reduction of the LCOE was similar to similar HRESs. Additionally, other economic (IRR) and environmental (CDE) indexes found in this study were consistent with the literature. Any inconsistency in the values may be due to the system's different components and input variables.

The main motivation behind this study is that sustainable energy generation is directly connected with the quality of life. The overpopulation and the continually increasing industrialization of the society result in higher energy consumption per capita and overall. Developing countries and islands rely on fossil fuels to meet energy requirements. It is important to develop new energy solutions with a low environmental footprint to help with problems such as energy poverty and climate change. Hybrid energy systems that use a CHP are a promising solution to the increased volatility of other RES sources such as PV and wind.

Based on the conducted literature review, a few research gaps are identified, where only a small number of research articles are published concerning the supply of thermal demand using RES, especially in an industrial setting. Additionally, there are no scientific research papers (to the best of the authors' knowledge) that incorporate two or more waste-to-energy technologies concurrently in HOMER Pro. In this diploma thesis, different HRESs were modeled, optimized, and later evaluated to find the industrial facility's optimal and most cost-effective HRES. Different system configurations were modeled and assessed. The primary differentiation of the proposed scenarios modeled in this diploma thesis is the waste-to-energy technology employed for energy production. In one category of systems, only gasification is used; in the other, a combination of gasification and AD is used.

The first novelty of this study is the proposal of a methodological framework to model biomass gasification and AD plants in HOMER Pro. This methodology fills the gap in the literature where these technologies have only been used individually.

Another novelty is the use of realistic inputs for techno-economic analysis of grid-connected HRESs. Real hourly consumption data, biomass raw material information/availability, market price data, and location-specific resources data were used to assess the economic and environmental performance of the abovementioned methodological framework.

Lastly, a sensitivity analysis was performed to identify the impacts of changes in the predefined system control variables on the system's economic performance.

The main limitation of this study lies in the fact that the HOMER Pro software does not provide enough tools for thermal energy analysis. Another source of weakness in this study is the fact that the optimal system is ranked based on the NPC of the system. However, more variables can affect the feasibility of the system and should not be ignored. Despite its limitations, the study certainly adds to our understanding of HRES developed to meet the needs of industrial facilities.

As abovementioned, the optimization of a HRES is a problem with multiple variables that affect the system's performance. Therefore, in future investigations, it might be beneficiary to use a multi-objective optimization algorithm for the investigation of the proper sizing of the system. Another future recommendation is the inclusion of demand-side management strategies such as electrification and energy efficiency. Additionally, in the future, a more advanced energy management system might provide opportunities such as flexible load shaping based on economic incentives. The idea that industries with energy-intensive processes could be utilized as energy sinks is a prominent issue for future research. Lastly, one of the main barriers to the decarbonization of the industrial sector, and more particularly in the food and beverage sector, are the policy options and business models used. Further research could usefully explore how policy options and business models affect HRES adaptation.

Further studies, which take the abovementioned limitations and future recommendations into account, will need to be undertaken to develop better and more cost-effective HRESs. Ultimately, this study's findings have several important implications for future practice.

References

- 7η ΥΠΠΕ - Γεωγραφία Δήμων Νομού Χανίων. (n.d.). Retrieved July 8, 2022, from <https://www.hccrete.gr>
- Aguado, R., Vera, D., López-García, D. A., Torreglosa, J. P., & Jurado, F. (2021). Techno-economic assessment of a gasification plant for distributed cogeneration in the agrifood sector. *Applied Sciences (Switzerland)*, *11*(2), 1–18. <https://doi.org/10.3390/app11020660>
- Ahmad, J., Imran, M., Khalid, A., Iqbal, W., Ashraf, S. R., Adnan, M., Ali, S. F., & Khokhar, K. S. (2018). Techno economic analysis of a wind-photovoltaic-biomass hybrid renewable energy system for rural electrification: A case study of Kallar Kahar. *Energy*, *148*, 208–234. <https://doi.org/10.1016/j.energy.2018.01.133>
- Almeida, P. v., Rodrigues, R. P., Gaspar, M. C., Braga, M. E. M., & Quina, M. J. (2021). Integrated management of residues from tomato production: Recovery of value-added compounds and biogas production in the biorefinery context. *Journal of Environmental Management*, *299*. <https://doi.org/10.1016/j.jenvman.2021.113505>
- Almeida, P. v., Rodrigues, R. P., Teixeira, L. M., Santos, A. F., Martins, R. C., & Quina, M. J. (2021). Bioenergy production through mono and co-digestion of tomato residues. *Energies*, *14*(17). <https://doi.org/10.3390/en14175563>
- Al-Najjar, H., Pfeifer, C., al Afif, R., & El-Khozondar, H. J. (2022). Performance Evaluation of a Hybrid Grid-Connected Photovoltaic Biogas-Generator Power System. *Energies*, *15*(9). <https://doi.org/10.3390/EN15093151>
- Arregi, A., Amutio, M., Lopez, G., Bilbao, J., & Olazar, M. (2018). Evaluation of thermochemical routes for hydrogen production from biomass: A review. *Energy Conversion and Management*, *165*, 696–719. <https://doi.org/10.1016/J.ENCONMAN.2018.03.089>
- Beier, J. (2017). *Simulation Approach Towards Energy Flexible Manufacturing Systems* (S. Kara & C. Herrmann, Eds.). Springer. <http://www.springer.com/series/10615>
- Bhattacharjee, S., & Dey, A. (2014). Techno-economic performance evaluation of grid integrated PV-biomass hybrid power generation for rice mill. *Sustainable Energy Technologies and Assessments*, *7*, 6–16. <https://doi.org/10.1016/J.SETA.2014.02.005>
- Bird, L., Milligan, M., & Lew, D. (2013). *Integrating Variable Renewable Energy: Challenges and Solutions*. www.nrel.gov/publications.
- Boehm, R., Wilde, P. E., ver Ploeg, M., Costello, C., & Cash, S. B. (2018). A Comprehensive Life Cycle Assessment of Greenhouse Gas Emissions from U.S. Household Food Choices. *Food Policy*, *79*, 67–76. <https://doi.org/10.1016/J.FOODPOL.2018.05.004>
- Braimakis, K., Charalampidis, A., & Karellas, S. (2021). Techno-economic assessment of a small-scale biomass ORC-CHP for district heating. *Energy Conversion and Management*, *247*. <https://doi.org/10.1016/J.ENCONMAN.2021.114705>

- Cara, C., Ruiz, E., Ballesteros, I., Negro, M. J., & Castro, E. (2006). Enhanced enzymatic hydrolysis of olive tree wood by steam explosion and alkaline peroxide delignification. *Process Biochemistry*, *41*(2), 423–429. <https://doi.org/10.1016/j.procbio.2005.07.007>
- Castellanos, J. G., Walker, M., Poggio, D., Pourkashanian, M., & Nimmo, W. (2015). Modelling an off-grid integrated renewable energy system for rural electrification in India using photovoltaics and anaerobic digestion. *Renewable Energy*, *74*, 390–398. <https://doi.org/10.1016/J.RENENE.2014.08.055>
- Chambon, C. L., Karia, T., Sandwell, P., & Hallett, J. P. (2020). Techno-economic assessment of biomass gasification-based mini-grids for productive energy applications: The case of rural India. *Renewable Energy*, *154*, 432–444. <https://doi.org/10.1016/J.RENENE.2020.03.002>
- COMPANY PROFILE - *plastikakritis.com*. (n.d.). Retrieved March 22, 2022, from <https://www.plastikakritis.com/en>
- Contreras, M. del M., Romero, I., Moya, M., & Castro, E. (2020). Olive-derived biomass as a renewable source of value-added products. In *Process Biochemistry* (Vol. 97, pp. 43–56). Elsevier Ltd. <https://doi.org/10.1016/j.procbio.2020.06.013>
- Copa, J. R., Tuna, C. E., Silveira, J. L., Boloy, R. A. M., Brito, P., Silva, V., Cardoso, J., & Eusébio, D. (2020). Techno-economic assessment of the use of syngas generated from biomass to feed an internal combustion engine. *Energies*, *13*(12). <https://doi.org/10.3390/EN13123097>
- Curto, D., Franzitta, V., Viola, A., Cirrincione, M., Mohammadi, A., & Kumar, A. (2019). A renewable energy mix to supply small islands. A comparative study applied to Balearic Islands and Fiji. *Journal of Cleaner Production*, *241*, 118356. <https://doi.org/10.1016/J.JCLEPRO.2019.118356>
- Danevad, D., & Carlos-Pinedo, S. (2021). Exploring Interactions Between Fruit and Vegetable Production in a Greenhouse and an Anaerobic Digestion Plant—Environmental Implications. *Frontiers in Sustainability*, *2*. <https://doi.org/10.3389/frsus.2021.770296>
- Department of Energy and Climate Change and the Department for Business, I. and S. (2015). *Industrial Decarbonisation & Energy Efficiency Roadmaps to 2050*.
- Després, J., Mima, S., Kitous, A., Criqui, P., Hadjsaid, N., & Noirot, I. (2017). Storage as a flexibility option in power systems with high shares of variable renewable energy sources: a POLES-based analysis. *Energy Economics*, *64*, 638–650. <https://doi.org/10.1016/j.eneco.2016.03.006>
- Eamonn Lannoye, Damian Flynn, & Mark O'Malley. (2012). Evaluation of power system flexibility. *IEEE Transactions on Power Systems*, *27*(2), 922–931. [10.1109/TPWRS.2011.2177280](https://doi.org/10.1109/TPWRS.2011.2177280)
- Eziyi, I., & Krothapalli, A. (2014). Sustainable rural development: Solar/Biomass hybrid renewable energy system. *Energy Procedia*, *57*, 1492–1501. <https://doi.org/10.1016/j.egypro.2014.10.141>

- Francesco, A., & Umberto, D. (Eds.). (2019). *Handbook of Energy Efficiency in Buildings*. Elsevier. <https://doi.org/10.1016/C2016-0-02638-4>
- Fryda, L.-E. (2006). *Development of advanced electricity production systems with biomass*. DOI: 10.12681/eadd/17790
- García Martín, J. F., Cuevas, M., Feng, C. H., Mateos, P. Á., García, M. T., & Sánchez, S. (2020). Energetic valorisation of olive biomass: Olive-tree pruning, olive stones and pomaces. In *Processes* (Vol. 8, Issue 5). MDPI AG. <https://doi.org/10.3390/PR8050511>
- Griffin, P. W., Hammond, G. P., & Norman, J. B. (2016). Industrial energy use and carbon emissions reduction: a UK perspective. *WIREs Energy Environ*, 5, 684–714. <https://doi.org/10.1002/wene.212>
- Haghighat Mamaghani, A., Avella Escandon, S. A., Najafi, B., Shirazi, A., & Rinaldi, F. (2016). Techno-economic feasibility of photovoltaic, wind, diesel and hybrid electrification systems for off-grid rural electrification in Colombia. *Renewable Energy*, 97, 293–305. <https://doi.org/10.1016/J.RENENE.2016.05.086>
- Hansen, T. L., Jansen, J. la C., Davidsson, Å., & Christensen, T. H. (2007). Effects of pre-treatment technologies on quantity and quality of source-sorted municipal organic waste for biogas recovery. *Waste Management*, 27(3), 398–405. <https://doi.org/10.1016/J.WASMAN.2006.02.014>
- Herenčić, L., Melnjak, M., Capuder, T., Andročec, I., & Rajšl, I. (2021). Techno-economic and environmental assessment of energy vectors in decarbonization of energy islands. *Energy Conversion and Management*, 236, 114064. <https://doi.org/10.1016/J.ENCONMAN.2021.114064>
- Hersh, M. A. (2006). The Economics and Politics of Energy Generation. *Improving Stability in Developing Nations through Automation 2006*, 77–82. <https://doi.org/10.1016/B978-008045406-1/50011-2>
- Iáñez-Rodríguez, I., Martín-Lara, M. Á., Blázquez, G., Osegueda, Ó., & Calero, M. (2019). Thermal analysis of olive tree pruning and the by-products obtained by its gasification and pyrolysis: The effect of some heavy metals on their devolatilization behavior. *Journal of Energy Chemistry*, 32, 105–117. <https://doi.org/10.1016/J.JECHEM.2018.07.002>
- Independent Power Transmission Operator / IPTO*. (n.d.). Retrieved June 18, 2022, from <https://www.admie.gr/en>
- Indrawan, N., Simkins, B., Kumar, A., & Huhnke, R. L. (2020). Economics of distributed power generation via gasification of biomass and municipal solid waste. *Energies*, 13(14). <https://doi.org/10.3390/EN13143703>
- Intergovernmental Panel on Climate Change (IPCC). (2007). *Climate Change 2007 - Mitigation of Climate Change: Working Group III contribution to the Fourth Assessment Report of the IPCC (Climate Change 2007)*.
- Jagadabhi, P. S., Kaparaju, P., & Rintala, J. (2011). Two-stage anaerobic digestion of tomato, cucumber, common reed and grass silage in leach-bed reactors and upflow anaerobic sludge

- blanket reactors. *Bioresource Technology*, 102(7), 4726–4733. <https://doi.org/10.1016/j.biortech.2011.01.052>
- Jahangir, M. H., & Cheraghi, R. (2020). Economic and environmental assessment of solar-wind-biomass hybrid renewable energy system supplying rural settlement load. *Sustainable Energy Technologies and Assessments*, 42. <https://doi.org/10.1016/j.seta.2020.100895>
- Jahangiri, M., Shahmarvandi, F. K., & Alayi, R. (2021). Renewable Energy-Based Systems on a Residential Scale in Southern Coastal Areas of Iran: Trigeneration of Heat, Power, and Hydrogen. *Journal of Renewable Energy and Environment (JREE)*, 8(4), 67–76. <https://doi.org/10.30501/jree.2021.261980.1170>
- Kerr, T. (2008). *Combined Heat and Power: Evaluating the Benefits of Greater Global Investment*. <http://www.iea.org/Textbase/about/copyright.asp>
- Kougioumtzis, M.-A., Karampinis, E., Grammelis, P., & Kakaras, E. (2019). *EXPLOITATION OF OLIVE TREE PRUNINGS. EVALUATION OF AN INTEGRATED HARVESTING DEMONSTRATION IN CENTRAL GREECE*.
- Kumar, K. R., Dashora, K., Krishnan, N., Sanyal, S., Chandra, H., Dharmaraja, S., & Kumari, V. (2021). Feasibility assessment of renewable energy resources for tea plantation and industry in India - A review. In *Renewable and Sustainable Energy Reviews* (Vol. 145). Elsevier Ltd. <https://doi.org/10.1016/j.rser.2021.111083>
- Kumar, P., & Vallabhbai, S. (2016, February 27). Analysis of Hybrid Systems: Software Tools. *International Conference on Advances in Electrical, Electronics, Information, Communication and Bio-Informatics (AEEICB16)*. <https://doi.org/10.1109/AEEICB.2016.7538302>
- Kumar, R., & Channi, H. K. (2022). A PV-Biomass off-grid hybrid renewable energy system (HRES) for rural electrification: Design, optimization and techno-economic-environmental analysis. *Journal of Cleaner Production*, 349, 131347. <https://doi.org/10.1016/J.JCLEPRO.2022.131347>
- Ladha-Sabur, A., Bakalis, S., Fryer, P. J., & Lopez-Quiroga, E. (2019). Mapping energy consumption in food manufacturing. *Trends in Food Science & Technology*, 86, 270–280. <https://doi.org/10.1016/J.TIFS.2019.02.034>
- Looney, B. (2021). *Statistical review of world energy globally consistent data on world energy markets*.
- Lynn, P. A. (2012). *Onshore and offshore wind energy : An introduction*. Wiley.
- Malik, P., Awasthi, M., & Sinha, S. (2020). Study of grid integrated biomass-based hybrid renewable energy systems for Himalayan territory. *International Journal of Sustainable Energy Planning and Management*, 28, 71–88. <https://doi.org/10.5278/ijsepm.3674>
- Mamaní, A., Maturano, Y., Mestre, V., Montoro, L., Gassa, L., Deiana, C., & Sardella, F. (2021). Valorization of olive tree pruning. Application for energy storage and biofuel production. *Industrial Crops and Products*, 173. <https://doi.org/10.1016/j.indcrop.2021.114082>

- Martínez, J. D., Mahkamov, K., Andrade, R. v., & Silva Lora, E. E. (2012). Syngas production in downdraft biomass gasifiers and its application using internal combustion engines. *Renewable Energy*, 38(1), 1–9. <https://doi.org/10.1016/J.RENENE.2011.07.035>
- Martínez-Patino, J. C., Romero, I., Ruiz, E., Cara, C., Romero-García, J. M., & Castro, E. (2017). Design and Optimization of Sulfuric Acid Pretreatment of Extracted Olive Tree Biomass Using Response Surface Methodology. *BioResources*, 12(1), 1779–1797.
- Martín-Lara, M. A., Ronda, A., Zamora, M. C., & Calero, M. (2017). Torrefaction of olive tree pruning: Effect of operating conditions on solid product properties. *Fuel*, 202, 109–117. <https://doi.org/10.1016/J.FUEL.2017.04.007>
- Mata-Alvarez, J., Dosta, J., Romero-Güiza, M. S., Fonoll, X., Peces, M., & Astals, S. (2014). A critical review on anaerobic co-digestion achievements between 2010 and 2013. *Renewable and Sustainable Energy Reviews*, 36, 412–427. <https://doi.org/10.1016/J.RSER.2014.04.039>
- McIlwaine, N., Foley, A. M., Morrow, D. J., al Kez, D., Zhang, C., Lu, X., & Best, R. J. (2021). A state-of-the-art techno-economic review of distributed and embedded energy storage for energy systems. *Energy*, 229, 120461. <https://doi.org/10.1016/J.ENERGY.2021.120461>
- Meegoda, J. N., Li, B., Patel, K., & Wang, L. B. (2018). A review of the processes, parameters, and optimization of anaerobic digestion. In *International Journal of Environmental Research and Public Health* (Vol. 15, Issue 10). MDPI AG. <https://doi.org/10.3390/ijerph15102224>
- Meyers, R. A., & Kaltschmitt, M. (2019). *Energy from Organic Materials (Biomass)*. <https://link.springer.com/bookseries/15436>
- Meyers, S., Schmitt, B., Chester-Jones, M., & Sturm, B. (2016). Energy efficiency, carbon emissions, and measures towards their improvement in the food and beverage sector for six European countries. *Energy*, 104, 266–283. <https://doi.org/10.1016/J.ENERGY.2016.03.117>
- Mizanur, M., Kent, M. D., & Kopacek, P. (2021). Techno-economic analysis of HRES in south-east of Ireland. *IFAC-PapersOnLine*, 54(13), 454–459. <https://doi.org/10.1016/j.ifacol.2021.10.490>
- Mlaik, N., Karray, F., Sayadi, S., Feki, F., & Khoufi, S. (2022). Semi-continuous anaerobic digestion of the organic fraction of municipal solid waste: digester performance and microbial population dynamics. *Journal of Environmental Chemical Engineering*, 107941. <https://doi.org/10.1016/J.JECE.2022.107941>
- Molino, A., Chianese, S., & Musmarra, D. (2016). Biomass gasification technology: The state of the art overview. *Journal of Energy Chemistry*, 25(1), 10–25. <https://doi.org/10.1016/J.JECHEM.2015.11.005>
- Mu, L., Zhang, L., Zhu, K., Ma, J., & Li, A. (2018). Semi-continuous anaerobic digestion of extruded OFMSW: Process performance and energetics evaluation. *Bioresour Technol*, 247, 103–115. <https://doi.org/10.1016/J.BIORTECH.2017.09.085>
- Najafi, E., Castro, E., & Karimi, K. (2021). Biorefining for olive wastes management and efficient bioenergy production. *Energy Conversion and Management*, 244. <https://doi.org/10.1016/j.enconman.2021.114467>

- NASA POWER / *Prediction Of Worldwide Energy Resources*. (n.d.). Retrieved April 1, 2022, from <https://power.larc.nasa.gov/>
- Pane, C., Celano, G., Piccolo, A., Vилlecco, D., Spaccini, R., Palese, A. M., & Zaccardelli, M. (2015). Effects of on-farm composted tomato residues on soil biological activity and yields in a tomato cropping system. *Chemical and Biological Technologies in Agriculture*, 2(1). <https://doi.org/10.1186/s40538-014-0026-9>
- Pantaleo, A. M., Camporeale, S., & Fortunato, B. (2015). Small scale biomass CHP: Techno-economic performance of steam vs gas turbines with bottoming ORC. *Energy Procedia*, 82, 825–832. <https://doi.org/10.1016/J.EGYPRO.2015.11.819>
- Pellera, F. M. (2017). *Integrated solid organic waste treatment and valorization in the Mediterranean area using anaerobic digestion*. DOI: 10.12681/eadd/39804
- Pfenninger, S., & Staffell, I. (2016). Long-term patterns of European PV output using 30 years of validated hourly reanalysis and satellite data. *Energy*, 114, 1251–1265. <https://doi.org/10.1016/J.ENERGY.2016.08.060>
- Pierri, E., Hellkamp, D., Thiede, S., & Herrmann, C. (2021). Enhancing Energy Flexibility through the Integration of Variable Renewable Energy in the Process Industry. *Procedia CIRP*, 98, 7–12. <https://doi.org/10.1016/j.procir.2020.12.001>
- Pierri, E., Schulze, C., Herrmann, C., & Thiede, S. (2020). Integrated methodology to assess the energy flexibility potential in the process industry. *Procedia CIRP*, 90, 677–682. <https://doi.org/10.1016/j.procir.2020.01.124>
- Rajbongshi, R., Borgohain, D., & Mahapatra, S. (2017). Optimization of PV-biomass-diesel and grid base hybrid energy systems for rural electrification by using HOMER. *Energy*, 126, 461–474. <https://doi.org/10.1016/J.ENERGY.2017.03.056>
- Ram, K., Swain, P. K., Vallabhaneni, R., & Kumar, A. (2021). Critical assessment on application of software for designing hybrid energy systems. *Materials Today: Proceedings*, 49, 425–432. <https://doi.org/10.1016/j.matpr.2021.02.452>
- Renewable Energy Agency, I. (2015). *Renewable Energy Options for the Industry Sector: Global and Regional Potential until 2030*. www.irena.org/remap.
- Ribó-Pérez, D., Herraiz-Cañete, Á., Alfonso-Solar, D., Vargas-Salgado, C., & Gómez-Navarro, T. (2021). Modelling biomass gasifiers in hybrid renewable energy microgrids; a complete procedure for enabling gasifiers simulation in HOMER. *Renewable Energy*, 174, 501–512. <https://doi.org/10.1016/J.RENENE.2021.04.083>
- Riley, D. M., Tian, J., Güngör-Demirci, G., Phelan, P., Rene Villalobos, J., & Milcarek, R. J. (2020). Techno-economic assessment of chp systems in wastewater treatment plants. *Environments - MDPI*, 7(10), 1–32. <https://doi.org/10.3390/ENVIRONMENTS7100074>
- Salehin, S., Islam, A. K. M. S., Hoque, R., Rahman, M., Hoque, A., & Manna, E. (2014, July 21). Optimized model of a solar PV-biogas-diesel hybrid energy system for Adorsho Char island, Bangladesh. *Proceedings of 2014 3rd International Conference on the Developments in Renewable Energy Technology, ICDRET 2014*. <https://doi.org/10.1109/icdret.2014.6861692>

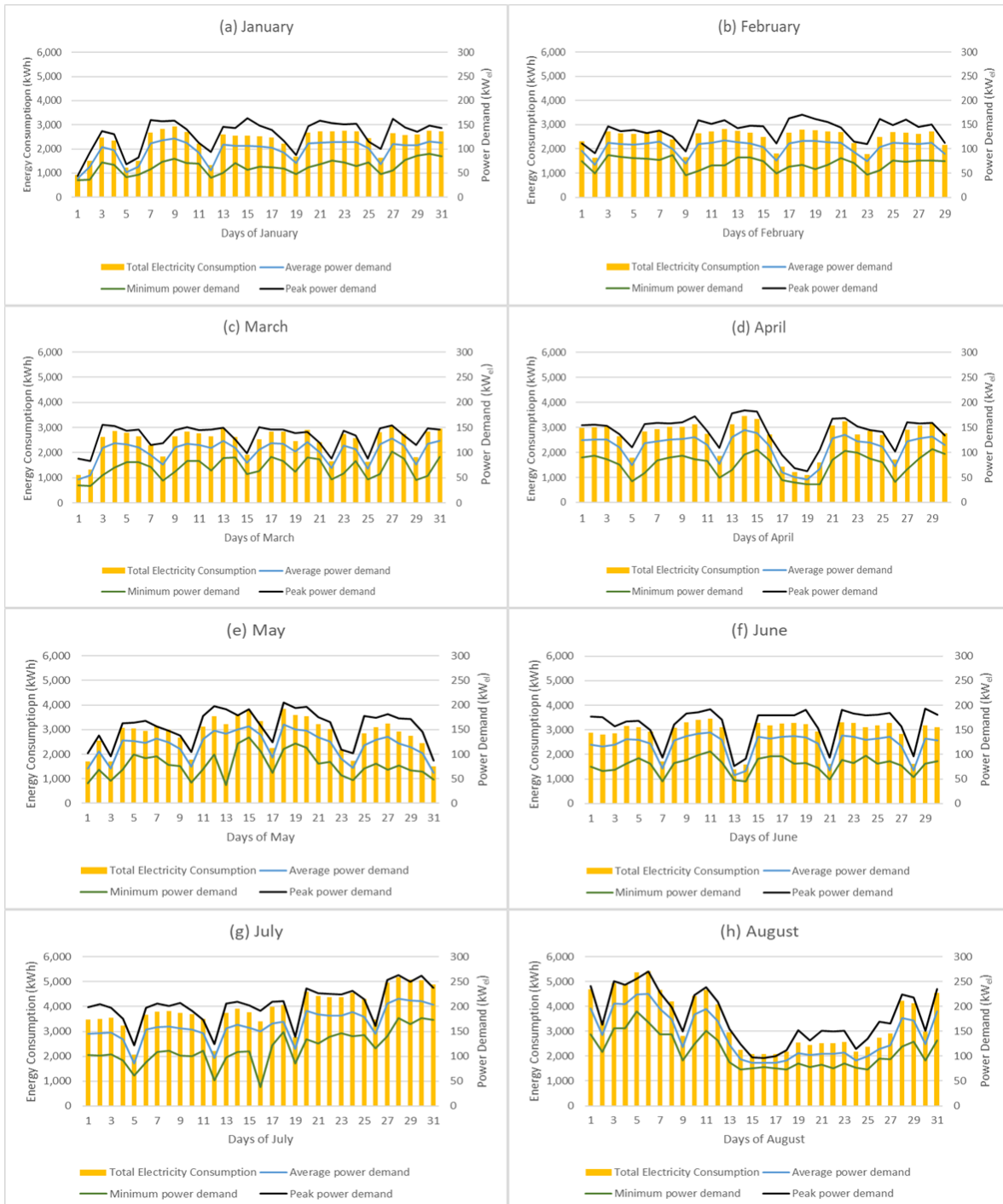
- Sánchez, F., & San Miguel, G. (2016). Improved fuel properties of whole table olive stones via pyrolytic processing. *Biomass and Bioenergy*, *92*, 1–11. <https://doi.org/10.1016/J.BIOMBIOE.2016.06.001>
- Shahzad, M. K., Zahid, A., Rashid, T., Rehan, M. A., Ali, M., & Ahmad, M. (2017). Techno-economic feasibility analysis of a solar-biomass off grid system for the electrification of remote rural areas in Pakistan using HOMER software. *Renewable Energy*, *106*, 264–273. <https://doi.org/10.1016/J.RENENE.2017.01.033>
- Sifakis, N., Konidakis, S., & Tsoutsos, T. (2021). Hybrid renewable energy system optimum design and smart dispatch for nearly Zero Energy Ports. *Journal of Cleaner Production*, *310*. <https://doi.org/10.1016/j.jclepro.2021.127397>
- Sigarchian, S. G., Paleta, R., Malmquist, A., & Pina, A. (2015). Feasibility study of using a biogas engine as backup in a decentralized hybrid (PV/wind/battery) power generation system - Case study Kenya. *Energy*, *90*, 1830–1841. <https://doi.org/10.1016/J.ENERGY.2015.07.008>
- Skoulou, V. (2009). *Design and development of a gasification reactor for energy production from biomass* [PhD Thesis, Aristotle University of Thessaloniki (AUTH)]. DOI: 10.12681/eadd/27195
- Solar Permit Package Software | SolarDesignTool*. (n.d.). Retrieved June 10, 2022, from <https://get.solardesigntool.com/>
- Sovacool, B. K., Bazilian, M., Griffiths, S., Kim, J., Foley, A., & Rooney, D. (2021). Decarbonizing the food and beverages industry: A critical and systematic review of developments, sociotechnical systems and policy options. *Renewable and Sustainable Energy Reviews*, *143*, 110856. <https://doi.org/10.1016/J.RSER.2021.110856>
- Staffell, I., & Pfenninger, S. (2016). Using bias-corrected reanalysis to simulate current and future wind power output. *Energy*, *114*, 1224–1239. <https://doi.org/10.1016/J.ENERGY.2016.08.068>
- Strezov, V., & Anawar, H. M. (Eds.). (2019). *Renewable Energy Systems from Biomass Efficiency, Innovation, and Sustainability edited by*. CRC Press Taylor & Francis Group.
- Tang, H., Wang, S., & Li, H. (2021). Flexibility categorization, sources, capabilities and technologies for energy-flexible and grid-responsive buildings: State-of-the-art and future perspective. In *Energy* (Vol. 219). Elsevier Ltd. <https://doi.org/10.1016/j.energy.2020.119598>
- Tazay, A. (2020). Techno-Economic Feasibility Analysis of a Hybrid Renewable Energy Supply Options for University Buildings in Saudi Arabia. *Open Engineering*, *11*(1), 39–55. <https://doi.org/10.1515/eng-2021-0005>
- Terlouw, T., & Bauer, C. (2021). *Smart integRation Of local energy sources and innovative storage for flexiBle, secure and cost-efficient eNergy Supply ON industrialized islands D5.1-Technology specifications*. www.robinson-h2020.eu
- Thirunavukkarasu, M., & Sawle, Y. (2022). An Examination of the Techno-Economic Viability of Hybrid Grid-Integrated and Stand-Alone Generation Systems for an Indian Tea Plant. *Frontiers in Energy Research*, *10*. <https://doi.org/10.3389/fenrg.2022.806870>

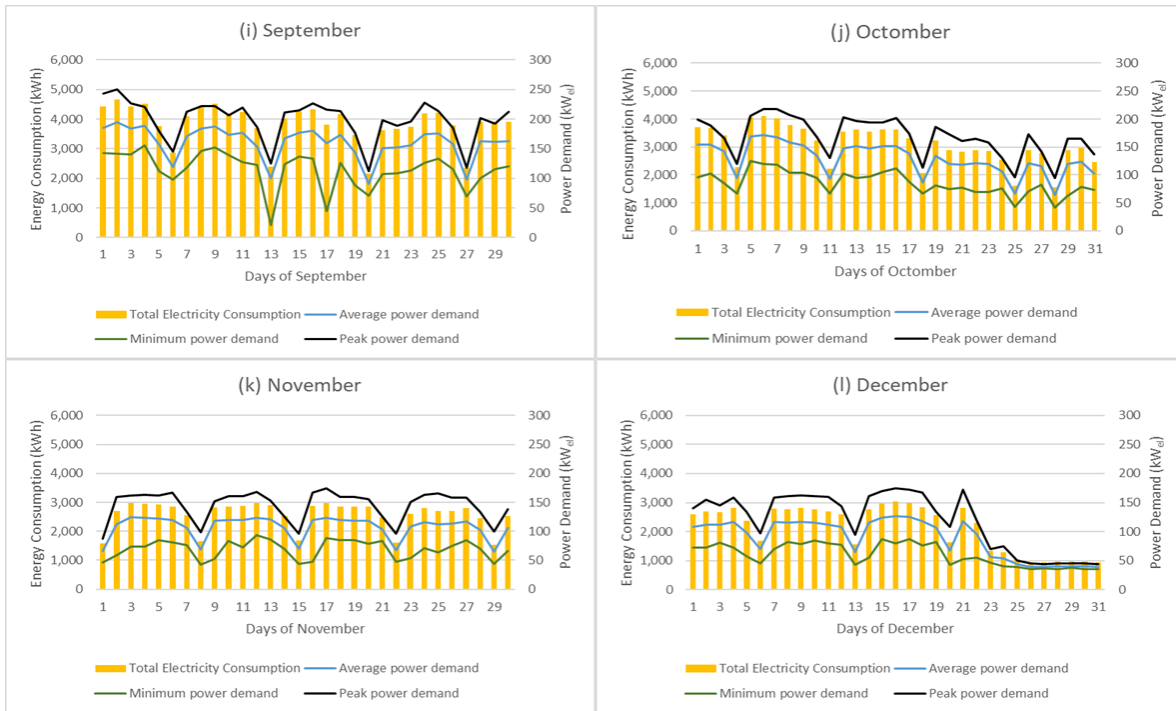
- Tial Kio, T. M. L., Anne M, M., Arampatzis, G., Peter, B., Mohammad, M., & Magnus, D. (2021). *Smart integRation Of local energy sources and innovative storage for flexiBle, secure and cost-effiCient eNergy Supply ON industrialized islands D 1.1 – Islands documentation and mapping reports*. www.robinson-h2020.eu
- Trabold, T. A., & Badditt, C. W. (2018). *Sustainable Food Waste-to-Energy Systems* (T. A. Trabold & C. W. Badditt, Eds.). Academic Press ELSEVIER.
- TRADING ECONOMICS | 20 million INDICATORS FROM 196 COUNTRIES. (n.d.). Retrieved June 10, 2022, from <https://tradingeconomics.com/>
- Velázquez-Martí, B., Fernández-González, E., López-Cortés, I., & Salazar-Hernández, D. M. (2011). Quantification of the residual biomass obtained from pruning of trees in Mediterranean olive groves. *Biomass and Bioenergy*, 35(7), 3208–3217. <https://doi.org/10.1016/j.biombioe.2011.04.042>
- Vendoti, S., Muralidhar, M., & Kiranmayi, R. (2021). Techno-economic analysis of off-grid solar/wind/biogas/biomass/fuel cell/battery system for electrification in a cluster of villages by HOMER software. *Environment, Development and Sustainability*, 23(1), 351–372. <https://doi.org/10.1007/S10668-019-00583-2>
- Vera, D., Jurado, F., Margaritis, N. K., & Grammelis, P. (2014). Experimental and economic study of a gasification plant fuelled with olive industry wastes. *Energy for Sustainable Development*, 23, 247–257. <https://doi.org/10.1016/j.esd.2014.09.011>
- Wang, L. (2014). Energy efficiency technologies for sustainable food processing. In *Energy Efficiency* (Vol. 7, Issue 5, pp. 791–810). Kluwer Academic Publishers. <https://doi.org/10.1007/s12053-014-9256-8>
- Waste statistics - Statistics Explained. (2021, May 4). https://ec.europa.eu/eurostat/statistics-explained/index.php?title=Waste_statistics
- Yimen, N., Hamandjoda, O., Meva`a, L., Ndzana, B., & Nganhou, J. (2018). Analyzing of a photovoltaic/wind/biogas/pumped-hydro off-grid hybrid system for rural electrification in Sub-Saharan Africa - Case study of Djoundé in Northern Cameroon. *Energies*, 11(10). <https://doi.org/10.3390/en11102644>
- Yimen, N., Monkam, L., Tcheukam-Toko, D., Musa, B., Abang, R., Fon Fombe, L., Abbasoglu, S., & Dagbasi, M. (2021). *IET Renewable Power Generation Optimal design and sensitivity analysis of distributed biomass-based hybrid renewable energy systems for rural electrification: Case study of different photovoltaic/wind/ battery-integrated options in Babadam, northern Cameroon*. <https://doi.org/10.1049/rpg2.12266>
- Yin, S., Xia, J., & Jiang, Y. (2020). Characteristics analysis of the heat-to-power ratio from the supply and demand sides of cities in northern China. *Energies*, 13(1). <https://doi.org/10.3390/en13010242>
- O.I.E.K.E.II.E. - Home Page. (n.d.). Retrieved April 5, 2022, from <https://www.opekepe.gr/en/>
- Σαββάκης, Ν., Τουρνάκη, Σ., & Τσούτσος, Θ. (2018). *Μελέτη Σκοπιμότητας για αξιοποίηση του δυναμικού βιομάζας ξυλείας στον Δήμο Ανωγείων*.

- Τσούτσος, Θ. Δ., & Κανάκης, Ι. Ν. (2013). *Ανανεώσιμες Πηγές Ενέργειας Τεχνολογίες & Περιβάλλον*. Εκδόσεις Παπασωτηρίου.
- Υπ. Ανάπτυξης, Ανταγωνιστικότητας, Υποδομών, Μεταφορών και Δικτύων - Παρατηρητήριο Τιμών Υγρών Καυσίμων. (n.d.). Retrieved May 26, 2022, from <http://www.fuelprices.gr/>
- Χατζηγιάννη, Ε. (2016). *Περιφερειακός Σχεδιασμός Διαχείρισης Αποβλήτων Κρήτης (ΠΕΣΔΑΚ) | Περιφέρεια Κρήτης Περιφέρεια Κρήτης*. <https://www.crete.gov.gr/prefecture/perifereiakos-schediasmos-diacheirisi/>

APPENDIX A

Appendix A presents the electricity profiles, for every month, of the reference industrial facility.

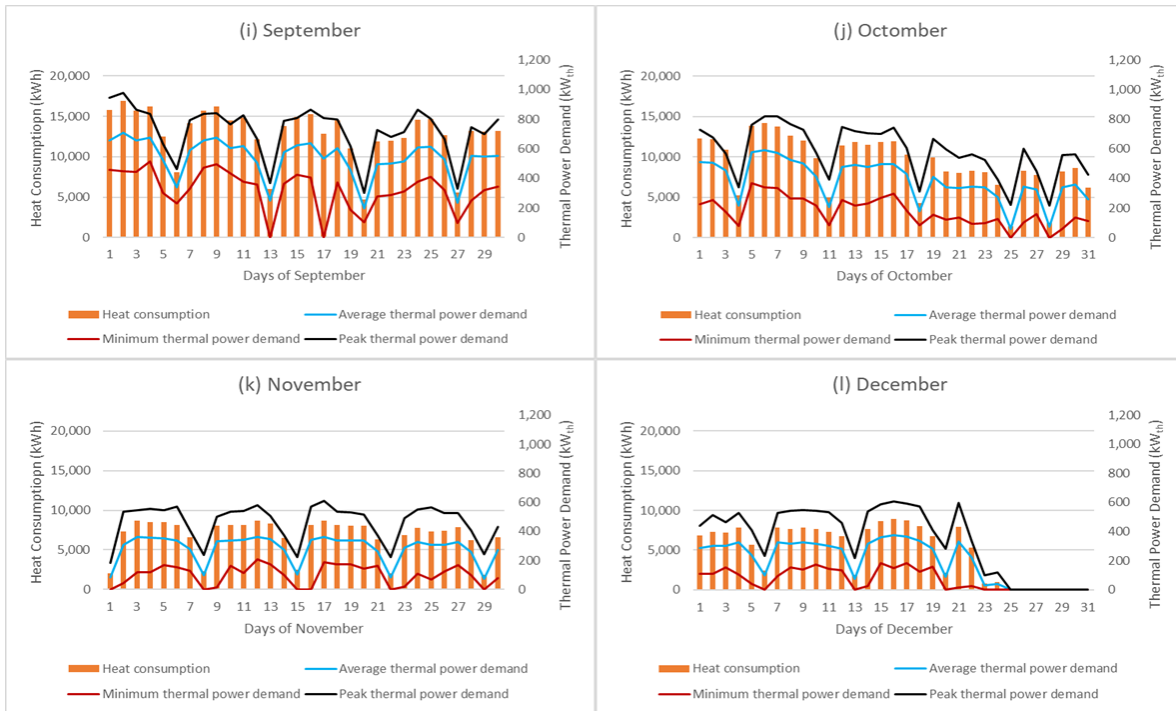




APPENDIX B

Appendix B presents the thermal energy usage profiles, for every month, of the reference industrial facility.





APPENDIX C

Appendix C presents the proposed methodological framework flowchart.

